THE MESSENGER

EL MENSAJERO

Paranal
La Silla
La Serena
Santiago
Munich

No. 98 – December 1999

First Scientific Results with the VLT in Visitor and Service Modes

Starting with this issue, The Messenger will regularly include scientific results obtained with the VLT. One of the results reported in this issue is a study of NGC 3603, the most massive visible H II region in the Galaxy, with VLT/ISAAC in the near-infrared J_S, H, and K_S-bands and HST/WFPC2 at Hα and [N II] wavelengths. These VLT observations are the most sensitive near-infrared observations made to date of a dense starburst region, allowing one to investigate with unprecedented quality its low-mass stellar population. The sensitivity limit to stars detected in all three bands corresponds to 0.1 $M_\odot$ for a pre-main-sequence star of age 0.7 Myr. The observations clearly show that sub-solar-mass stars down to at least 0.1 $M_\odot$ do form in massive starbursts (from B. Brandl, W. Brandner, E.K. Grebel and H. Zinnecker, page 46).

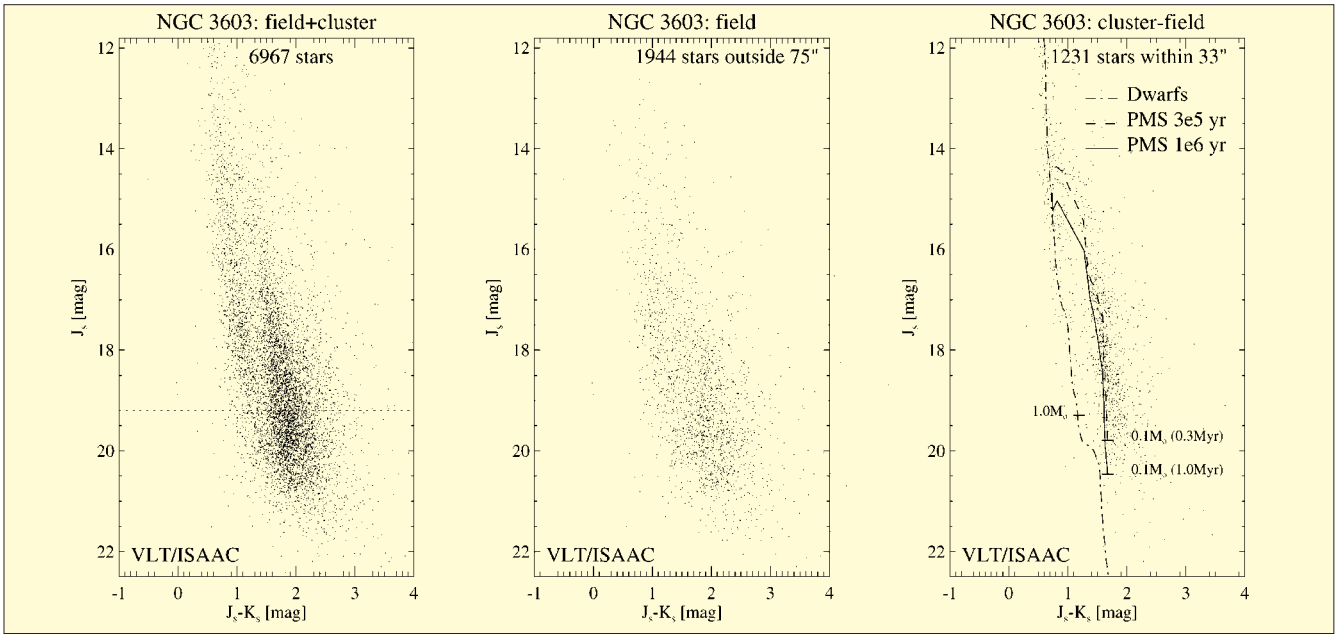

J_S versus J_S–K_S colour-magnitude diagrams of NGC 3603. The left-hand panel contains all stars detected in all three wavebands in the entire field of view (3.4′ × 3.4′, or 6 pc × 6 pc); the centre panel shows the field stars at r > 75″ (2.25 pc) around the cluster, and the right-hand panel shows the cluster population within r < 33″ (1pc) with the field stars statistically subtracted. The dashed horizontal line (left-hand panel) indicates the detection limit of the previous most sensitive NIR study (Eisenhauer et al. 1998). The right-hand panel also shows the theoretical isochrones of pre-main-sequence stars of different ages from Palla & Stahler (1999) and the main sequence for dwarfs. For comparison, some corresponding stellar masses have been plotted next to the isochrones.

The VLTI – The Observatory of the 21st Century

A. GLINDEMANN, R. ABUTER, F. CARBOGNANI, F. DELPLANCKE, F. DERIE, A. GENNAI, P. GITTON, P. KERVELLA, B. KOEHLER, S. LÉVÊQUE, G. DE MARCHI, S. MENARDI, A. MICHEL, F. PARESCE, T. PHAN DUC, M. SCHÖLLER, M. TARENGHI and R. WILHELM

European Southern Observatory

1. Introduction

After several years on a bumpy road, the support for the VLT Interferometer project has increased dramatically over the last year with the appointment of eight new staff members, with the foundation of the NOVA[1]-ESO VLTI Expertise Centre (NEVEC) at the Leiden Observatory and with institutes and institutions from other European countries (Italy, Switzerland and Belgium) on the verge of joining the project in one way or another.

Major contracts for the Delay Line Systems and for the Auxiliary Telescope Systems (ATs) were signed in 1997 and 1998 respectively, the work on the science instruments MIDI and AMBER has progressed very well in the last two years and the commissioning instrument VINCI is coming closer to reality. Several smaller contracts for the Test Siderostats, for the Coudé Optical Trains of the four Unit Telescopes (UTs), and for a Feasibility Study of the dual-feed facility PRIMA were also placed.

We are now planning for first fringes with the commissioning instrument and the Siderostats before the beginning of the new Millenium.

In this article we will give a report on the status of the project and we will describe the strategy for making the VLTI the observatory of the 21st century.

[1]NOVA is the Netherlands Research School for Astronomy.

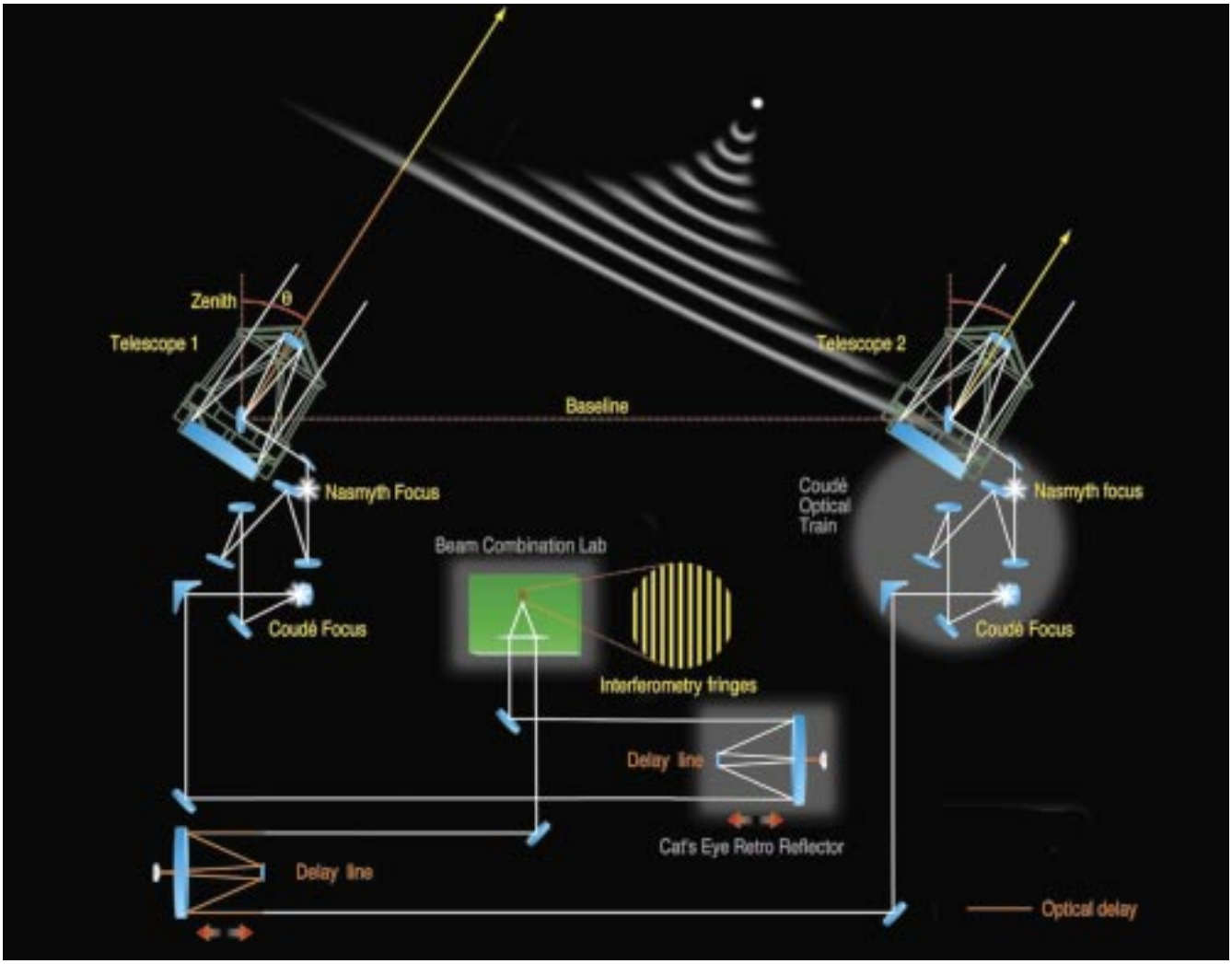

Figure 1: The optical layout of the VLTI with two telescopes. The telescopes represent both UTs and ATs that have the same optical design. The Coudé Optical Trains are the mirrors after the tertiary mirror up to the Coudé Focus. Two Delay Lines are shown to demonstrate the principle of operation. The VLTI laboratory is represented by the beam-combining lens forming fringes.

2. The Sub-Systems of the VLTI

The layout of the VLTI is displayed in Figure 1, for the sake of simplicity with only two telescopes. A star at infinity illuminates the apertures in the two telescopes with a plane wave that is guided through the Coudé Optical Trains into the Delay Line Tunnel. The delay in arrival of the light at telescope 1 with respect to telescope 2 is compensated by the delay lines so that the beams have zero Optical Path Difference (OPD) when they interfere on the detector in the VLTI laboratory. The field of view of the VLTI is 2 arcsec. However, the dual-feed facility PRIMA will allow picking two stars at the Coudé focus of ATs or UTs each in a 2 arcsec field of view and separated by up to 1 arcmin.

The measurements of the contrast of the fringe pattern and of its phase, i.e. the position of the white light fringe with respect to the nominal zero OPD position are the tasks of the VLT Interferometer. Doing these measurements for many different baselines (different in length and orientation) allows reconstructing an image with the angular resolution of a single telescope with a diameter equal to the longest baseline. Since the longest baselines are 130 m for the Unit Telescopes and 200 m for the Auxiliary Telescopes and since the specified precision for the measurements of the fringe contrast is very high, the requirements e.g. for the Delay Line systems are very tough. Here, the beam tilt accuracy has to be better than 1.5 arcseconds (15 milliarcsec on the sky) and the absolute position accuracy is 1μm over 65 m of travel in the tunnel. Similar accuracy values are required for all mirrors and mirror mounts of the VLTI, including the 8-m primary mirrors. Also, the environmental conditions have to be very stable in order to minimise internal turbulence.

It is the advantage of the VLTI that these considerations have been driving the design of the Unit Telescopes and of the Auxiliary Telescopes, as well as the construction of the infrastructure. Several measurement campaigns have confirmed that both optomechanical and environmental specifications are met.

The status of the VLTI sub-systems is as follows:

Test Siderostats

For tests with the VLTI and the instruments, two Test Siderostats were designed and built (for details see [3]). The free aperture of 400 mm allows for about 20 stars to be observed in the N-band at 10 μm. Since for the VLTI Control System the Siderostats will 'look' the same as the UTs and ATs, it is planned to commission the VLTI with the Siderostats. They will be located on the AT stations and will thus be able to use baselines between 8 and 200 m. The systems are readily manufactured and they will be delivered to Paranal in January 2000. The implementation of the Siderostat control software will be finished by May 2000. It is planned to have first fringes with the Siderostats and VINCI in December 2000.

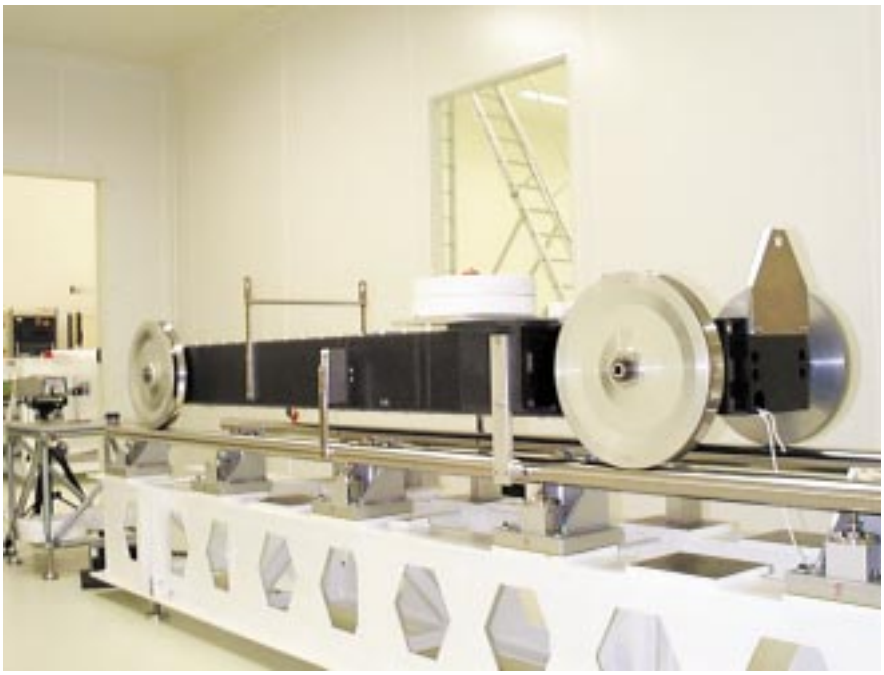

Figure 2: The carriage for the cat's-eye of the Delay Line System in the Clean Room at Fokker in Leiden. The carriage has three wheels running on the 65-m steel rails. The diameter of the wheels is about 40 cm and the length of the carriage 2.25 m.

Delay Line Systems

Three Delay Lines have been ordered; the first two will be installed in the Delay Line Tunnel in July 2000, the third one in December 2000. The systems consist of the cat's-eye mirror system retro-reflecting the incoming parallel beam, and of the carriage transporting the cat's-eye along the delay lines. Figure 2 shows the carriage on its three wheels in the cleanroom at the manufacturer. The three-mirror optical design of the cat's-eye has a variable curvature mirror (VCM, see [4]) in the focus of the cat's eye in order to re-image the telescope pupil into a fixed position in the VLTI laboratory while the Delay Line System is tracking. The cat's-eye can handle two input beams as required for a dual feed system. A total of eight Delay Line Systems can be hosted in the Delay Line Tunnel.

Auxiliary Telescope Systems

In June 1998, two 1.8-m Auxiliary Telescopes were ordered, and in June 1999, the option for the third AT was exerted. A model of the telescope is displayed in Figure 3. The first two telescopes will be ready for the VLTI in June 2002, the third in October 2002. The telescopes are relocatable on 30 stations of the VISA (VLT Interferometer Sub-Array) providing baselines between 8 and 200 m. Using three telescopes and thus three baselines at the same time will allow the application of closure phase techniques eliminating the influence of atmospheric turbulence on fringe position. Each AT will be equipped with a tip-tilt system correcting for the fast image motion induced by atmospheric turbulence. Under the seeing conditions at Paranal, tip-tilt correction on a 1.8-m telescope in the near infrared means almost diffraction limited image quality. One should note that the ATs are available exclusively for the VLTI, forming an observatory that is operated independently of the Unit Telescopes.

Coudé Optical Trains and Transfer Optics

The five mirrors after the tertiary mirror of the Unit Telescopes form the Coudé Optical Train with a field of view of 2 arcmin (see Fig. 1). The last mirror before the Coudé Focus is very close to the telescope exit pupil and can be replaced by the deformable mirror of the adaptive optics system. The image quality at 2.2 μm is diffraction limited on the optical axis and better than 97% over the full field of view. The Coudé Optical Trains for all four UTs have been ordered and will be installed at Paranal in October 2000.

The transfer optics between the Coudé Focus and the Delay Lines are currently being designed. The concept is to avoid the need of human intervention in the delay line tunnel when switching between AT stations or UTs. Thus, the mirrors in the Delay Line Tunnel reflecting the light into the Delay Lines and from the Delay Lines into the VLTI Laboratory will be remotely controlled.

Figure 3: A model of an Auxiliary Telescope during Observations. The 1.8-m telescope (with an Alt-Az mount like the Unit Telescopes) is rigidly anchored to the ground by means of a special interface. The light is directed via the Coudé Optical Train to the bottom of the Telescope. From the Coudé Relay Optics it is sent on to the underground Delay Line Tunnel

VLTI Laboratory

The concept driver for the optical layout of the VLTI Laboratory (see Fig. 4) was to provide the same beam diameter for the interferometric instruments both when observing with UTs or ATs. Therefore, a beam compressor reduces the 80 mm beam diameter from the UTs to 18 mm matching the diameter of 18 mm provided by the ATs. The nominal position of equal optical path length is set for all beams at the same distance after the switchyard (indicated by the red line ZOPD in Fig. 4) to simplify the optical alignment of the interferometric instruments.

3. Phase A – Two Telescope Interferometry

In accordance with the recommendation by the Interferometry Science Advisory Committee (ISAC) laid out in the VLTI New Plan [12], the VLTI in its first phase will combine two telescopes, and near- and mid-infrared instrumentation will be available. An adaptive optics system for the UTs and a fringe sensor unit (FSU) will be implemented as well. In the near infrared, adaptive optics on the UTs is mandatory if the effective telescope aperture is not to be reduced to the size of the Fried Parameter, r_0, which is about 1 m in the near infrared.

Figure 4: The layout of the VLTI Laboratory. The switchyard can direct the beam into four directions: (1) to the interferometric instruments on the left without beam compression, (2) to the interferometric instruments after beam compression, (3) to the Differential Delay Lines (DDLs) after beam compression, and (4) to the Differential Delay Lines without beam compression. The beam compressor reduces the beam diameter from 80 mm to 18 mm and it re-images the telescope pupil into the PRIMA FSU, MIDI and VINCI (the position of the pupil is indicated by a diagonal line). A possible location for a visitor instrument is shown on the right.

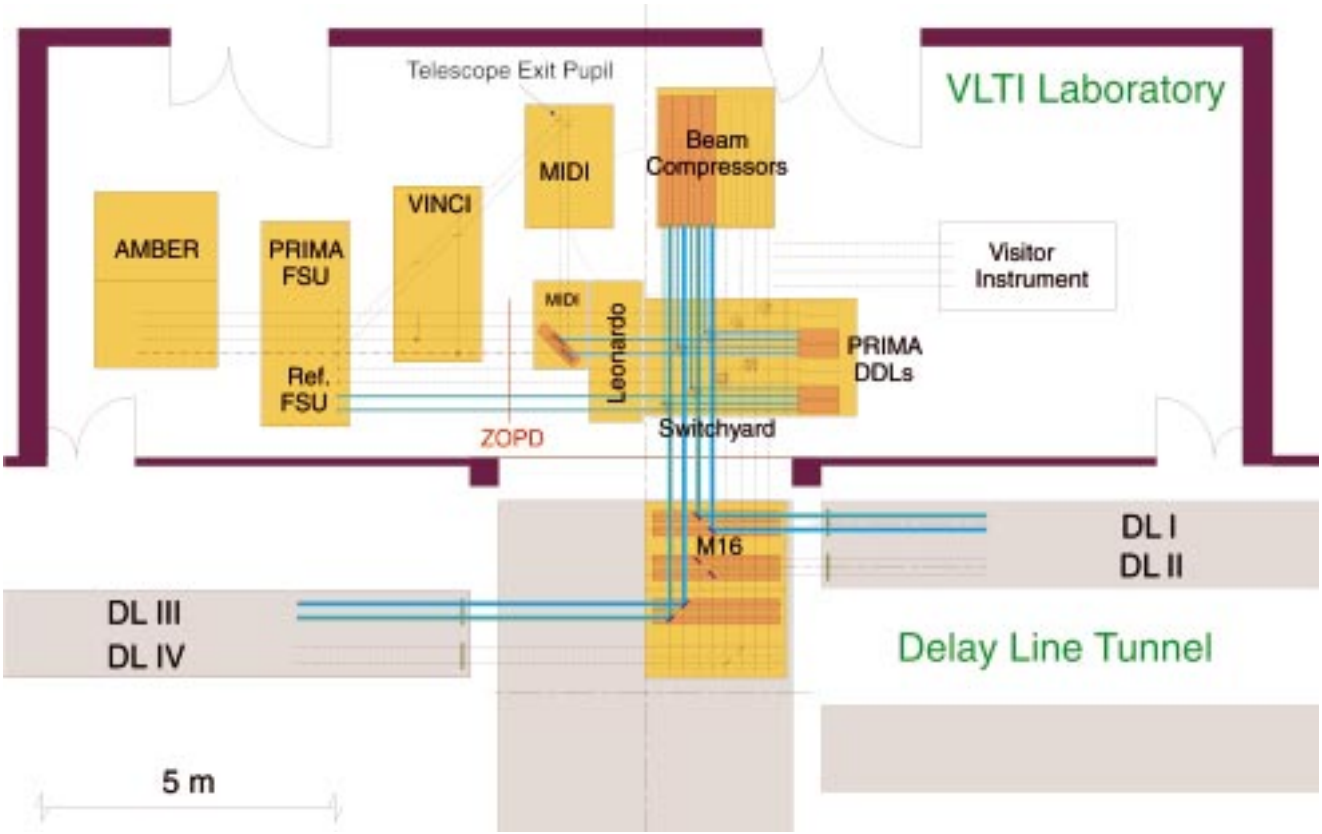

VINCI – The Commissioning Instrument

The commissioning instrument of the VLTI is a conceptual copy of FLUOR, the near-infrared interferometric instrument of the IOTA interferometer on Mount Hopkins in Arizona (US) [2]. The idea is to limit the technical risk and to facilitate the commissioning of the VLTI by using the design of an existing well functioning instrument (see e.g. [6]). The main component of VINCI (see Fig. 5) is a fibre beam combiner using the light from two telescopes as input and producing four outputs, two photometric and two interferometric signals. By varying the OPD between the beams with an internal modulator, a temporally modulated fringe pattern is produced on the detector. In addition to serving as the interferometric instrument, VINCI provides alignment tools and reference sources for the VLTI and the scientific instruments. VINCI will be delivered to Paranal in October 2000.

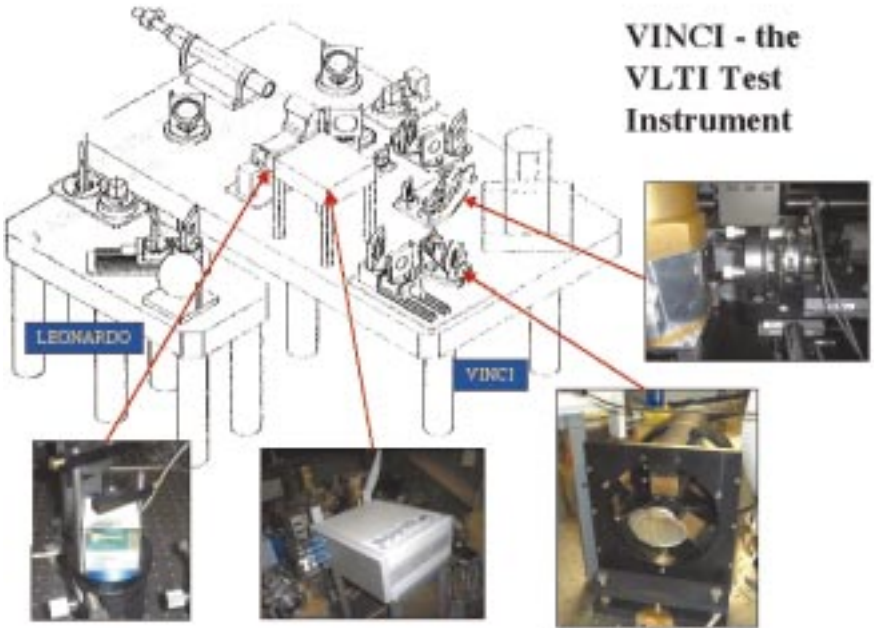

Figure 5: The concept of the VLTI commissioning instrument VINCI. The beam combining unit, VINCI, and the reference source unit, LEONARDO, are placed on individual tables. Their respective positions in the VLTI Laboratory are shown in Figure 4. The main elements on the VINCI table are the fibre beam combiner and the dewar of the infrared detector. The inserted photographs show details of the FLUOR instrument at the IOTA interferometer. VINCI is a conceptual copy of FLUOR.

MIDI

An interferometric instrument in the mid-infrared at 10 μm in combination with 8-m telescopes is a novelty, promising exciting results on new types of objects.

MIDI is being designed and built by a European consortium led by the Max-Planck-Institute for Astronomy in Heidelberg. The design philosophy is to have a simple instrument concept combining two beams and providing a moderate spectral resolution (≈ 200). The challenge lies in controlling the high thermal background. It is estimated that the individual beams will have an emissivity of about 50%, which corresponds to an equivalent photon noise on the sky of 53 mJy per Airy disk (with $\lambda/D = 0.26''$ for an aperture of 8 m) for a broad band 10 μm filter ($\Delta\lambda$ = 4 μm). Since the signal-to-noise-ratio scales as $S/N \propto D^2$ the availability of the Unit Telescopes is a huge advantage over smaller apertures. The details of the instrument are described in [7]. MIDI will be delivered to Paranal in June 2001; first light with the Siderostats is planned for September 2001.

AMBER

The near infrared instrument of the VLTI, AMBER, will operate between 1 and 2.5 μm, at first with two telescopes with a spectral resolution up to 10,000. As noted above, for UT observations in the near-infrared adaptive optics is mandatory. The magnitude limit of AMBER on the UTs is expected to reach K = 20 when a bright reference star is available (i.e. with a dual feed facility) and K = 14 otherwise. The European consortium in charge of designing and manufacturing this instrument is led by the Universities of Nice and Grenoble. AMBER has been designed for three beams to enable imaging through phase closure techniques [10]. It is planned to start commissioning AMBER with the Siderostats in February 2002.

MACAO

The adaptive optics system MACAO will have a 60-actuator bimorph mirror and a curvature wavefront sensor. The deformable mirror will replace one of the mirrors of the Coudé optical train, thus requiring no additional optical elements. As noted above, MACAO is essential for all near-infrared instrumentation to be used with the Unit Telescopes including the Fringe Sensor Unit operating in the H-band. This means that also a mid-infrared instrument like MIDI needs adaptive optics in order to improve the limiting magnitude by using a Fringe Tracker.

The first MACAO system will be installed on one of the Unit Telescopes in December 2001. It is planned to have MACAO ready for interferometric observations with two UTs in June 2002. Clones of the MACAO system will be used for future VLT instrumentation like SINFONI. MACAO is an in-house development [1].

4. Phase B – Imaging

The main drivers for the second phase of the VLTI are increasing the sensitivity of the interferometer and adding imaging modes. In addition, an astrometric mode will open the door for many thrilling scientific programmes.

Increasing the sensitivity of the VLTI calls for a dual feed facility. Then, the sensitivity is improved by using a bright guide star for fringe tracking – similar to the guide star in adaptive optics for wavefront sensing – in one of the two 'feeds' allowing increasing the exposure time on the science object in the other feed up to 10–30 minutes depending on the position in the sky. With a high-precision laser metrology system used to determine the internal optical path length, a dual feed system also provides an imaging mode. The VLTI dual feed facility PRIMA is described in the following.

Imaging with an interferometer relies on filling efficiently the UV plane with many different baseline vectors. Although this can be done by observing with two telescopes in many different positions using a dual feed system, it is more efficient to use three or more telescopes at the same time and eliminate the influence of atmospheric turbulence by applying phase closure techniques. Therefore, the third and fourth delay lines as well as the third Auxiliary Telescope are included in this phase.

PRIMA

The Phase Referenced Imaging and Micro-arcsec Astrometry (PRIMA) facility is a dual-feed system adding a faint-object imaging and an astrometry mode to the VLTI [5, 11]. PRIMA enables simultaneous interferometric observations of two objects – each with a maximum size of 2 arcsec – that are separated by up to 1 arcmin, without requiring a large continuous field of view. One object will then be used as a reference star for fringe tracking whilst the other object will be the

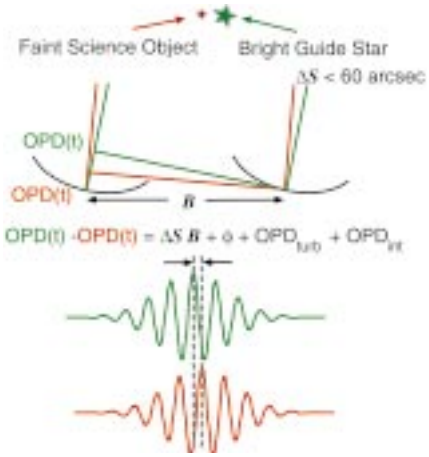

Figure 6: Principle of phase referenced imaging and astrometry with an interferometer. The difference in the positions of the white light fringes of object and reference star are determined by the OPD given by the product of ΔS, the angular separation vector of the stars, and B, the baseline vector, by the phase ϕ of the visibility function of the science object, by the OPD caused by the turbulence, and by the internal OPD.

science target. As a detector for PRIMA either the two scientific instruments MIDI and AMBER can be used making use of the fringe stabilisation provided by PRIMA, or a dedicated PRIMA detector for high-precision astrometry that will be designed in the next years.

PRIMA is the key to access: (1) Higher sensitivity, the limiting magnitude will be about K = 20, (2) imaging of faint objects with high angular resolution (<10 milliarcsec), (3) high-precision astrometry (≈ 10 μarcsec over a 10-arcsec field).

The principle of operation relies on finding within the isoplanatic angle (≈ 1 arcmin) of the science target a sufficiently bright star (H ≈ 12) that can be used as a reference star for the stabilisation of the fringe motion induced by atmospheric turbulence (see Fig. 6). Controlling all optical path lengths of the reference star and of the science star inside the interferometer (OPD_{int}) with a laser metrology system introduces the capability of imaging faint objects and of determining the precise angular separation between the two stars. The measurement has to be repeated for up to 30 min in order to average out the variations of the differential OPD caused by atmospheric turbulence (OPD_{turb}).

PRIMA can be subdivided into the four sub-systems (see Fig. 7): Star Separator, Laser Metrology System, Differential Delay Lines and Fringe Sensor Unit. These sub-systems contain a number of technological challenges, in particular in the area of laser metrology, that require careful analysis of the possible technical solutions. Therefore, a feasibility study for the four subsystems was performed by Dornier Satellite Systems, Friedrichshafen, and by ONERA, Paris, to find the best technical solutions and to obtain a thorough financial estimate for the manufacturing of the subsystems. The results of the study became available in July 1999 and a Call for Tender for the manufacturing of the system is planned early in 2000.

Dual feed observations with PRIMA can start as soon as the star separator, the fringe sensor unit and the differential delay lines are ready. Then, a reference star can be used for fringe tracking while integrating on the fainter science object as described above. If the fringe pattern can be stabilised over 10–100 sec the expected limiting magnitudes are about K ≈ 16 and N ≈ 8.

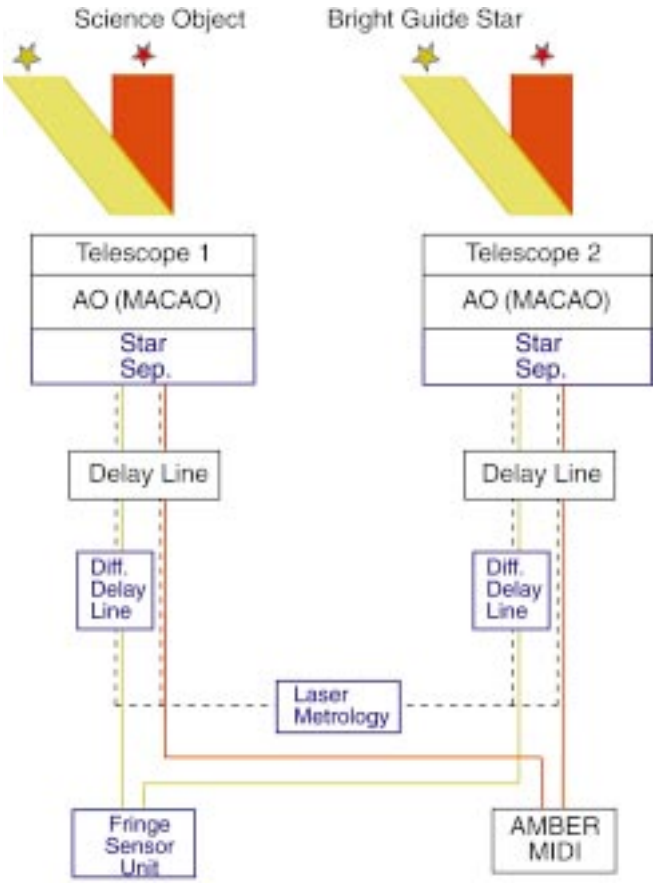

Figure 7: Functional block diagram of the VLTI and the PRIMA components. The VLTI has the following subsystems: Telescope 1 and 2 – two UTs or two ATs, AO – Adaptive Optics, Delay Lines, AMBER/MIDI – Science Instruments. The PRIMA subsystems are: Star Separator, Differential Delay Line, Laser Metrology, Fringe Sensor Unit.

Phase information required for imaging and astrometry becomes available if the laser metrology system is installed. An OPD measurement accuracy of 500 nm rms over 10 min sets the limiting magnitudes to about K ≈ 20 and N ≈ 11. The Strehl ratio in the reconstructed image can be as good as 30% in the K-band and 80% in the N-band depending on the UV coverage. Reaching the final goal of 5 nm rms over 30 min allows 10 μarcsec astrometry. PRIMA shall be operational by 2003.

5. First Fringes and Beyond

The major challenge in making the VLTI work is the complexity of the system. Not only are the individual sub-systems high-tech instruments but they are also scattered over an area up to 200 m in diameter. The quality of the control sys-

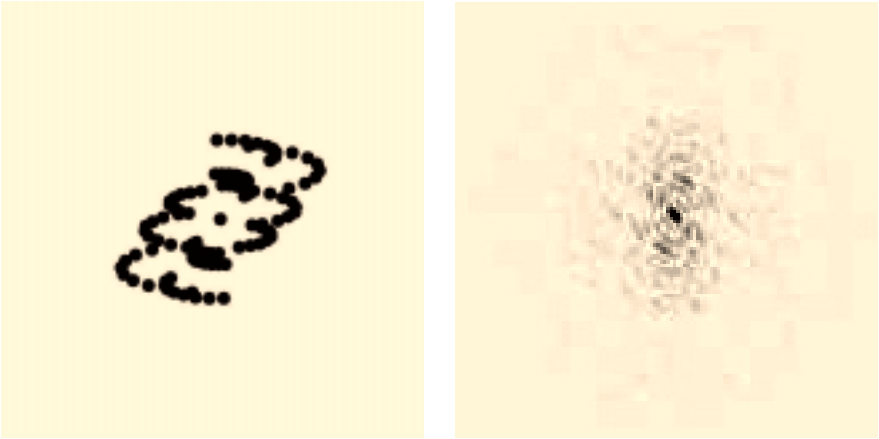

Figure 8: The UV coverage on the left and the point spread function (PSF) on the right with a full width at half maximum of 4 mas respectively 8 mas in the narrow respectively wide direction of the PSF at 2.2 μm. The UV coverage and the PSF are calculated for –15° declination and 8 hours of observing when combining all four UTs. Producing images with this quality is the ultimate goal for the VLTI.

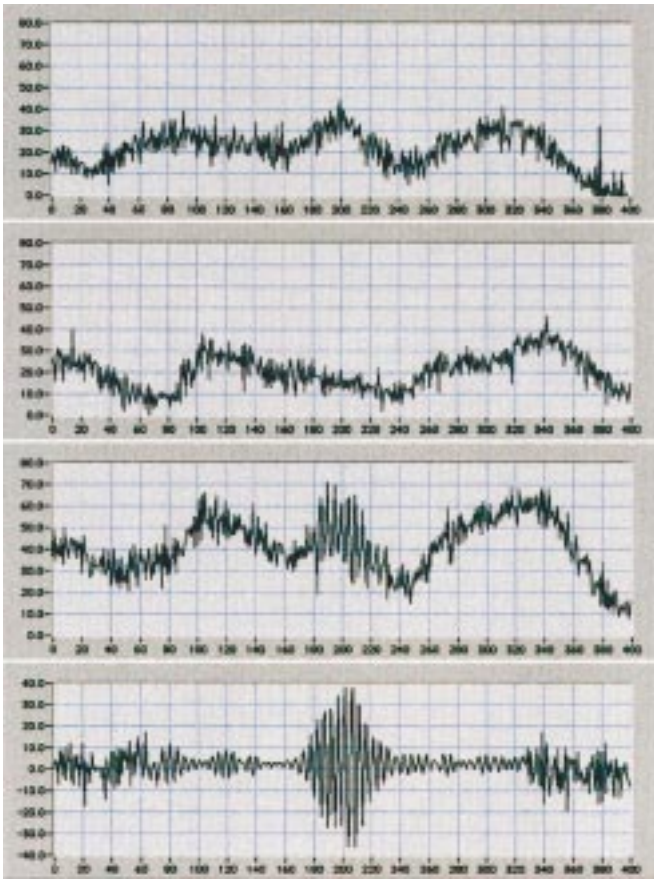

Figure 9: The type of results obtained with VINCI. The two top rows display the photometric signals from each telescope, the third row displays one of the interferometric outputs and the fourth row displays the same signal as in the third row calibrated with the photometric signals to obtain a clean fringe pattern.

tem is a key issue for the smooth operation of the complete system. From the beginning of 2000 onwards, every 6 months major new sub-systems and instruments arrive at Paranal and have to be integrated into the VLTI. Thus, the strategy for commissioning has to be defined very carefully.

For the first milestone of the VLTI programme, First Fringes with the Siderostats and VINCI, we have adopted the following approach: after installation and commissioning of the Siderostats, of the Delay Lines and of the Transfer Optics, the optical alignment of the full system will be done with a Technical CCD. Then, all degrees of freedom but one can be adjusted and the dynamic behaviour of the delay lines can be tested with a star observed with the siderostats. With the commissioning instrument VINCI the last remaining degree of freedom, the optical path difference, will be adjusted to produce interferometric fringes before the end of 2000. After first fringes, in the first half of 2001, the VLTI will be optimised by using different AT stations for the Siderostats and by integrating the third Delay Line into the system. While this is taking place the Coudé Optical Trains in the UTs and the remaining transfer optics are being installed.

The next instruments to arrive at Paranal are MIDI in the middle and AMBER at the end of 2001. Both science instruments will be commissioned with the Siderostats. MIDI can be tested shortly after first fringes on the Siderostats with the UTs even before the adaptive optics system MACAO arrives. After installation and commissioning of MACAO with the VLTI and with VINCI in the second half of 2002, AMBER will be tested on the UTs.

Also in 2002, a total of three Auxiliary Telescopes will be commissioned, first individually then with the VLTI and VINCI. The science instruments will follow suit. The first sub-systems of PRIMA arrive as well in 2002. During the course of 2003 both dual feed and closure phase operation can be tested with the VLTI.

In order to operate the VLTI as an observatory, support astronomers, instrument operators and engineers are required for regular operations and for maintenance. Although the number of nights with two (or more) UTs is probably restricted to a small fraction of the total number of available nights in the first few years, first the Siderostats and then the Auxiliary Telescopes are available every night for VLTI observations. Thus, the planning for the VLTI has to foresee a full-time coverage with technical and scientific personnel. One has to keep in mind that the VLTI is running in parallel to the VLT observatory with Unit Telescopes and requires the same level of technical support for telescopes and instruments.

The final goal of the VLTI is to produce images with a few milliarcseconds resolution. Figure 8 shows a simulated point spread function when observing for eight hours with all four UTs. The result shows a very impressive albeit elongated PSF with a full width at half maximum (FWHM) of about 4×8 milli- arcsec for a wavelength of 2.2 μm. Having this goal in mind, one must not forget that for several years the results will be individual measurement points in the UV plane represented by curves like those in Figure 9. However, this does not diminish the scientific content of these results. The full scientific potential of the VLTI in its different phases is described in [9] summarised by F. Paresce [8].

6. The Future

The scenario of VLTI observations described in the article will without any doubt provide a wealth of scientific discoveries but it still does not exploit the full capacity of the infrastructure at Paranal. The layout of the interferometric tunnel and of the VISA array allows combining more than three telescopes providing either an even better coverage of the UV plane or the operation of different instruments at the same time.

Therefore, the four final Delay Line Systems and all remaining Auxiliary Telescopes for a total of 8 ATs shall be installed for VLTI operations. The completion of the final phase will allow VLTI observations with 28 simultaneous baselines. The planning also has to include new, the second-generation, instrumentation allowing the combination of six to eight telescopes and at the same time providing a dual feed facility for each pair of telescopes.

Beyond the fully equipped VLTI there have to be kilometric arrays with 8+ m telescopes in order to drive the angular resolution into the sub-milliarcsec range and to improve the sensitivity well beyond K = 20. The VLTI will be the stepping stone towards these observatories.

References

[1] Bonaccini, D., Rigaut, F., Glindemann, A., Dudziak, G., Mariotti, J.-M. and Paresce, F. 1998, *Proc. SPIE* **3353**, 224–232.

[2] Coudé du Foresto, V., Perrin, G., Mariotti, J.-M., Lacasse, M. and Traub, W.A. 1996, *Integrated Optics For Astronomical Interferometry, Grenoble,* P. Kern and F. Malbet eds., 110–125.

[3] Derie, F., Brunetto, E. and Ferrari, M. 1999, *The Messenger* **97**, 12–13.

[4] Ferrari, M. and Derie, F. 1999, *The Messenger* **97**, 11.

[5] Glindemann, A. and Lévêque, S. 1999 *VLT Opening Symposium,* in press.

[6] Kervella, P., Coudé du Foresto, V., Traub, W. A. and Lacasse, M.G.1999, *ASP Conf. Series XX,* 51.

[7] Leinert, Ch. and Graser, U. 1998, *Proc. SPIE* **3350**, 389–393.

[8] Paresce, F., et al. 1996, *The Messenger* **83**, 14–21.

[9] Paresce, F., Ed. 1997 *Science with the VLT Interferometer.* Springer-Verlag.

[10] Petrov, R., Malbet, F., Richichi, A. and Hofmann, K.-H. 1998, *The Messenger* **92**, 11–14.

[11] Quirrenbach, A., Coudé du Foresto, V., Daigne, G., Hofmann, K.-H., Hofmann, R., Lattanzi, M., Osterbart, R., Le Poole, R., Queloz, D., Vakili, F. 1998, *Proc. SPIE* **3350**, 807–817.

[12] von der Lühe, O., Bonaccini, D., Derie, F., Koehler, B., Lévêque, S., Manil, E., Michel, A. Verola, M. 1997, *The Messenger* **87**, 8-14.

E-mail: aglindem@eso.org

Laser Guide Star Facility for the ESO VLT

D. BONACCINI, W. HACKENBERG, M. CULLUM, M. QUATTRI, E. BRUNETTO, J. QUENTIN, F. KOCH, E. ALLAERT, A. VAN KESTEREN

European Southern Observatory

1. Introduction

ESO has been studying the possibility of introducing a Laser Guide Star Facility (LGSF) for the VLT to serve the adaptive optics (AO) instruments foreseen on the UT3 telescope of the Paranal Observatory: NAOS-CONICA and SINFONI.

Although full project funding, according to the ESO Long Range plan, will only start in 2001, we have performed a comprehensive feasibility study, with some innovative developments, especially on the possible injection of the laser light through a single-mode fibre (see the following article). The LGSF concept is the basis of this article.

The LGSF is foreseen as an add-on to the VLT telescope, able to create an artificial guide star in the mesospheric sodium layer, at 90 km average altitude. The LGSF would be used as a slave system to the AO systems, to produce an artificial reference star for the wavefront sensor, close to the observed object, whenever necessary. Figure 1 illustrates how the baseline LGSF concept would be implemented on the VLT.

The activities reported here have been carried out at ESO, with the enthusiastic scientific collaboration of the Max-Planck-Institut für Extraterrestrische Physik (MPE) in Garching,. MPE has built the Calar Alto Laser for the ALFA system (Davies et al, 1999).

The definition of the LGSF is at the conceptual design stage, with a solid baseline solution explored in detail and two open options: the final choice for the laser, and the use of a fibre relay for the laser beam instead of a mirror system. The final choices will be made during the LGSF Conceptual Design Review.

This article gives an overview of the conceptual design we are currently working on.

2. Project Rationale

The most important limitation of current NGS-AO systems, is the scarcity of a good reference star for the wavefront sensor (WFS) to exploit the full potential gain of the adaptive optics loop. The NGS should be bright enough to overcome both sensor read-out and photon noise. If it lies outside of a small field, optimum correction cannot be achieved, due to anisoplanetism effects.

To minimise the former, wavefront sensors with a high quantum efficiency and very low read noise are required. Thus photon noise is the only unavoidable contributor to the WFS noise. Even so, with Natural Guide Stars (NGS) the performance in the K-band of a medium-sized AO system drops significantly when $m_V \geq 15$. Figure 2 shows the expected K-band Strehl performance for a 60-element curvature system with the VLT as a function of NGS magnitude and its angular distance from the science target. Note that Strehl curves depend by the seeing at 6th power. Our analytical computations are for 0.66" seeing at 0.5 μm, 6 msec τ_o, and 0.4 Strehl contribution from field anisoplanatism at 20" elongation, in K-band.

The analytical simulations allow a parametric exploration of the AO performance. Although this is less accurate than a full numerical simulation, the results are according to our estimates accurate to within 10-15%, and serve well the purpose of this discussion. The effect of anisoplanatism on AO systems is very evident in Figure 2. For example, a 10th magnitude NGS which is 25 arcseconds away from the science target

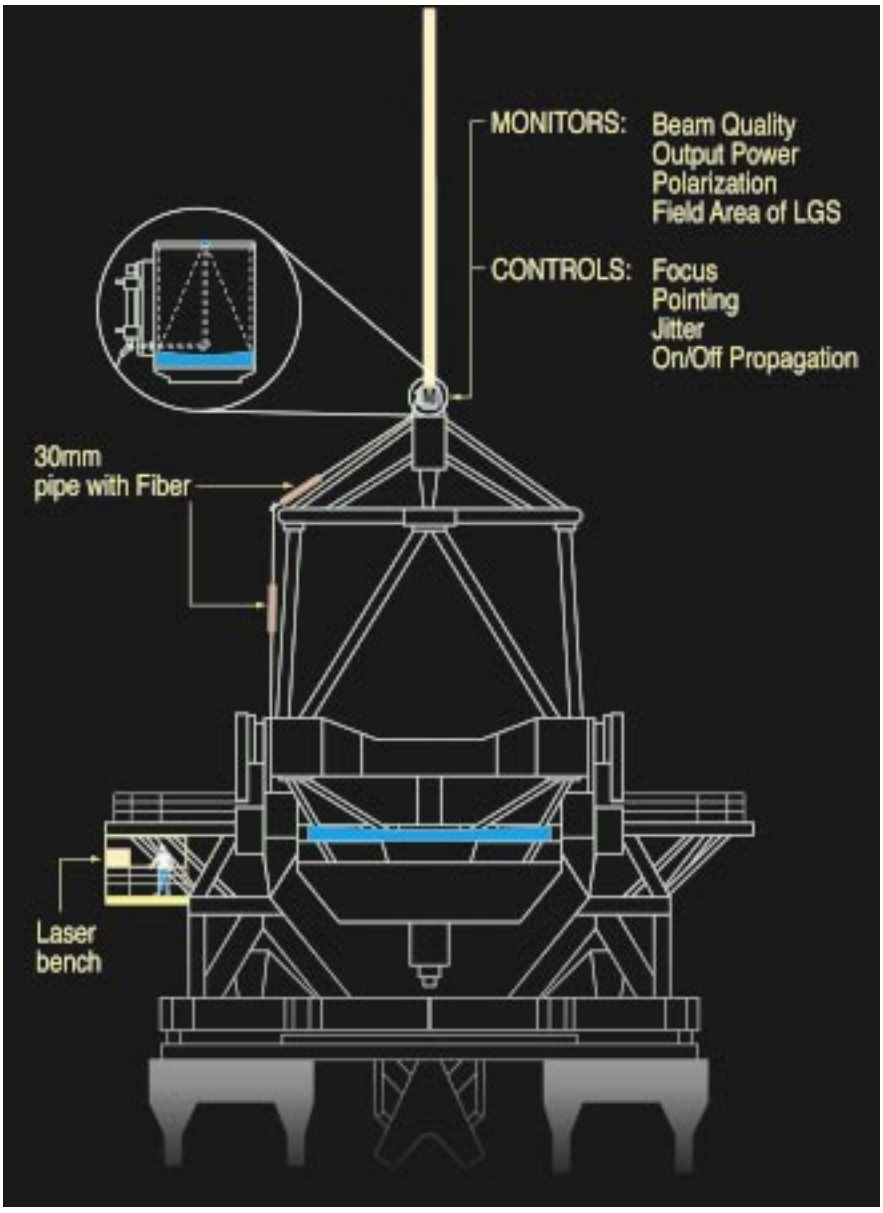

Figure 1: Layout of the LGSF. The laser and its controls are mounted under the Nasmyth platform, in a well-insulated laser room. The laser beam is relayed to the 50-cm-diameter launch telescope located behind the UT secondary mirror.

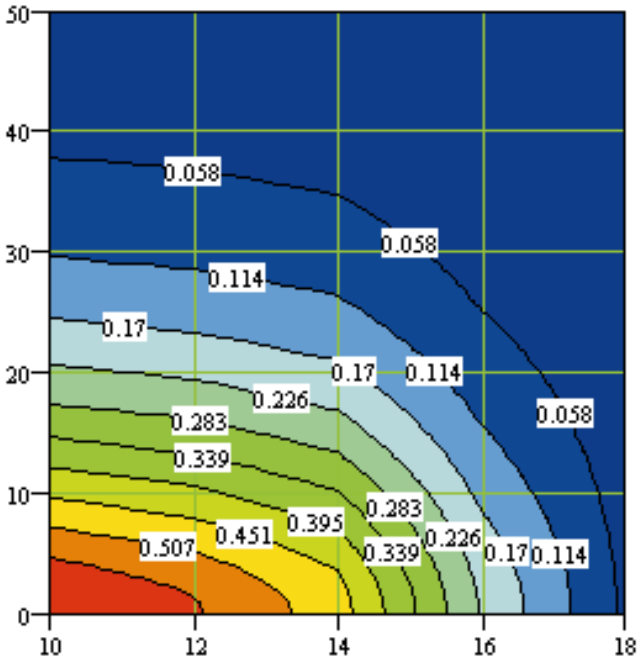

Figure 2: K-band iso-Strehl curves, computed for a 60-element curvature system, vs NGS magnitude (x-axis) and elongation between science object and NGS (y-axis, arcsec).

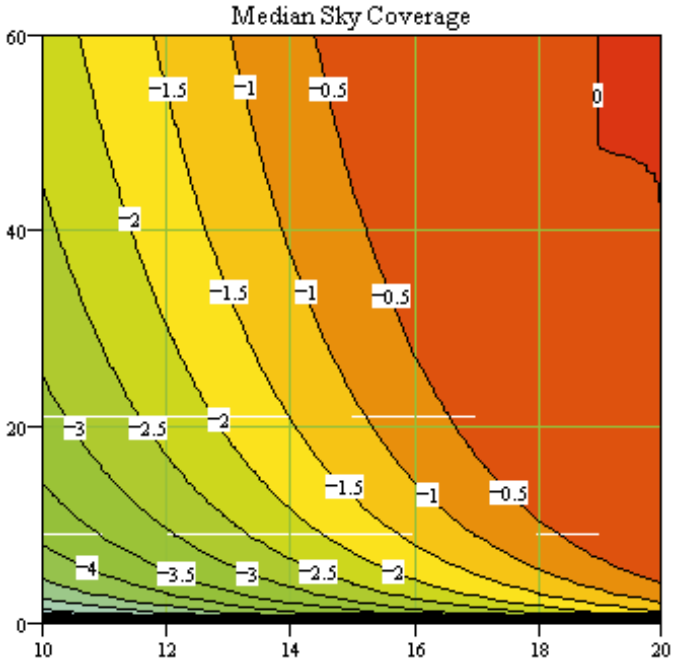

Figure 3: Logarithmic iso-probability curves for NGS. V-band NGS magnitude on the horizontal axis, NGS elongation from the science object in arcsec, on the vertical axis.

gives the same Strehl ratio as a 17th magnitude NGS on-axis.

The scientific justification of the LGSF comes from sky-coverage considerations. Put in simple terms, we need the answer to the question: 'what fraction of the sky can be observed with AO, and how many of my objects can be observed?' (Le Louarn et al., 1998, Di Serego Alighieri et al., 1994) The requirement of a relatively bright NGS, at short distance from the science object, limits the use of AO systems. The higher the Strehl Ratio required the greater the limitation. Figure 3 shows the median sky coverage iso-probability curves for a NGS plotted on a logarithmic scale.

Using a LGS, the reference signal for the AO wavefront sensor can be made equivalent to that of a NGS of $m_V \cong 9.5$ with seeing-limited diameter. It is rather like providing the telescope with a headlight, enabling the AO system to find a reference star wherever the telescope points. This opens the possibility of observing many more extragalactic targets than with a NGS-AO system. Two problems still prevent us reaching complete (100%) sky coverage: (a) the 'focus anisoplanatism' or cone effect (Tyler, 1994), and (b) the intrinsic indetermination of the image motion (tip-tilt) signal. The cone effect, for an 8-m telescope in the Near Infra-Red (NIR), and one single LGS, gives an unavoidable but tolerable reduction of the Strehl performance.

The tilt problem can be overcome by using a natural star in the field in addition to the LGS. The image blur is corrected using the LGS, the image motion (tip-tilt) using a NGS. The NGS for tip-tilt can, however, be much fainter and typically 2.5 times further away than a high-order NGS reference.

The ultimate sky coverage and AO performance depends largely on the tip-tilt sensor and is one of the reasons why ESO has put considerable effort to develop a high-performance tip-tilt correction subsystem, the so-called STRAP system. We will report on the STRAP system in a next issue of *The Messenger*.

The K-band iso-Strehl contours for a LGS-AO 60-element curvature sensing system are shown in Figure 4. The NGS magnitude and elongation axis refer to the tip-tilt reference star. The LGS is assumed to be pointed close to the science target. Compared to Figure 2, the gain in sky coverage is very evident even though the cone effect limits the maximum achievable Strehl. There is an even larger gain if one looks at the encircled energy improvement for a spectrograph (Le Louarn et al., 1998, Bonaccini, 1996).

Figure 5 combines the information contained in Figures 2 and 4, and shows the overall sky coverage (combining NGS magnitude and elongation) achieved with a given Strehl ratio, for NGS-AO and LGS-AO systems. The simulated system corrects 80 Karhunen-Loewe modes[1]. Using a LGS-AO,

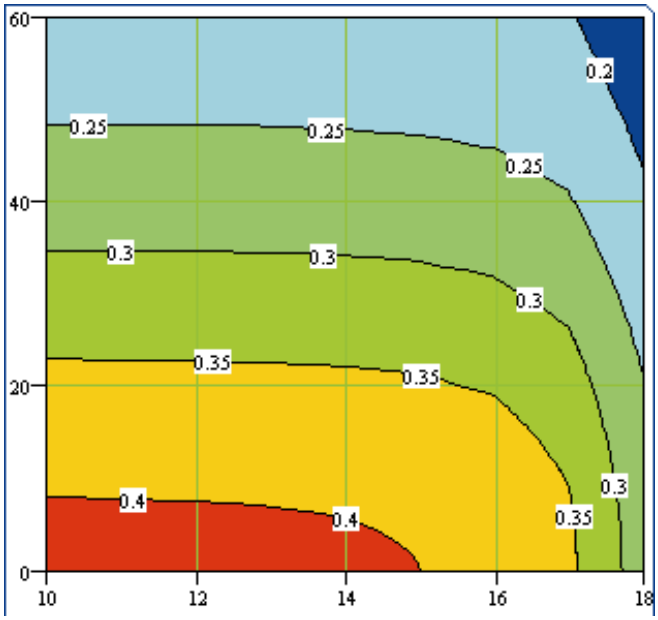

Figure 4: K-band iso-Strehl curves, for a 60-element curvature sensing AO system with a LGS, using a tip-tilt natural guide star. The NGS V-magnitude and elongation (arcsec) from the science target are the horizontal and vertical axes respectively. This plot should be compared with Figure 2.

[1]Karhunen-Loewe modes: they are an orto-normal basis for the expansion of the wavefront. They are often used in AO systems, as the modes are also statistically independent (see e.g. Adaptive Optics in Astronomy, p. 31, F. Roddier ed., Cambridge Press University 1999).

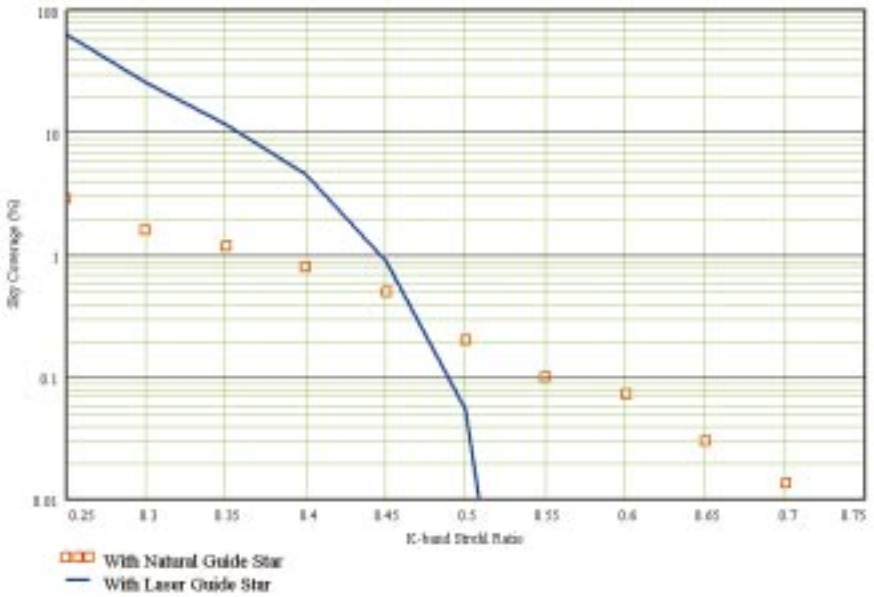

Figure 5: Sky coverage of an AO system correcting 80 Karhunen-Loewe modes, as a function of the K-band Strehl Ratio. The model atmosphere is as described in the article. NGS and LGS curves are plotted. The assumed single sodium LGS has a $m_V = 10$ and 1 arcsec FHWM. The saturation of the LGS curve at SR = 0.52 is due to the cone effect: Irrespective of how good the tip-tilt reference signal is, higher Strehl ratios are not possible.

the maximum K-band Strehl obtainable is 0.52 in our example, and this is seen in the saturation of the LGS-AO sky coverage curve. The sky coverage for a Strehl Ratio < 0.45 in K-band is always larger than NGS-AO in this configuration.

The LGS-AO system foreseen for the VLT will not reach Strehl ratios much greater than 40% in K-band, due to the cone effect. Note that the PSF core achieves the resolution of the diffraction limit (0.057″ in K-band), therefore the spatial information can be recovered. The images may be further boosted using post-processing techniques such as deconvolution if necessary (Conan et al. 1998, Christou et al., 1999). Figure 6 shows the long-exposure Modulation Transfer Function (MTF) for the uncorrected seeing, for the LGS-AO and for the 'perfect' telescope. The LGS-AO system allows the attenuation of all the spatial frequencies transmitted by the telescope to be restored by post-facto deconvolution.

Techniques to reduce or remove the LGS cone-effect are being studied at various institutes, for example by using multiple guide stars (Fried and Belsher, 1994), or with a hybrid system where the low orders are corrected with the NGS, the remaining high orders with the LGS. These will be necessary for visible AO compensation on future extremely large aperture telescopes.

3. Project Status

ESO's Scientific Technical Committee has confirmed the scientific relevance of the LGSF, and asked to prepare a proposal for equipping with it the VLT Unit Telescope hosting AO systems. A baseline solution has been studied in detail during 1998, for the subsystems of the laser, the beam relay and the launch telescope. The preliminary design activities were frozen in February 1999, except for the studies on a single-mode fibre relay. This was to allow the feasibility of the fibre relay system to be thoroughly investigated before proceeding further.

The past months have been spent on the development of a prototype single-mode fibre relay system, from the laser output to the launch telescope. The fibre-optics industry has been involved in order to have access to state-of-the-art fibre production technologies. We have used a 532 nm, 5W Continuous Wave (CW), *Verdi** laser from Coherent GmbH, to do the laboratory experiments and studies. The results of our studies and tests so far indicate that the fibre relay solution, although not as easy as it seems, is feasible and also very attractive. We plan to conclude this development with working fibre relays in June 2000, and resume LGSF detailed design activities in the summer 2000. Assuming that funding is forthcoming as planned, one could envisage commissioning of the LGSF on the VLT by the end of 2003.

A brief explanation of the baseline LGSF design is given below and represents the present conceptual design around which we are working. It is likely to be modified somewhat during the preliminary and final design phases.

4. High Level Operational and Functional Requirements

The LGSF is seen by the AO instruments as a telescope server facility. It is therefore compliant with the VLT requirements/standards and integrated hardware and software with the telescope environment. The AO systems (NAOS and MACAO) on UT3 will be able to send basic commands and receive the diagnostic status.

The LGSF will never take independent initiatives except for safety reasons, such as air-traffic alerts from the dedicated monitoring camera. In this case, it notifies to the clients that it is going to shut down the beam propagation before doing it.

Concerning light pollution from the LGS, work is in progress to determine it quantitatively (Delplancke et al., 1998). The monochromatic laser beam scattering does not disturb the IR instruments. The operational scheme proposed is to create an area-of-avoidance around the laser beam: the LGSF monitors the pointing of the other Paranal telescopes, and creates an alert status

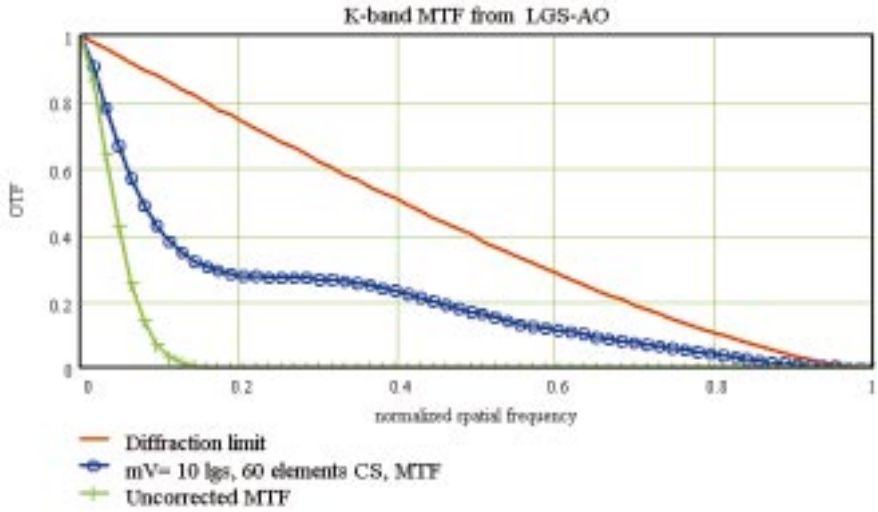

Figure 6: MTF in K-band, for the VLT with uncorrected seeing, LGS-AO correction, and the perfect telescope

*The *Verdi* is an all-solid-state diode pumped Nd:YVO4 laser, recently produced by Coherent.

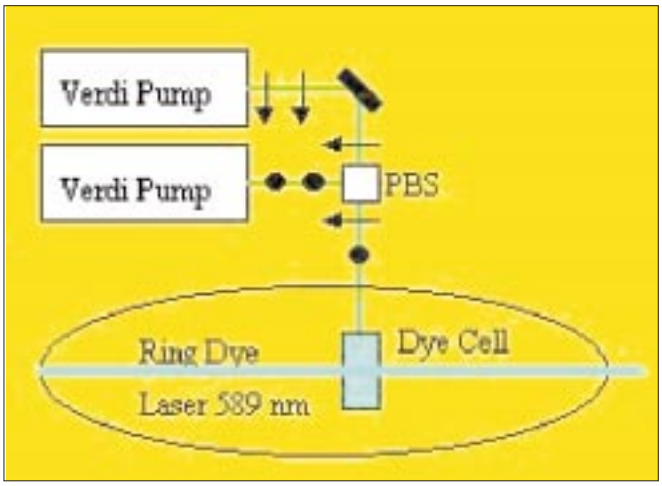

Figure 7: Baseline laser conceptual scheme. Two solid-state pump lasers are combined in a single beam, 20W at 532 nm, pumping a ring-dye resonator laser, using Rodhamine 6G as dye and servo-tuned to 589 nm.

when another telescope is pointing close to the cone-of-avoidance. The actions to take in this case are still to be decided.

The LGSF is required to produce a m_V = 9.5 equivalent artificial reference star with a FWHM of 1.5″ (seeing limited as goal). For median Paranal seeing, down to 60 degrees zenith distance, a 6.5W CW Sodium laser will serve the purpose. For worse seeing conditions, or in the presence of thin cirrus clouds, a laser power in the range of 10W would be preferable.

The LGS has to be independently pointed within 20″ from the defined optical axis of the VLT, with a relative pointing accuracy of 0.3″. Automatic focussing of the LGS on the sodium layer will be performed, up to zenith angles of 60 degrees.

The safety measures of the LGSF will comply with the Paranal observatory strict safety regulations, Chilean law, and the FAA regulations as applicable in Chile.

5. LGSF Baseline Design Solution

The baseline solution study has divided the LGSF into three different subsystems: (a) the laser room, including the laser and its servo-controls, (b) the beam relay and (c) the launch telescope with its diagnostics. We report here briefly on (a) and (c). A companion article in this issue describes the prototype fibre beam relay subsystem in detail. We will report in future issues of *The Messenger* design details on subsystems (a) and (c).

We propose to use a relatively low-consumption laser (4KW), and to build a thermally stabilised laser room under the Nasmyth platform of UT3. The laser choice takes into account commercial availability, support, stability and servicing issues, so as to minimise the LGSF operation and overhead costs.

The baseline solution for the relay of the 20-mm-diameter laser beam from the laser room to the launch telescope could in principle use flat mirrors in a shielded light-path. The laser beam would be hidden behind one of the secondary mirror (M2) support spiders when crossing above the primary mirror. The mirror relay system was investigated in detail. It is cumbersome and difficult to implement in practice. Turbulence effects in the relay path as well as dust contamination and thermal effects on the optics, can degrade the LGS quality considerably. Air tightness, several servo-controls and also frequent maintenance would be necessary.

The alternative solution for the laser relay we propose uses a 30 m long, single-mode optical fibre. This is an innovative solution and not easy, given the power densities involved: one Watt of injected power in a 5.5 micron core fibre corresponds to a power density of 4 MW/cm^2. We have found a viable solution to this problem. It will deliver a diffraction-limited beam at the launch telescope input, with >70% throughput. The use of a single-mode fibre would result in savings in laser power, money and manpower.

A 50-cm diameter laser launch telescope is located behind M2. The aperture is dictated by the optimisation of the LGS beam diameter for the best Paranal seeing conditions. The projected beam diameter will be adjusted to the actual seeing conditions. The telescope is a polychromatic reflective design, which allows the LGS to be positioned within a 1-arcminute field on the sky, with a visible monitoring camera. Figure 1 shows a schematic diagram of the foreseen set-up.

The level of automatism to be built into the LGSF is large, in order to allow routine and reliable operation at the VLT. This increases the initial cost and complexity of the facility, but we believe it will prove highly beneficial later, during operation. A number of servo-systems and automatic computations are planned, based on dedicated hardware/software.

6. Baseline Laser and Laser Options

Only a complex micro-macro pulse modulation scheme would allow slightly greater flux returns from the mesospheric sodium than a CW laser (Milonni and Fugate 1997). Considering that CW lasers are intrinsically more stable and simpler, that coatings for CW lasers

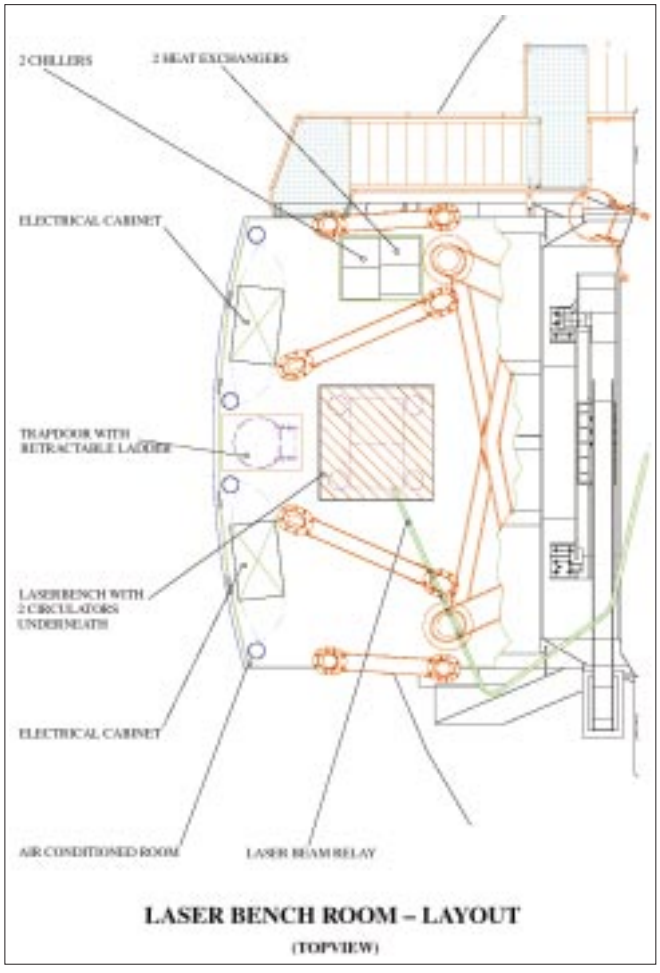

Figure 8: Layout of the laser room designed, with the laser optical table and the necessary accessories. The room is thermally isolated and conditioned.

are less demanding, and that CW lasers safety issues are easier to handle than for pulsed lasers, we are concentrating on CW lasers solutions.

The baseline laser is a modified version of a commercial product from Coherent, made of two 10W Nd-$YV0_4$ CW Verdi diode laser pumps at 532 nm, combined into the Coherent jet-streamed ring dye resonator model 899-21, using Rhodamine 6G as dye. The general advantages of solid state lasers as compared to ion-lasers for pumping, are the much higher conversion efficiency and greater compactness.

In addition the wavelength of frequency-doubled light from Nd-doped laser crystals is around the maximum of the absorption spectrum of Rh6G, whereas the light of argon-ion lasers is clearly off the absorption peak.

This laser configuration delivers > 6.5W of CW power on a 20 MHz FWHM TEM_{00}* line, or a LGS with $m_V \cong 9$ after beam conditioning. A similar ring-dye laser has proven to be robust and stable during the past years at Calar Alto.

The laser line is broadened to 500 MHz, to avoid both the saturation of mesospheric sodium atoms and non linear effects in the fibre.

We have the capability of doubling this power in the future, by adding two such laser systems on the same optical table. This scenario would produce 13W CW of sodium laser power, and would use two independent single-mode fibres to relay the beams to the launch telescope. The orthogonally polarised beams at the fibre output would be combined in the launch telescope.

For safety and operational stability reasons, the laser bench would be installed in an isolated room underneath the Nasmyth platform. This room also contains the dye solution chiller, the pump laser heat-exchanger, two electronics cabinets and workspace for maintenance work (Fig. 8).

The dimensions of the laser room allow convenient access to the optical table. The room is temperature stabilised and supplied with filtered air to avoid contamination of the optics. In order not to impact on the telescope seeing the laser room is thermally insulated, with the outer walls at the same temperature as the air in the telescope enclosure.

Vibration, air turbulence, temperature variations and dust contamination directly influence the line width as well as the power and beam-pointing stability of a jet-streamed dye laser. The dye-laser oscillator therefore is installed in a fixed spatial position on a rigid optical table that de-couples the laser head from vibrations, e.g. when the telescope is moving.

Figure 8 shows the layout of the laser room together with the accessory devices. The laser optical table size is chosen so as to allow a later addition of a second 6.5W laser. The room is thermally isolated and conditioned.

The total mass of the laser bench equipment is estimated to be 1.3 metric tons. We estimate the entire laser room to weight not more than 4 tons. An analysis of the static and dynamic impact of the laser room mounted under the Nasmyth platform on UT3 has been done and found to be negligible. The power, communication and cooling budgets have indicated that one VLT Service Connection Point (SCP) will be sufficient for the laser room.

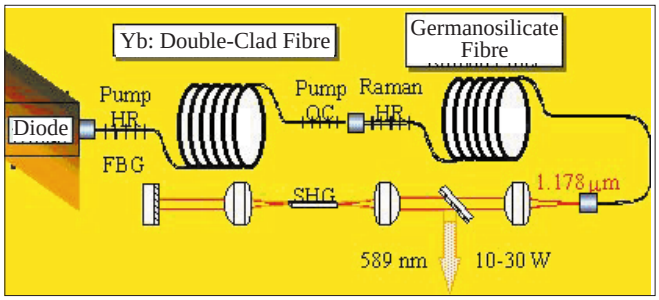

Figure 9: Fibre laser layout. The pump laser is a diode-pumped double-clad Yb-doped fibre that outputs 1.1137 µm. The Raman is a high-delta germanosilicate single-mode fibre, which is directly coupled to the pump fibre. Feedback for both the pump and Raman fibres are provided by FBGs. The second harmonic of the 1.178 µm first Stokes is generated within the fibre Raman laser cavity, and is ejected by a dichroic mirror. (Courtesy J. Murray, LiteCycles Inc.)

7. Alternative Laser Choices

Two alternative laser choices are currently being monitored.

One solution, in which the fibre itself is the laser, is being studied by Litecycles Inc. (Murray et al., 1998). This is still in the feasibility phase and it has

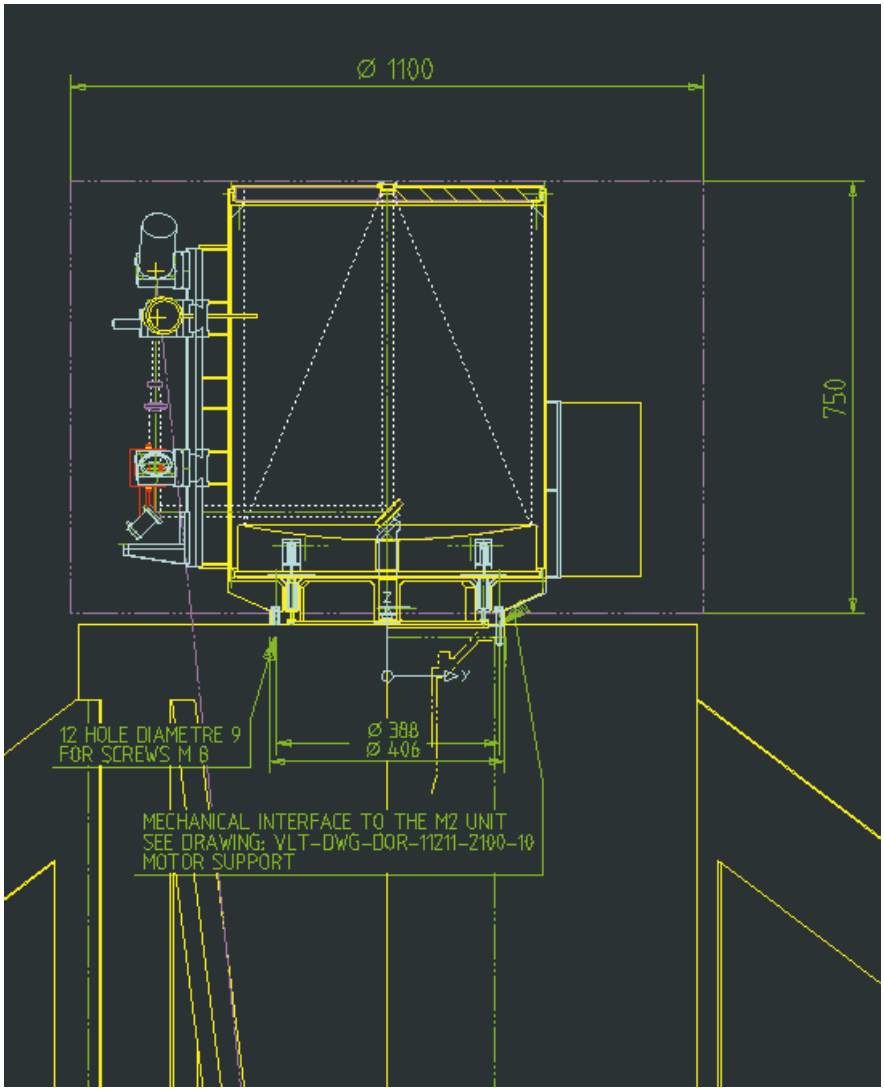

Figure 10: The launch telescope is a 25X beam expander. It is mounted behind the M2 unit, together with its accessory beam monitors: power, alignment, polarization meters, and beam pointing/focussing servos. Two cameras are present, one to monitor the LGS in the field, and one for air-traffic surveillance.

*TEM_{00} is the fundamental Transversal Electromagnetic Mode of the resonator.

recently attracted the interest of the Gemini AO project as well. The concept is shown in Figure 9.

Two 100W CW laser diode-bar arrays are used, efficiently coupled in a double-clad Yb-doped fibre which outputs >50% of the input power at 1.1137 μm from the single-mode fibre core. The Yb-doped fibre is fusion-spliced with a single-mode germanosilicate fibre 1 km long. The Stimulated Raman Scattering (SRS) effect in this long fibre is used to stretch the wavelength and tune it to 1.178 μm, i.e. twice the 0.589 μm of the D_2 sodium line, by the use of fibre Bragg gratings (FBG) written on the fibre and servo-tuned by piezos. The fibre output beam is focused on a second harmonic generation crystal (SHG) for intracavity doubling, which will convert the 1.178 μm photons to 0.589 μm. The longitudinal mode spacing of such a long fibre Raman laser is 100 kHz, giving a truly broad-band excitation of the mesospheric sodium. The goal for the line FWHM is ≤ 2 GHz, and the CW output power should be in excess of 10W CW, with a goal of 30W. However, an unpolarised sodium 2 GHz laser line would return about half the flux of a 20 MHz FWHM line. A 10W broad-band laser would therefore be equivalent to 5W of 'narrow-band' power. Perceived risks of this technology are the larger than expected linewidth, excessive non-linearity (Stimulated Brillouin Scattering) losses and a lower than expected efficiency of the intracavity SHG crystal. We are taking advantage of our models of the non-linear effects, developed for the fiber relay studies, to further investigate this laser design.

The great advantages of this solution are that the single-mode fibre output plus frequency doubling crystal give a high beam quality, the long fibre length (1 km!) allows the laser source to be placed far away from the telescope, in a VME-rack sized box. If this laser would be commercially available, it would be the ideal solution.

The second laser choice under investigation is a recent development at MPE in Garching. It is a two-stage laser with a seeded dye-laser amplifier which would deliver at least 10 W CW with 500 MHz line width. This laser would give an equivalent LGS magnitude $m_V = 8$.

8. Launch Telescope

The input interface to the launch telescope (LT) is a collimated beam 20-mm in diameter. The output is a diffraction limited spot at 90 km altitude with the possibility to focus it between 70 and 200 km. The LT optical quality specification is to have a Strehl ratio >0.95 within 10 arcsec of field radius, and with 80% encircled energy diameter of 0.7" within 1 arcminute field radius. This is required to ease the alignment tolerances and to have a CCD monitoring camera looking at the surrounding sky field (notching out the LGS). The launch telescope is thus a 25X beam expander. We have explored a reflective solution based on a two-parabolic-mirror stigmatic design and verified the feasibility of its opto-mechanical tolerances. Lightweight mirrors can be used; the total weight of the LT and its structure is estimated to be 80 kg.

A wedged, anti-reflection coated exit window provides shielding from turbulence and dust, and a 10^{-3} laser flux return, to monitor the exit beam quality and power. We will also monitor the beam polarisation state and its frequency spectrum. The volume from the fibre end to the exit window is airtight.

Figure 11: View of the laboratory setup where the fibre experiments have been carried out. The setup allows the measurement of the spectrum, power and propagation properties of the laser beam. The injection, fibre output and SBS return beams can also be characterised.

The space available behind the UT3 secondary mirror is limited and we are forced to expand the beam by a factor 25 within 600 mm of design space. The current design is shown in Figure 10. It delivers a very good performance with a central obscuration of 0.7% in area for a 2-arcminute-diameter field (see Table 1). However it has tight tolerances and requires an athermalised design: its feasibility has been checked. We will also have to introduce alignment diagnostics. The pointing has to be remotely controlled within a minimum range of 1 arcmin radius. Fast steering is also necessary to compensate the LGS jitter induced by the atmosphere on the upward-going 50 cm beam which differs from the downward path toward the collecting 8-m telescope. The expected rms jitter is 0.34 arcsec for the median Paranal atmosphere and therefore a fast steering range of ± 2-arcsec is specified. The steering signal is provided by the AO high order WFS that is looking at the LGS. The bandwidth of the steering device has to be better than 200Hz at –3dB.

The pointing and steering would be done at the level of the fibre output. The range of fibre motion is ± 0.79 μm for slow pointing with 0.1 μm precision, and ± 12 μm for fast steering. Commercial devices are available which meet these specifications together with their control electronics.

We plan to enclose the launch telescope and its liquid-cooled electronics in an aerodynamic wind-shield, behind M2 unit. The static and dynamic impact on M2 structural stability have been studied and shown to be negligible.

Conclusion

The conceptual design of the LGSF has been completed and the main interfaces with UT3 as well as the environmental and structural impacts have been assessed. Further optimisation will be carried out in the next phases. Laser beam relay system designs using both conventional optics and mono-mode fibre have been explored. This latter solution has many advantages

Table 1: Launch Telescope Design – Optical Performance

	Design Requirements / Value Achieved	
Field	10 arcsec radius	1 arcmin radius
Strehl Ratio at 589 nm	>0.95 / 0.99	-- / 0.975
80% Encircled energy diam. (“)	-- / 0.45	0.7 / 0.5

and we now feel confident that this solution can be adopted.

We have however to finish the tests of the final fibre-relay modules in the laboratory. A burn-in test is being discussed with MPE, to be performed with the 4.5W CW sodium laser at Calar Alto. After these tests have been satisfactorily completed, the detailed design activities for the LGSF can be resumed by the second half of next year, pending approval by the ESO management.

References

Ageorges N., Delplancke F., Hubin N., Redfern M. and Davies R.: "Monitoring of laser guide star and light pollution", *SPIE Proceedings* **3763**, in press, 1999.

Avicola et al.: 'Sodium Layer guide-star Experimental Results', *JOSA A*, Vol.**11**, 825–831, 1994.

Bonaccini, D: 'Laser Guide Star Adaptive Optics Performance Analysis', ESO Technical Report VLT-TRE-ESO-11630-1202, 1996.

Christou, J.C., Bonaccini, D., Ageorges, N. and Marchis, F: 'Myopic Deconvolution of Adaptive Optics Images', *The Messenger* No. **97**, 14, Sept. 1999.

Conan, J.M., Fusco, T., Mugnier, L.M., Kersale, E. and Michau, V: 'Deconvolution of Adaptive Optics Images with imprecise knowledge of the point spread function: results on astronomical objects', in ESO/OSA Topical meeting on Astronomy with Adaptive Optics: Present Results and Future Programs, p. 121, D.Bonaccini ed., 1998.

Davies,R, Hackenberg, W., Eckart, A., Ott, T., Butler, D., and Casper, M: 'The ALFA Laser Guide Star operation and results, accepted for publication in *Experimental Astronomy.*

Delplancke F., Ageorges N., Hubin N., O'Sullivan C.: "LGS light pollution investigation in Calar ALto" Proceedings of the ESO/OSA topical meeting on Astronomy with Adaptive Optics, Present Results and Future Programs – Sonthofen, September 1998.

Di Serego Alighieri, S., Bonaccini, D., Oliva, E., Piotto, G., Ragazzoni, R. and Richichi, A: 'Adaptive Optics for the Telescopio Nazionale Galileo', Technical Report No. 41, Astronomical Observatory of Padua-Asiago, 1995.

Fried, D.L. and Belsher, J.F.: 'Analysis of fundamental limits to artificial guide star adaptive optics system performance for astronomical imaging', *JOSA A*, Vol. **11**, p. 277, 1994.

Le Louarn, M., Foy, R., Hubin, N. and Tallon, M.: 'Laser Guide Star for 3.6 and 8m telescopes: performance and astrophysical implications', *MNRAS* **295**, 756, 1998.

Le Louarn, M, Hubin, N., Foy, R. and Tallon, M: 'Sky coverage and PSF shape with LGS-AO on 8m telescopes', *SPIE Proceedings* Vol. **3353**, 364, 1998.

Milonni, P. W. and Fugate, R.Q.: 'Analysis of measured photon returns from Sodium Guide Stars', in Proceedings of the ESO Workshop on Laser Technology for Laser Guide Star Adaptive Optics Astronomy, N. Hubin ed., p. 77, 1997.

Milonni, P.W., Fugate R.Q. and Telle, J.M.: 'Analysis of Measured Photon Returns from Sodium Beacons', *JOSA A*, Vol. **15**, p. 217–233, 1998.

Murray, J.T., Roberts, W.T., Austin, L. and Bonaccini, D.: 'Fiber Raman laser for sodium guide star', in *SPIE Proc.* Vol. **3353**, p. 330, 1998.

Tyler, G.A.: 'Rapid Evaluation of d0: the effective diameter of a laser guide star adaptive optics system', *JOSA A*, **11**, 325, 1994.

Viard E., Delplancke F., Hubin N. and Ageorges N.: "LGS Na spot elongation and Rayleigh scattering effects on Shack-Hartmann wavefront sensor performances", *SPIE Proceedings* **3762**, in press, 1999.

Viard E., Delplancke F., Hubin N., Ageorges N. and Davies R.: "Rayleigh Scattering and laser spot elongation problems at ALFA", accepted for publication in *Experimental Astronomy*.

E-mail: dbonacci@eso.org

VLT Laser Guide Star Facility Subsystems Design

Part I: Fibre Relay Module

W. HACKENBERG, D. BONACCINI, G. AVILA, ESO

The advantages of the LGSF fibre relay approach are twofold: (1) we avoid the cumbersome optomechanical relay, and (2) transfer a diffraction limited beam. The opto-mechanical relay system would require a sealed tube for the laser beam optical path to avoid turbulence and dust contamination, with air-tight sliding joints at the elevation axis, two servo-controlled steering mirrors to keep the optical alignment and several safety interlocks if the beam has lost alignment. Point (2) is very important, as much effort needs to be spent to ensure a good beam quality. Assuming the LGS is an extended object, the adaptive optics wavefront sensor error is proportional to the area of the LGS divided by its flux. As it is both costly and difficult to increase the laser power, all possible efforts have to be taken to minimise the LGS spot size, i.e. the laser beam quality. Some laser relay systems in other LGS projects are even considering incorporating active or low order adaptive optics in the laser beam relay optical path, to ensure a good outgoing beam quality.

Incidentally, injection of high laser power in a single-mode fibre is very useful in long distance fibre communication systems to save repeaters. In fact, much work has been done and literature is available on the subject (Tsubokawa et al., 1986; Cotter, 1982). However the successful injection of several watts of continuous wave (CW) visible laser power has not been demonstrated for long fibres. As we are concerned with a fibre length of 30 m for the VLT LGSF system, we have been able to achieve this in the laboratory and have also learned a few tricks in the process. A fibre relay (Figure 1) provides a very flexible solution and significantly simplifies the integration. It would also be readily applicable to multiple LGS systems needed for future high-order AO systems on large telescopes.

The potential causes of power losses in the fibre are:

1. Coupling losses from the laser beam to the fibre core. These include Fresnel reflections and laser to waveguide mode mismatches..

2. Extinction losses in the bulk material. In a 30 m long low-loss, pure fused silica fibre, the bulk losses from scattering and absorption are expected to be about 8%.

3. Scattering at the fibre core-cladding interfaces.

4. Mode conversion from low-loss trapped modes to high-loss cladding modes.

5. Stimulated Raman Scattering (SRS).

6. Stimulated Brillouin Scattering (SBS).

7. Four-wave mixing between forward and backward Stokes modes.

Points 1 and 6 are the most important causes of losses in our case.

The basic requirements of our fibre relay system (Fig. 1) are:

(i) stable throughput above 70 % over 30 m for 589-nm CW laser light in the multi-Watt regime

(ii) diffraction limited output for the smallest possible LGS spot size

(iii) polarisation preserving.

The latter allows the output of several fibres to be combined, and to circularly polarise the light for the optical pumping of the mesospheric sodium atoms. In order to achieve these requirements, three fundamental problems have to be solved:

1. Efficient coupling of a free-space laser beam into a small-frame optical fi-

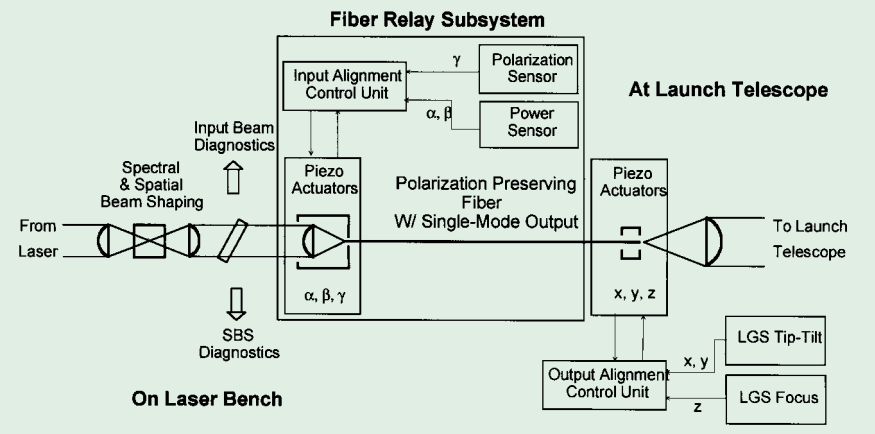

Figure 1: LGSF fibre relay subsystem layout. The fibre input is on the laser optical table, the output is at the launch telescope. The power and polarisation sensors at the fibre end are used to drive the alignment actuators at the fibre input.

bre. This demands an accuracy and long term stability of the order of a fraction of a micron.

2. Handling of high power densities at air-glass interfaces. The power density at the fibre core interface is in the order of several tens of MW/cm^2. This is above the damage threshold of high power anti. reflection coatings (0.5 MW/cm^2). A careful thermal management in the fibre connectors is therefore crucial.

3. Nonlinear effects. At high power levels the scattering processes become stimulated and influence both effective throughput efficiency and spectral purity of the transmitted light.

Three simple measures have been taken to overcome these problems: We have (i) maximised the area of the illuminated air-glass surface, (ii) maximised the effective cross-sectional fibre mode area and (iii) maximised the effective laser line width.

The limits are set by: (i) the numerical aperture of the fibre, (ii) the requirement of having single-mode output, (iii) the finite bandwidth of the mesospheric sodium excitation process.

Design of the Single-Mode Fibre and Input Coupling Unit

The input laser beam at the fibre-waveguide is assumed to be in TEM$_{00}$ mode, i. e. the lowest-order resonator mode. Gaussian beam propagation has to be considered in the design of the coupling optics and their tolerances, so that the mode fields of the input beam and of the optical waveguide optimally match. If we consider a fibre, which is single-mode over its entire length for a given wavelength, the field distribution of the guided fundamental mode can be approximated by a Gaussian. That mode field diameter increases not only with increasing core radius but also with decreasing numerical aperture. The latter is a measure of the light acceptance angle of a fibre. Restricting the waveguide losses due to bending and micro-bending to no more than 1% (minimum bend radius 10 cm) results in a minimum numerical aperture NA = 0.08. For operation as close as possible at the single-mode cut-off wavelength, the maximum fibre core diameter is 5.5 µm for light at 589 nm.

The linear loss coefficient of fibre with a core of pure synthetic fused silica is 0.003 m^{-1} at 589 nm. With antireflection coatings on the fibre ends the theoretical maximum throughput of a 30-m fibre becomes 90%. Since the damage threshold of high-power antireflection coatings is around 500 kWcm^{-2} in the visible, the air-glass surface has to be enlarged at the fibre ends. For this we use a fused silica window, either in optical contact with the fibre or fusion spliced (Fig. 2). To avoid Fabry-Perot effects between the fibre ends, the output surface has to be wedged.

The state of polarisation at the exit of a polarisation-preserving fibre is stable and linear if the input state of polarisation is stable, linear and aligned to the birefringence axis.

For focusing the free-space laser beam onto the fibre we use an aspheric lens, mounted and pre-aligned to the fibre input inside an athermalised housing. We first carried out an analytical optical design, and then verified numerically the coupling efficiency using CODE V. The experiments reported in the last section of this article confirm the design model. Figure 3 shows the dependence of coupling efficiency on decentre between the optical axis and the fibre axis, for various angles of incidence. For optimum coupling efficiency, the incoming laser beam has to be shaped so that the waist diameter of the focal spot produced by the external lens exactly matches the fibre mode field diameter. In our case this is 15 % larger than the nominal core diameter.

Aligning the coupling unit with respect to the incoming beam requires three degrees of freedom. A power and polarisation sensor analysing the fibre output will provide the error signal for a piezo-based servo-loop stabilisation of the optimum injection.

In order to prevent the single-mode contaminating cladding modes (i. e. higher order modes that are not guided by the core), as well as for an optimal heat removal, the fibre connectors have to be fabricated out of glass that matches the fibre core index. A protective and flexible stainless steel sheath is required over the entire length of the fibre.

Critical Fibre Input Power Density

The most important nonlinear loss process in the fibre is stimulated Bril-

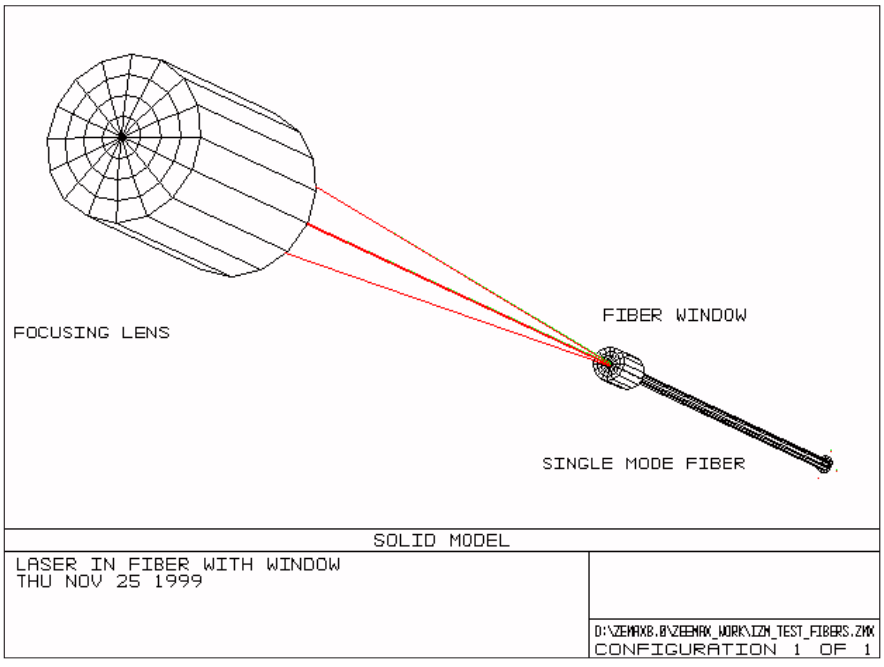

Figure 2: The glass-air interface area of the fibre is enlarged using a window of the same material of the fibre core. The window is either spliced to the fibre, or optically contacted. Both fibre ends have a fibre window.

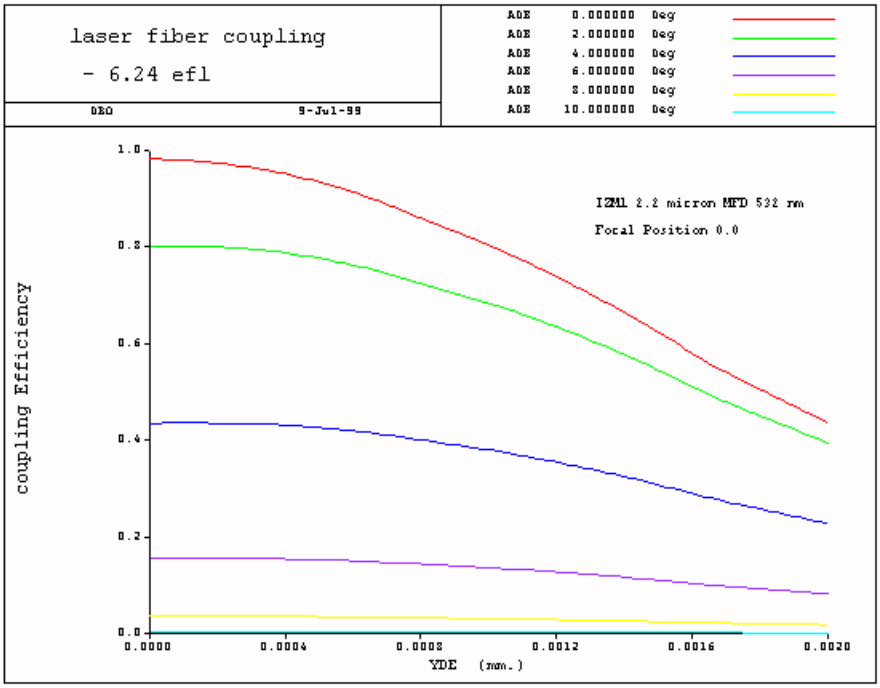

Figure 3: Coupling efficiency for the designed optics. The coupling efficiency is plotted against decentring error between the laser beam and the waveguide axis. Several curves for different beam incident angles are shown.

louin scattering (SBS). This is the scattering of light by sound waves that are created in the fibre by the incident light due to electrostiction[1] in a phonon-photon interaction process. The standing acoustic waves create a regular density grating along the fibre. As a consequence of the selection rules in the waveguide, only scattering in the backward direction occurs in the fibre due to SBS.

[1]The type of piezoelectric effect where the induced material deformation depends on the square of the electrical field amplitude is called electrostiction.

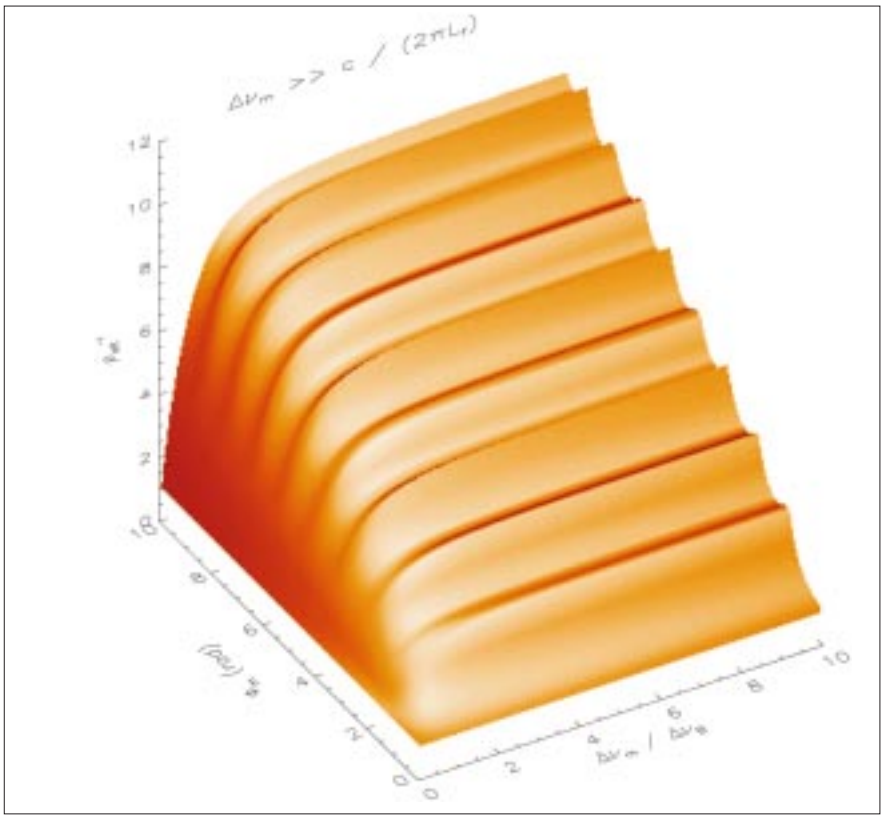

Figure 4: Increase of the SBS threshold pump power, ρ_{eff}^{-1}, under multiline excitation, normalised to the single-mode threshold, as a function of the frequency modulation bandwidth to Brillouin linewidth ratio $\Delta\nu_m / \Delta\nu_B$, and the achievable peak phase shift ϕ_m. It has been assumed that the pump coherence length is much smaller than the fibre length, L_f, and that the frequency modulation is achieved with a single transverse electro-optical modulator.

Energy conservation demands that the amplified backward light (the Stokes wave) is shifted downwards in frequency with respect to the incoming (pump) light, by an amount equal to the acoustic frequency of the material excited. The Stokes line frequency shift is in our case about 30 GHz, and the spectral (or Brillouin) width of the backscatterd light is $\Delta\nu_B$ = 110 MHz FWHM.

The effect of SBS is that a fraction of the light injected in the fibre is sent backwards, shifted in frequency and with a characteristic linewidth of $\Delta\nu_B$. SBS is a non-linear effect and its onset is abrupt, once the pump laser power exceeds a certain threshold. This threshold depends on the fibre material and the frequency distribution of the pump. Solving the differential equations for the Stokes and pump intensities in the steady regime, we obtain a critical pump power[2] of 720 mW. This is for single-frequency, narrow-band sodium light injected into a 30-m single-mode fused silica fibre whose parameters are optimised for minimum power density in the core. In an equivalent polarisation-maintaining fibre the SBS threshold power is reduced by a factor of two due to polarisation scrambling.

As long as the coherence length of the pump light is much smaller than the fibre length, the frequency-dependent SBS gain coefficient is given by the convolution of the pump spectral profile and the SBS gain profile. This is a key point. As it means the critical pump power can be increased, if the effective laser linewidth is broadened, for example by means of phase or frequency modulation of the laser beam.

If we assume a narrow-band single-frequency CW laser source whose effective linewidth is broadened externally by a simple phase modulation scheme (see below), then the pump spectrum will consist of several longitudinal modes equally separated by a frequency $\Delta\nu_m$ corresponding to the modulation bandwidth. The modes of the Stokes wave will be also equidistant, separated by the same distance $\Delta\nu_m$. If again the pump coherence length is much smaller than the characteristic SBS interaction length, i.e. for fibres more than a few metres long, each of the Stokes modes interact with all of the pump modes, and vice versa. Since the interaction strength is determined by the de-tuning from resonance, the interaction bandwidth is limited to the Brillouin linewidth $\Delta\nu_B$. In other words, if $\Delta\nu_m >> \Delta\nu_B$ then the SBS source polarisations generated by different pump modes are not phase matched and do not interfere coherently, as each pump mode generates its own Stoke wave. In this situation and with equal power pump modes, the resulting SBS gain is

[2]Here defined as that input power for which the total SBS power equals 1% of the pump power at the fibre entrance.

reduced by a factor equal to the number of pump modes. This reduction of the SBS gain in case of multimode excitation can be summarised in a factor ρ_{eff}, averaged over all modes and normalised to the SBS gain for a single pump mode with the same total intensity and intrinsic linewidth. In general, ρ_{eff} will also depend on the relative power distribution within the pump modes. For a frequency modulation scheme with a transverse electro-optic light modulator (see below), the relative strength of pump mode *j* is given by the square of the Bessel function of order *j*, evaluated at the peak phase shift ϕ_m which can be achieved with the modulator. The inverse of ρ_{eff} (or the effective increase in the critical input power) is shown in Figure 4 as a function of the externally applied peak phase shift and the frequency modulation bandwidth to Brillouin linewidth ratio. It can be seen that at ϕ_m = 1.5 rad, 2.7 rad, 3.8 rad (etc.) local maxima in ρ_{eff}^{-1} appear. Those extremes correspond to the most equal power distribution within the generated pump modes.

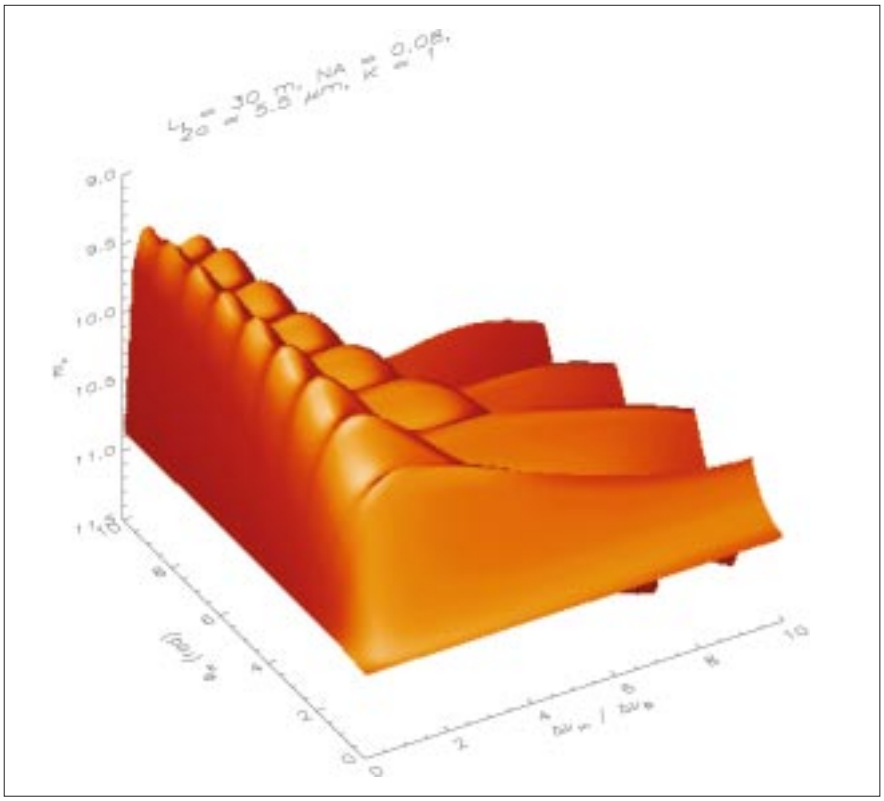

Figure 5: Predicted LGS brightness m_V in case of laser light relay with an optimised single mode, 30-m-long, polarisation-preserving, pure fused silica fibre. The LGS brightness is computed as a function of the frequency modulation bandwidth to Brillouin linewidth ratio, $\Delta\nu_m / \Delta\nu_B$, and peak phase shift ϕ_m, achieved with a single electro-optic modulator. The parameters for the atmosphere are chosen to represent median values. For the transmission of the launching optics 90 % was assumed with the LGS at zenith.

Mesospheric Sodium Excitation Efficiency

The effective backscatter cross section of the mesospheric sodium atoms is given by the convolution of the spectral illumination profile and the sodium absorption profile. We want to maximise it.

With a fixed LGS spot size and increasing layer illumination, saturation of the atoms can be avoided by broadening the effective laser linewidth. Since the width of the Doppler-broadened sodium D_2 absorption profile is about 2 GHz, there is an optimum effective laser linewidth, which optimises the LGS photon return. In Figure 5 the predicted LGS brightness is shown as a function of the phase modulation parameters, in case of a beam relay with an optimised polarisation preserving 30-m-fibre that is single-mode over its entire length.

The throughput of the laser launching optics has been assumed to be 90%. The atmospheric parameters (seeing, transparency, sodium column density, layer height and temperature) assumed for Figure 5 represent median Paranal values, with the telescope pointing the LGS to zenith. As can be seen, the maximum brightness occurs at modulation bandwidth to Brillouin linewidth ratios in the range between 1 and 2. For smaller ratios the lower critical input power limits the brightness, independently of the peak phase shift. For larger bandwidth ratios, the decrease in the overlap integral between the excitation spectral profile and the Doppler-broadened absorption profile limits the LGS magnitude. The brightness gain starts to saturate for optimum peak phase shift values above 2.7 rad. This, together with a minimisation of the electrical power requirements for the laser light modulation, implies an overall optimum peak phase shift of ϕ_m = 3.8 rad. The corresponding optimum modulation to SBS bandwidth ratio is $\Delta\nu_m / \Delta\nu_B$ = 1.0. With these parameters the maximum LGS brightness will be limited to 9.5 equivalent V-band magnitude in case of unpolarised excitation.

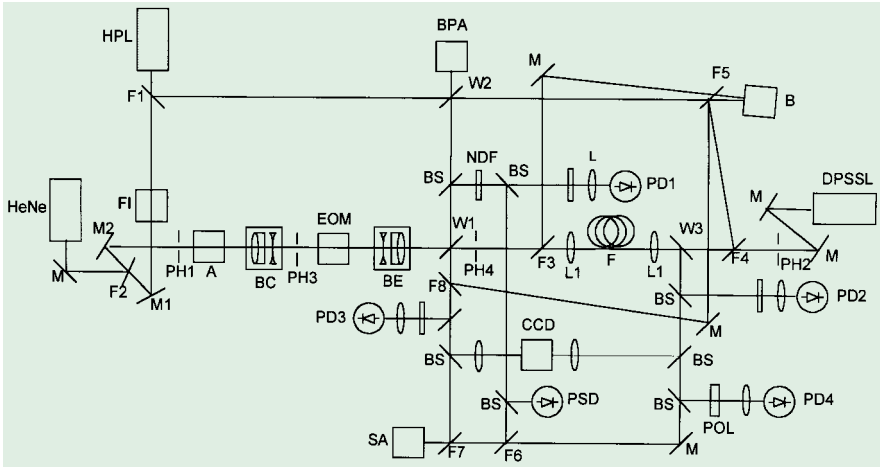

Figure 6: Layout of the laboratory set-up for the results reported in this article. See text for explanation of the acronyms.

Experimental Results

Fibre-transmission experiments have been carried out with the ALFA sodium laser on Calar Alto in 1998. The results of the SBS threshold achieved agree well with theory. In Garching, a prototype injection setup has been built with a 532 nm, 5W CW all solid-state laser. The scheme is shown in Figure 6. HPL is the high power laser. For the laboratory experiment this is a diode-pumped Nd:$YV0_4$ laser (Coherent Verdi) capable of emitting 5.5 W of single-frequency CW power at 532 nm with high beam quality. To suppress any back-reflections into the

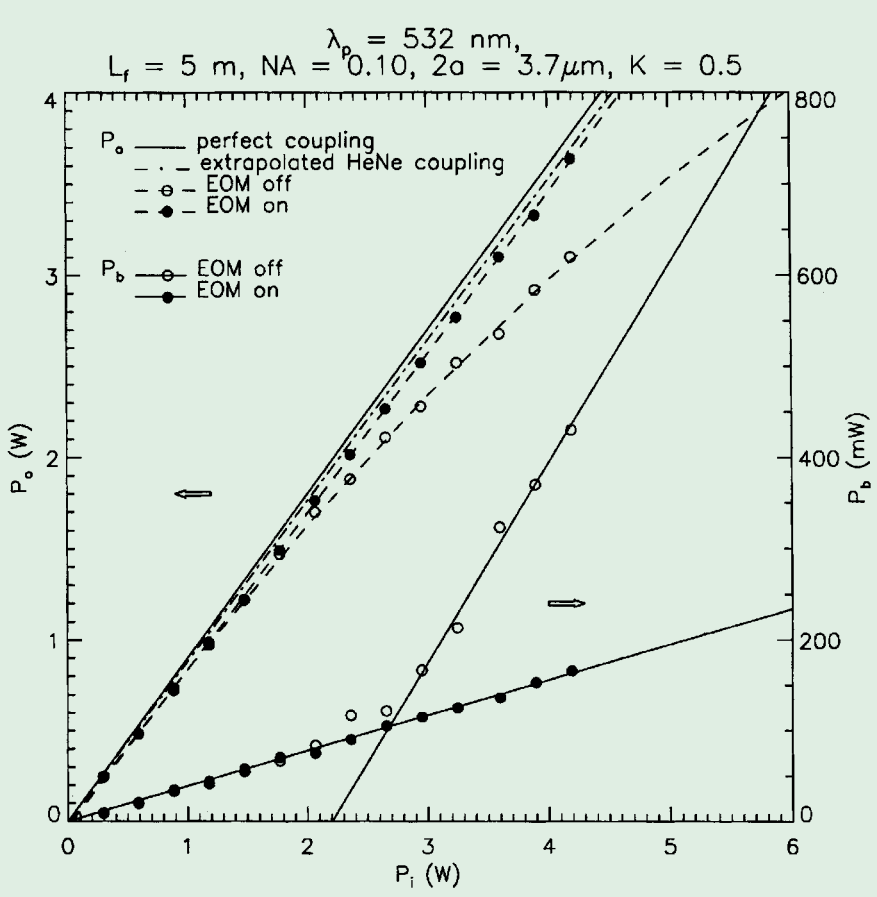

Figure 7: Measured fibre output power P_o and backscattered power P_b as a function of the input power P_i for a 5-m-long pure fused silica non-polarisation preserving single-mode fibre at 532 nm. The cases of unmodulated and frequency modulated input are shown (light modulator EOM on/off). For comparison, the extrapolated low power HeNe-laser transmission and the maximum theoretical throughput is displayed. See text for further details on the setup.

laser head a Faraday Isolator (FI) is installed near the laser output coupler. M1 and M2 are folding mirrors for controlling the four degrees of freedom of the laser beam. PH1-PH4 are pinholes for alignment purposes (see below). For the same reason an attenuator (A) is installed in the beam. Its working principle is based on Fresnel reflection at counter-moving glass plates, which ensures minimum beam position deviation during operation. In combination with the position angle of the exit polariser of FI, any attenuation between 0 dB (without insertion losses) and 27 dB can be selected. BC and BE form the beam shaping optics. These are 2-element 4x beam compressor and expander, respectively. The purpose of these two telescopes is twofold: First, BC reduces the beam size so that the beam can pass through the electro-optical light modulator (EOM) without clipping. The aperture of the electro-optical crystal is minimised in order to relax the electrical power requirements to drive it. Second, by slightly decollimating BC and BE, the waist location and diameter of the beam entering the focusing lens L1 is controlled for optimum launching, i. e. mode matching with the fibre waveguide.

Several diagnostics tools are integrated for on-line analysis of the launched beam, the back-reflected light from the fibre entrance and output. These allow the measurement of the light spectrum (SA), polarisation (POL), power (photodiodes PD 1–4, bolometer B), beam quality (BPA) and jitter as well as waist location and size (beam propagation analyser BPA, position sensitive device PSD). The diagnostics tools are fed with the help of windows (W1–3), beamsplitters (BS) and flipper mirrors (F1–8). Metallic coated neutral density filters (NDF) are used to adjust light levels. All high power lenses and windows including the phase modulator crystal are antireflection coated. The high power mirrors are dielectric coated. To reduce scattering and beam degradation, all high-power surfaces and the elements in the arm of the beam-propagation analyser have a surface quality of better than 60 nm PTV and are polished down to 10^{-5} scratch-dig. The throughput of the high power beam path is 80 %. HeNe and DPSSL are low power lasers for alignment purposes.

To allow the optics in the high-power arm to thermalise and also for safety reasons the coarse-alignment of the high power laser beam is started first with an attenuated beam. Figure 7 summarises the results on the high power transmission of a 5-m-long single-mode test fibre. The conclusion from this first experiment has been that it is possible to achieve an optimum launching and efficient SBS suppression for the test fibre. Moreover, our theoretical calculation and experimental results are in good agreement, which gives us confidence in the reliability of the model of the system. With the current HF amplifier driving the electro-optic light modulator, a maximum peak phase shift of $\phi_m = 2.1$ rad at $\Delta\nu_m = 110$ MHz can be achieved. At 532 nm this corresponds to a SBS gain reduction factor $\rho_{eff} = 0.41$. In Figure 7 the fibre output and backscattered power are shown as a function of the input power on a 5-m-long, non-polarisation-preserving single-mode fibre. Below 2.4 W input power only Fresnel reflection is observed in the backscattered light. This agrees with the calculated critical SBS pump power of 2.5 W. The slight discrepancy between the former values can be explained by the tolerances in the fibre parameters. For input powers higher than 2.5 W and with the laser frequency un-modulated, the SBS back-reflected power increases to 29% of the pump power above the Fresnel reflection. In the spectrum of the back-reflected light the Brillouin-shifted input started to appear at the critical input power. With the modulator switched on, no SBS was observed up to the maximum achievable input power level. This agrees with the calculated decrease of the SBS gain. The modulated throughput at the maximum input level of 4.2 W is 85 %. For comparison the throughput of a low power HeNe-laser is 88 %, measured with an optical setup optimised for the He-Ne laser, which had a mode quality comparable to the Verdi laser. The difference can be explained by the larger beam jitter of the Verdi laser, which should account for nearly 3% coupling loss due to concentricity errors. The maximum theoretical throughput is about 90% including Fresnel reflection at the uncoated fibre end surfaces (8% loss) and extinction (linear loss coefficient 0.005 m^{-1} at 532 nm) but neglecting all other loss sources. The maximum fibre output power was stable during the experiment. A burn-in test with longer fibres is scheduled.

Conclusions

We have demonstrated that a fibre relay module is feasible. The experimental results agree well with the theoretical model. Further work on an optimised, end-face-protected, 30-m-long single-mode fibre is in progress and the first experiments will be carried out in Garching. A burn-in trial on Calar Alto sodium laser is foreseen in the first half of next year.

There appear to be at least two possibilities for further increasing the LGS brightness within a fibre-fed relay system:

1. To combine the polarised output of two fibres at the launch telescope. The brightness limit would increase by 0.7 mag.

2. To separate the two purposes of the fibre relay, namely flexible transportation

of polarised high power light and diffraction-limited output, into two physical fibre sections: a longer multimode section and a shorter mode cleaning section.

The disadvantage of the first solution is the increase in complexity, however we know it is feasible. The advantage of a two-sectioned fibre is that its design would be no longer limited by the critical input power of a single-mode fibre of equivalent length. Instead higher power levels could be considered. For a sodium laser with 10 W output power, whose spectrum is optimised for maximum LGS return flux, a hybrid fibre is under study. Assuming the same launching and atmospheric parameters as for Figure 5, without optical pumping of the sodium atoms via circular polarisation, this laser setup should be able to provide a seeing-limited LGS of brightness V=8 magnitude. This would be sufficient for adaptive optics correction even under poor seeing conditions, pointing at 60 deg Zenith angle.

References

Cotter, D.: 'Suppression of Stimulated Brillouin Scattering during Transmission of High-power narrow-band laser light in monomode fibre', *Electronics Letters*, Vol. **18**, No. 15, p. 638–640, 1982.

Smith, R.G.: 'Optical Power Handling Capacity of Low Loss Optical Fibres Determined by Stimulated Raman and Brillouin Scattering', *Applied Optics*, Vol. **11**, p. 2489, 1992.

Tsubokawa, M, Seikai, S., Nakashima, T., Shibata, N.: 'Suppression of Stimulated Brillouin Scattering in a Single Mode fibre by an Acousto-Optic Modulation', *Electronics Letters,* Vo. **22**, No. 9, p. 473–475, 1986.

E-mail: dbonacci@eso.org

New Pictures from the VLT

Spiral Galaxy Messier 83: This photo shows the central region of a beautiful spiral galaxy, Messier 83, as observed with the FORS1 instrument at VLT ANTU. It is based on a composite of three images, all of which are now available from the ESO Science Data Archive. The three frames were taken in March 1999 through three different filters: B (wavelength 429 nm; Full-Width-Half-Maximum (FWHM) 88 nm; exposure time 10 min; here rendered as blue), R (657 nm; 150 nm; 3 min; green) and I (768 nm; 138 nm; 3 min; red) during a period of 0.8 arcsec average seeing. The field shown measures about 6.8 x 6.8 arcmin and the images were recorded in frames of 2048 x 2048 pixels, each measuring 0.2 arcsec. North is up; East is left.

First Images from FORS2 at VLT KUEYEN on Paranal

Top: Three-colour composite of the well-known Crab Nebula as observed on November 10, 1999.
It is the remnant of a supernova explosion at a distance of about 6000 light-years, observed for the first time almost 1000 years ago, in the year 1054.

Right: Three-colour composite of the young object Herbig-Haro 34 (HH-34), now in a protostar stage of evolution. It is based on CCD frames obtained with FORS2 in imaging mode, on November 2 and 6, 1999.
The object has a remarkable, very complicated appearance that includes two opposite jets (red straight line, down centre) that ram into the surrounding interstellar matter. This structure is produced by a machine-gun-like blast of "bullets" of dense gas ejected from the star at high velocities (approaching 250 km/sec). This seems to indicate that the star experiences episodic "outbursts" when large chunks of material fall onto it from a surrounding disk.
Note also the enigmatic yellow arc to the left, a feature that is still unexplained.

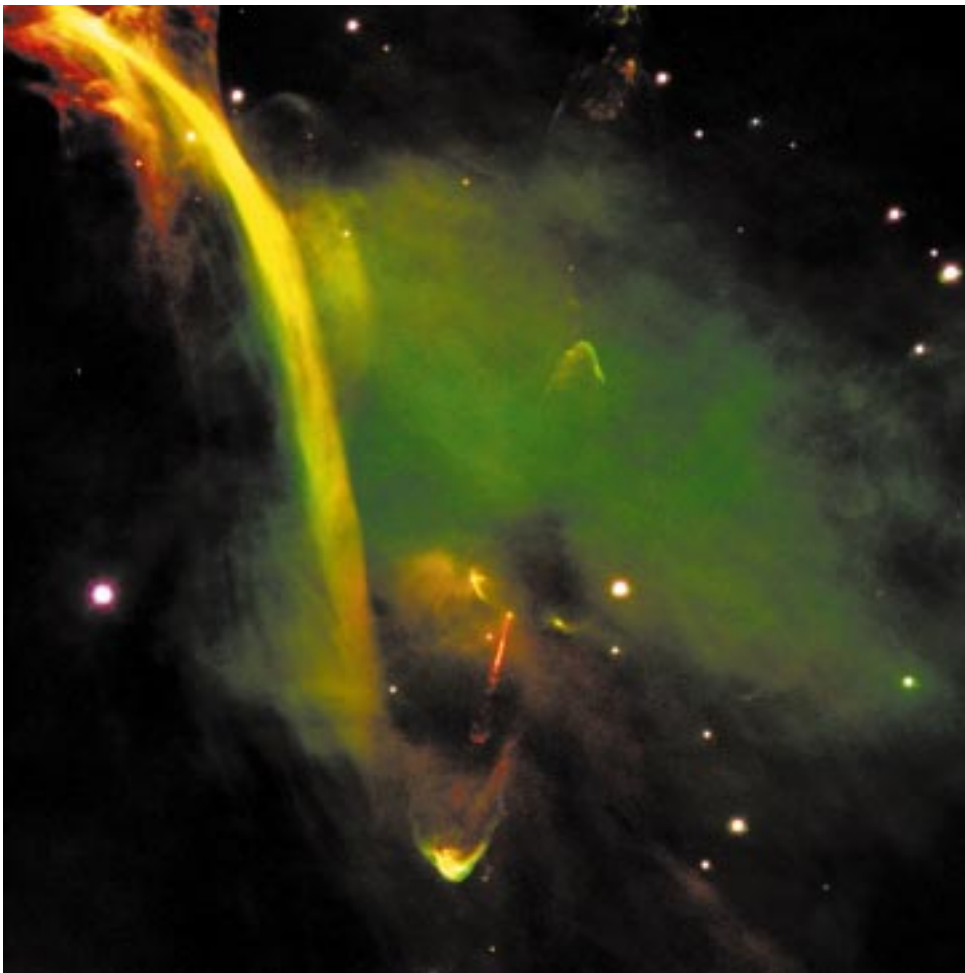

Commissioning of the Unit Telescopes of the VLT

J. SPYROMILIO, A. WALLANDER AND M. TARENGHI, ESO

In the June 1998 issue of *The Messenger* (No. 92) there was an article describing the hectic days and months before the first light for UT1. First light was a great public event and of great significance for the project and the organisation. From a technical point of view however, it was a non-event. The telescope had met all specifications for first light ahead of time and the weeks before the official announcement were more a sit tight, don't tell and don't break it time. Following the big event we were free again to work on the machine. For those with keen eyes looking back at the beautiful images taken for the first light, flaws could easily be found. In fact a number of messages and private comments arrived at Paranal describing in great detail what we already knew. A lot of work lay ahead of us.

The working schedule was set out. During the day Peter Gray, Toomas Erm, Gerd Hudepohl, Marc Sbaihi and Juan Osorio would fix all the things we broke during the night and continuously improved the opto-mechanical and electronic robustness of the system. During the night Jason would sleep on his sofa while the others tested out the latest and newest ideas that had been implemented the day before. Pretty pictures, which before first light were obtained when the seeing was better than 0.6 arcseconds, were banished to be taken at times when the seeing was better than 0.5 arcseconds. Then the limit was changed to 0.4 arcseconds as seeing was good too often and test time was being limited. It was often said that the seeing was best when Jason was asleep in the control room. Ivan Muñoz and Anders Wallander set out to prove this by obtaining a 0.27 arcsecond image in June under those operating conditions. A press release on the subject – politely avoiding the sleeping issue – can be found on the web.

Antu, or UT1 as it was still known in those early days, suffered from wind shake. The telescope was not stiff enough to remove the effects of the wind on the focal plane. This was not a surprise since from the design phase already it was known that the UTs would be susceptible to such problems. Before first light Gianlucca Chiozzi and Robert Karban had done a splendid job in getting field stabilisation to work in a matter of a couple of weeks. Now was the time to tune it up, remove the lag as much as possible and get every last millisecond out of the loop. Working with a 33 MHz 68040 processor as the central engine was a challenge. However, together with Birger Gustafsson, Antonio Longinotti and Philippe Duhoux (M2 and CCD experts) the field stabilisation was brought to an effective update frequency of 20 Hz. Now was the chance to have some real fun. Out of the drawer Birger produced the latest and best toy. A Power PC processor for our guiding LCU. It was tested on the control model in Garching, deemed to be good and hey presto! 50 Hz frequency on the M2. The secondary mirror of the VLT is 1.2 metres across. Moving it at 50 Hz is not for the weak of heart. If you got time on the VLT and you have got some data, the 'little' mirror at the top of the telescope was moving about all the time making the focal plane stay put while the big thing (telescope) shook in the wind. The weakness of the telescope in windshake rejection was thought to be with us for life. Toomas Erm would not accept that and continued working on this problem.

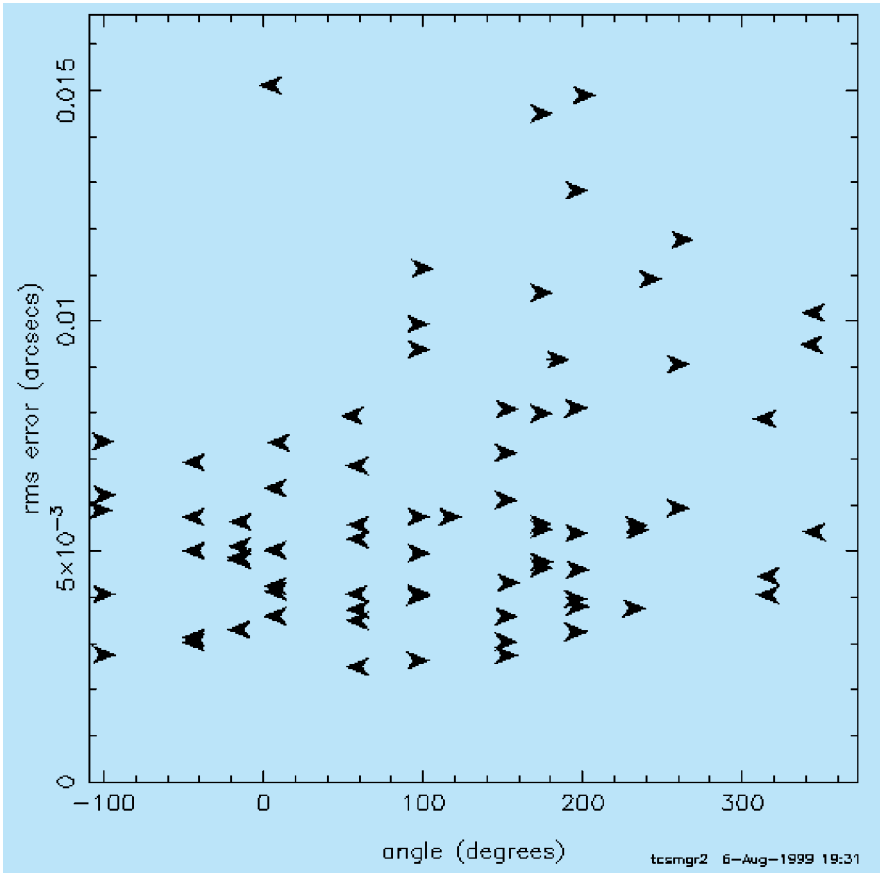

Figure 1: The plot shows the rms tracking error as measured on the telescope encoders for Azimuth on Kueyen. The specification is 0.1 arcsecond and the achieved performance is clearly much better than that. The direction of the arrow indicates the direction the telescope was moving during the measurements.

Before first light we only needed the telescope to point to 10 arcseconds or so. Even for a big machine like UT1 this was not very difficult to achieve thanks to the full integration of the pointing model into the tracking software. Now we had the real specifications to meet. Pointing any telescope to 1 arcsecond rms all over the sky is hard enough. Doing it with the UTs of the VLT is an interesting challenge. First we had to stabilise the pointing model which was varying from night to night. It does not take a rocket scientist to work out that if the primary mirror moves inside the cell then the pointing errors of the telescope change. Keeping the mirror in position was provided for with the mirror cell hardware, which permits us to position the mirror in x,y,z as well as the three angles about these axes. By re-positioning the mirror after each pre-set we stabilised the pointing model. A new set-up keyword for the telescope was needed and the food theme on Paranal began. When TEL.PSOUP (pronounced pea soup) is set to true the m1 cell Passive SuppOrt moves the mirror UP. Now we had a stable pointing solution and we could start worrying about the actual performance of the telescope. Trying as hard as we might, neither the residual of the fit nor the actual pointing performance could be brought below 1.5 or so arcseconds rms, and often the performance was worse. But then again we asked ourselves why are we bothering with this. The telescope guide probe moves automatically to find a guide star. Why not offset the telescope position to make the guide star land where the guide probe expected it to be. The pre-setting accuracy would then be equivalent to the as-

trometric accuracy of the guide star. Two birds killed with one stone. One was the pointing of the telescope. The other was the reproducibility of the pointing. The latter was to show its true worth later when FORS1 was being commissioned.

Now that some basic things were out of the way we could start having fun. Again Gianlucca Chiozzi and Robert Karban were set to work. We want to chop and field stabilise at the same time. Sure they said. It is part of the specs. One beam is always under control while the other is the sky beam that no one cares about. Somewhere in the specifications this had slipped through. Maybe it came from the days of single-element IR detectors. In any case, the new more complex specification was given out. Assuming the guide star is going to land on chip in both beams of the chop then we wish to field stabilise on both beams. Back to the drawing board. Philippe Duhoux to the rescue with a port of the DIMM software to the guider and again our wish was fulfilled. ISAAC folks would be happy. But what about the comet and moving-target community? Of course the VLT can track on a moving target. But could it guide on it as well? So the challenge was set. How would this be done? Back to the original design to see what was thought to be the way. Move the guiding box on the CCD with the appropriate speed and everything will be OK was the theory. But why do that? Why not tell the guide probe to simply track its star. Then if the centre moved or not was not a problem since the guide probe would happily hunt down its guide star. It actually turned out that Birger Gustafsson had already coded almost all of this simply to be able to pre-set the probe to the guide star. All he had to do was to keep the probe alive at all times. Easier said than done but, as usual, nothing is more fun than the impossible. So having this working, we could now chop and field stabilise while the telescope tracked a moving target. Unfortunately, in doing this we broke the combined offset mechanism. Traditionally the probe is offset in the other direction to the telescope. By making the probe live when the telescope offset the probe would automatically follow its own star. After a bit of soul searching we realised that this was actually the better way of doing things. The autoguider was promoted above the tracking software as the master and we were back in business.

While all of this was going on, from nowhere came a couple of Nasmyth adapters and were miraculously mounted on the telescope without interfering with our work (we suspect a phantom Francis Franza and his twin Paul Giordano had something to do with this but Martin Cullum denies all knowledge as to how this miracle occurred). The engineering crew was growing by the day. George Harding, the two Pablos (Gutiérrez and Barriga) and the formidable Patricio Ibanez all started putting their stamp on things. Toomas Erm kept worrying

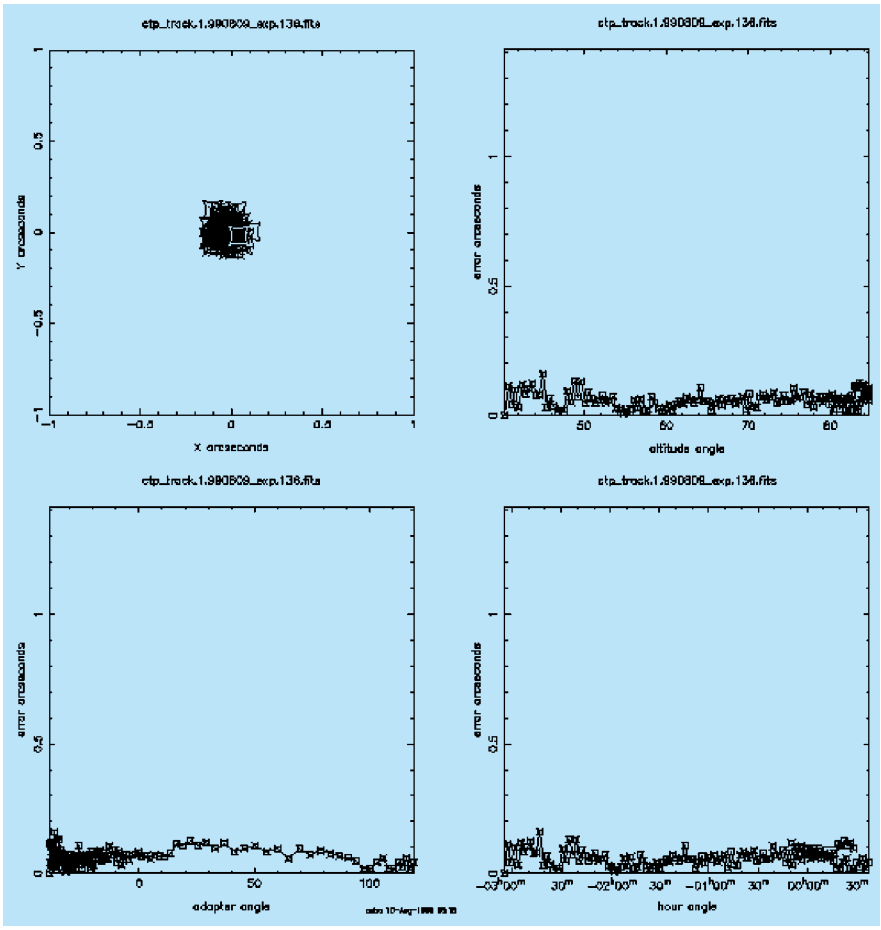

Figure 2: The top left plot shows the measured centroid for a star during successive 30 second exposures taken during a 3.5 hour track. The difference in the centroid between the first image and all successive images is the measured error in tracking. The three other plots show the error in tracking as a function of altitude, adapter angle and hour angle. The telescope crossed the meridian during this test and the peak error was below 0.15 arcsecond during the entire experiment.

about this wind shake thing. Gerd Hudepohl and Pierre Sangaset would fret about the cell while Gustavo Rahmer was finally about to get some serious work to do. Thanh Phan Duc would come and go and let us all know exactly how many cell operations we had made and would fix whatever needed fixing. It was like having a policeman checking up all the time. Ricardo Schmutzer moved between Garching and UVES and Paranal and the test camera without missing a beat on either of them. FORS1 arrived on the mountain and immediately aroused suspicions. Did they really think that big yellow thing would fit under our delicate telescope?

Meanwhile the final phases of the commissioning of another telescope on Paranal were taking place. The ASM (Astronomical Site Monitor) was getting to the phase where it could be left alone. Stefan Sandrock and Rodrigo Amestica would try to make our robotic telescope work. Anders expressed wishes that the UTs be so simple to operate. Switch it on and the ASM will know when to open and when to close, where to find a star and what to measure. Not too hard a requirement really. Only the ASM was having problems finding alpha Cen let alone any other star. A bit of investigating on the pointing problem and a few ingenious solutions by Stefan and Rodrigo and the ASM was up and running. Now the radio need not sound all night long with the call: “Julio! What is the seeing?”

Before putting FORS1 on to the telescope we had to satisfy another client. Bruno Leibundgut together with Mark Ferrari and Eline Tolstoy arrived for science verification with the test camera. Brilliant plans were laid out, astronomical challenges and problems to be solved. The first couple of nights went fine. In fact, a new image quality record was set at 0.26 arcseconds, the image taken with the ADC mounted. Then the weather changed, the seeing became poor, the control room was not a happy place and before you could say “bad luck” the two weeks of SV were over. Bruno took a copy of the data with him and the video conference to Garching fell silent.

Soon afterwards The FORS1 team led by Professor Appenzeller together with Gero Rupprecht as the ESO responsible put their pride and joy on the Cassegrain focus of UT1 and then had to take it off again due to a broken cooling pipe inside the adapter which dripped water inside their instrument. We apologised, helped to clean up the mess and on went FORS1 again. The moment of excitement arrived. The shutter was opened and the first im-

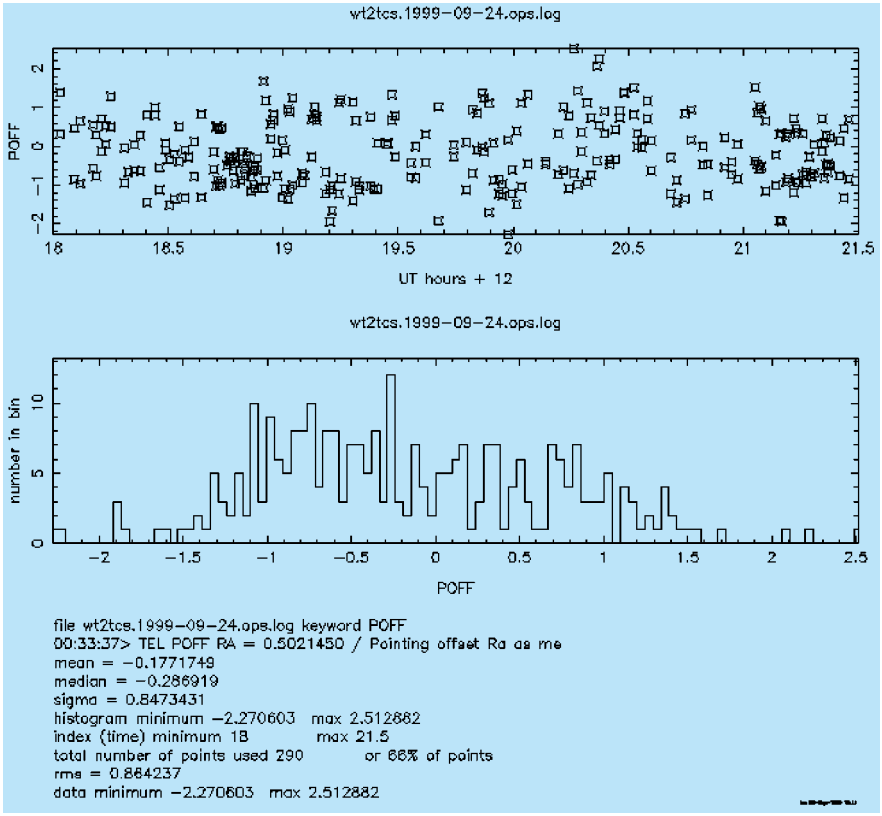

Figure 3: Measured pointing errors on 140 astrometric stars covering the whole sky. The measured rms pointing on this night was 0.85 arcsecond.

age obtained. The image quality was quickly derived to be 0.6 arcseconds. A quiet note of satisfaction was felt across the control room and now the real work commissioning FORS1 could start in earnest. A separate article on the FORS1 commissioning has already been published, so not much more will be said here.

In the mean time ISAAC was sitting in the integration lab waiting to be installed on the telescope. Jean-Luis Lizon had been working furiously under difficult conditions to complete the re-integration of the instrument. In the couple of weeks between FORS1 and ISAAC we checked out the Nasmyth A focus and verified all was well. ISAAC went on to the telescope on schedule and also produced beautiful images straight away. Finally we had an instrument that could exercise the telescope in all the weird and wonderful ways that only infrared astronomers can find. Alan Moorwood, Jean-Gabriel Cuby and Chris Lidman all worked furiously at characterising the instrument. Our first fellow on Paranal, Monica Petr, arrived around this time and immediately started learning and driving both instruments and telescope. Joar Brynnel finally could see all his electronics work used for astronomy rather than just tests. Manfred Meyer and Gert Finger got the last ounce of efficiency out their IRACE system to read the ISAAC detectors. Peter Biereichel was always at hand to make the instrument software that little bit better. Nicolas Devillard demonstrated the latest pipeline capabilities.

It was Christmas time by now and the FORS1 crew were back. To welcome them we put water inside their instrument again, but by now we were all experts at dismounting and cleaning FORS1 up. Our apologies were gracefully accepted again and we started to work together towards the final integration of the instrument into its new home. Unfortunately the weather did not co-operate and most of the second commissioning run was lost. We scheduled another run for January and with the help of Thomas Szeifert, Bernard Muschielok and Wolfgang Gaessler the instrument was Paranalised. Following this it was handed to Fernando Comerón to system test. Of course, Fernando kept on finding things we had missed. Roberto Gilmozzi would agree with him and then we had to change everything again. It was fun.

Time had come to welcome ISAAC back. Remember how well the telescope and instrument had behaved in the first commissioning run. Well, this time things were not to be so easy going. The UTs' direct drive motors (big fancy magnets with a protective metal cover) move the machine silently and very elegantly around the sky. On side A (not the ISAAC side) one of the covers came off and got crunched inside the motor. Patricio Ibanez, Pablo Gutiérrez, Gustavo Rahmer and Hans Gemperlein worked nonstop for a week to disassemble one whole side of the telescope and put it back together again. The badge of honour at the time was a piece of yellow duct tape, which was worn with great pride for the duration of the work. You might have thought that the control room would have been a quiet place with a broken telescope. Taking advantage of the absence of the head of commissioning, Michael Loose, our architect on Paranal, transformed the control room into Beirut at the height of the Lebanon troubles. The floor and the ceiling disappeared. If a small thermonuclear weapon had gone off it would have made a smaller mess. In spite of this, Jean-Gabriel, Jens Knudstrup and a few other brave souls continued working, wearing surgical masks to limit the amount of dust entering their lungs and the ear-plugs to reduce the noise level to that of a firing range.

All was brought together just in time for the end of the commissioning of ISAAC and we were ready for the operations dry runs which were scheduled for March. In the mean time two big events were on the horizon. UT2 (soon to be renamed to Kueyen) was getting ready for first light and the inauguration of Paranal was also rapidly approaching. Without commissioning really noticing, Peter Gray and his crew, with some help from the usual suspects in Garching – Bruno Gilli, Max Kraus and Fabio Biancat Marchet come immediately to mind – had another 8-metre telescope ready to go. Cells moving up and down the mountain, mirrors coated, servo loops tuned and all the things necessary to make a telescope ready somehow were all done without slowing UT1 work. Two telescopes running before the inauguration and a nice image to show from Antu would make a good showing. Massimo in a typically challenging order stated that nothing worse than a third of an arcsecond for the image from Antu would satisfy him. On the night before the inauguration, UT1 had already been handed to Science Operations for their dry runs. The telescope was theirs. What could they do? Just to set the standard for the future, Hermann Boehnhardt and Roberto Gilmozzi were at the controls with Massimo directing that FORS1 be switched to high-resolution mode since the seeing was good. It is a well-known fact that the presence of the director on Paranal improves the seeing. The combination of all of the effects described resulted in a 600-second I band image with quality better than 0.25 arcseconds. Now that the first goal was met we could have some extra fun. Lothar Noethe and Stephane Guisard had been labouring for some time to make the telescope spell its own name. Anyone they said could do it moving the telescope around until the star trails spelt out VLT. Even the NTT managed that. So they took charge of the shape of the primary mirror and they made stars whose shapes spelt out VLT! True control of the shape of the primary was demonstrated beyond a doubt.

On Kueyen as soon as we had a primary and a secondary mirror installed we had a look. It was not going to be as easy as Antu but it would work. Lothar Noethe, Stephane Guisard and Roberto Abuter set about their merry way to make the thing make stars that looked round.

Krister Wirenstrand sorted out the pointing with a bit of help from a big piece of paper being held at the Nasmyth Focus and using a real bright star. Two telescopes working and the best ever image. We now felt that the observatory could be inaugurated.

Before the telescope was released into full operations we threw away the old software. Giorgio Filippi came down with a present from Garching. A Y2K compliant system had been fully tested on the Garching control model and was installed on all systems on Paranal. Carlos Guirao brought some new data flow computers and Michèle Peron, Nick Kornweibel, Michele Zamparelli, Gerhard Mekiffer, Klaus Banse, Miguel Albrecht, Paola Amico, Reinhard Hanuschik, Palle Møller, Michael Rauch, Almudena Prieto, Dave Silva and Maurizio Chavan all spent quite some sleepless nights on Paranal ensuring the data-flow system was fully operational before and immediately after Antu was released.

Somewhere earlier in this story Toomas Erm was still worrying about this wind-shake problem. So, after a long think about it all, he asked if Stefan Sandrock could give him a helping hand with an idea he had. A couple of days later a new version of our tachometer was implemented in software and the enchilada was born (a soft taco being an enchilada). Wind shake is not a thing of the past but Kueyen is now stiffer than we had ever dreamed of. Enchilada gave way to Enchilada turbo and by now the azimuth axis of Kueyen was exceeding tracking specifications by over an order of magnitude and altitude was in great shape also exceeding specifications by a factor of 2 under most operating conditions. The windscreens of the enclosure have been improved and tested and retrofitted thanks to the work of Martina García (who somehow also managed to have a baby while all of this was happening) and Erich Bugueno. Juan Osorio fixed things on the electronics of the enclosure and German Ehrenfeld never seemed to stop making things and moving big pieces around. Nelson Montano is now our hydrostatic pad man and routine preventative maintenance started in earnest. The benefits of having more than one telescope to work on were coming to the fore. In any normal telescope observatory Antu would have been released and the improvements coming from Kueyen would have been implemented in some distant future. At Paranal the cycle still has some way to run.

On Antu, for each activity undertaken by commissioning, a test procedure was supposed to be followed documenting exactly how each test was to be performed. This was to be a self-documenting system with the procedure also providing the final documentation for the test. In some cases, such as tracking and field-stabilisation maps, this was done while for others the procedures were developed during the commissioning, as we better understood what needed to be done. On Kueyen this documentation effort was much improved and expanded. Also automation of a number of tests was undertaken. The use of the engineering data stream was expanded dramatically to provide input for preventive maintenance but also to better understand the system. The VLT control-system engineering-data stream includes for example every aberration measured by the system. In any given month, as many as 20 thousand active-optics corrections are made. Looking at the logs and using parallel measurements with the test camera wavefront sensor, we identified some cross-talk between defocus and spherical aberration. The effect was small resulting in additional noise in the system of order 0.03 arcseconds in the average image quality delivered. Lothar was looking at the data in Garching and promised a solution by the birth of his son. On schedule on the 3rd of August the problem was identified and corrected for. A baby boy was also born on the same day. The cross-talk was identified as being due to an incorrect sign in the force setting on the primary. The improvement in the stability of the defocus was obvious (the rms value of the aberration was reduced by 500 nanometres). The value of the engineering data stream cannot be overstated.

Continuing on the food theme (pea soup, enchilada) we started worrying about the sausages the telescope was producing. Close to the zenith and the meridian, when 430 tons of glass and metal are spinning around at an impressive pace, the stars were not coming out round but rather long like sausages. Here was a problem that had to have a solution. So we all worked on it. Krister changed the tracking software. Stefan changed it back and then back again and once more. Rodrigo and Anders measured in ever more imaginative ways. In parallel, continuous improvements in the system were made, all contributing in their own ways in attacking this problem and other annoyances. Mario Kiekebusch automated the adapter calibration procedures and gave us smarter secondary guiding. Ivan Muñoz made the pointing modelling trivial by automating it and introduced us to Pinky and the Brain. Francisco Delgado kept improving the active optics software to allow us to better control the mirror position. Sausage measurements were made, analysed, models and simulators written. The sausage problem was reduced by a factor of 10 and is now an operational annoyance. We keep working on it. Same with the pointing that has been measured as good as 0.85 arcseconds all over the sky. Roberto Rojas has inherited the thermal control software, from Roberto Abuter who escaped to Enteferometry [sic], and put it into full operation. This promises in the medium to long term to provide a significant improvement in how we manage the telescope environment.

This article is being written as UVES ended its first commissioning run on Kueyen. UVES is looking good. Very good! FORS2 is already mounted on the telescope and has seen stars. Kueyen is well on its way to be released on schedule for Period 65. Norma Hurtado and Julio Navarrete are driving the telescope and providing valuable operator feedback to the commissioning team. Baring unforeseen events in 2000 both Melipal and Yepun will have their first lights and we have new ideas for further improvements to the system.

To know who has made all of this possible, access the web and get a list of all ESO staff irrespective of location, position or function. We would like to thank Krister Wirenstrand personally for his tireless efforts towards building and commissioning the telescopes.

E-mail: jspyromi@eso.org

The Science Verification Plan for FORS2 and UVES at UT2/Kueyen

A. RENZINI and P. ROSATI, ESO

1. Introduction

The Science Verification (SV) observations for FORS2 and UVES at Kueyen (UT2) will follow the same approach and policy as already described for the SV of Antu (UT1) and its instruments (www.eso.org/science/utlsv/). SV observations are now planned as follows:

• UVES SV: February 6–17 (New Moon is February 5)

• FORS2 SV: February 28 – March 10 (New Moon is March 6). Raw, calibration and calibrated data will be made publicly available to the ESO community as soon as the reductions are completed and the data prepared for re-

lease. The SV Teams plan to release UVES data by March 31, 2000, and the FORS2 data by April 30, 2000. Observations will be made in Service Mode with SV Astronomers on Paranal for part of the time. SV observations may actually be taken from February 6 through March 31 in a flexible scheduling, depending on the needs of other commissioning and training activities that may arise.

SV observations will be conducted in coordination with the PIs of the two instruments, the Instrument Scientists, and the Kueyen (UT2) and instrument Commissioning Teams.

The scientific programmes have been selected in such a way as to produce first-quality data for cutting-edge science in areas of interest for a wide section of the potential users in the ESO community. Moreover, programmes that require very good seeing are complemented by others that would still be well feasible in less demanding conditions.

The SV Teams includes the following scientists: Joao Alves, Stephane Arnauts. Jacqueline Bergeron, Tom Broadhurst, Stefano Cristiani, Chris Gorski, Vanessa Hill, Richard Hook, Rodrigo Ibata, Tae-Sun Kim, Markus Kissler-Patig, Benoit Pirenne, Mario Nonino, Francesca Primas, Michael Rauch, Alvio Renzini, Piero Rosati, and Eline Tolstoy.

The following list of SV programmes has to be taken as indicative. In particular, some additional relatively small programme could be accommodated, depending on the actual observing conditions on Paranal. Any modification will be promptly reported in the SV WEB pages (http://http.hq.eso.org/science/ut2sv/), where more detailed information can be found, including target lists, modes and planned exposure times.

2. UVES SV Plan

Three main SV Programmes have been planned:

• **A Spectroscopic Survey of Intermediate Redshift QSOs**. Five out of a list of 8 QSOs with $2 \lesssim z \lesssim 3$ will be observed. These observations are meant to be the first step towards a public survey of QSO absorbers which aims at creating a large and homogeneous dataset to allow the study of the intergalactic medium in the redshift interval $z = 1.6–3$. A team co-ordinated by ESO will submit a proposal to carry out such a Public Survey in Period 66.

• **Abundance Ratios of Extremely Metal Poor Stars from the Hamburg ESO Survey**. At least 5 stars with [Fe/H] $\lesssim -3$ will be observed. The high S/N spectra will allow to determine the abundances of a number of interesting elements, such as Li, α-elements, and s- and r-process elements.

• **Chemical Abundances in LMC Clusters in a Wide Age Range**. A set of Red Giants ($16.5 < V < 17$) will be observed in seven LMC Globular Clusters with ages from 0.1 to ~ 14 Gyr. This should allow a detailed reconstruction of the chemical enrichment history of LMC.

3. FORS-2 SV Plan

The following programmes have been planned for the SV observations of FORS2:

• **Deep Imaging of the Cluster of Galaxies MS1008-1224**. This z = 0.3 cluster was extensively observed for SV of FORS1. With FORS2 SV one intends to complete the database by adding deep *U* and Gunn *z* images of the cluster.

• **Hα Rotation Curves of Dwarf Galaxies**. This is a "bad seeing" programme. Long slit spectra should allow to constrain the mass distribution at large radii in a set of three dwarf, dark matter dominated galaxies.

• **Kinematics of Previously Microlensed Stars in LMC**. Over two dozens microlensing events have been detected so far towards LMC. The plan foresees to take spectra of at least 10 of the stars that were microlensed, in order to obtain their radial velocity with an accuracy of ~ 10 km/s. Constraints on the nature and location of the lensing objects could then be derived.

• **Lyα emission at high redshift**. The NTT Deep Field will be imaged with a custom narrow-band filter (FW = 7Å) searching for Lyα emission from large-scale structure centred on a damped Lyα system at $z = 3.2$.

• **Near-IR Imaging of the NTT DF**. Imaging in IF_{915} and Gunn *z* filters will ensure the completion of the deep multicolour database of this deep field, thus allowing a photometric redshift search for very distant galaxies.

• **Spectroscopy of High Redshift Galaxies**. Distant, photometric redshift selected galaxies to $I_{AB} \simeq 25$ from public NTT data will be observed in MOS mode, possibly using the mask option.

• **Abundance Measurements in Giant Ellipticals**. MOS and long-slit spectroscopy for the abundance determination of globular clusters and the dwarf galaxies surrounding NGC4472 and of the galaxy itself out to ~ $3R_e$.

E-mail: arenzini@eso.org

The First Six Months of VLT Science Operations

R. GILMOZZI, ESO

Science Operations started at UT1 Antu on April 1, 1999. This article is a brief account of the first six months (Period 63). As the statistics below will show, operations have been fairly successful. Visitor and Service modes were intermixed during P63, in a 50/50 ratio for the available time (i.e. discounting Guaranteed time, which is by definition in Visitor mode): we had 62 nights in Visitor, and 60 in Service. To this one should add 10 Service nights for the Calibration Plans, and any time allocated but not used for technical time, target of opportunity time and director discretionary time (so that in the end, more than 85 nights were devoted to Service Mode observations and calibrations).

Period 63 started under less than promising omens: the mask wheel of ISAAC had just had to be taken out of the instrument to be repaired, so ISAAC could only work in imaging mode; the decontamination of the FORS1 CCD had not resolved the infamous "quadrangle" problem, and the CCD had to be taken out to be baked more thoroughly, so FORS could not be used. And the weather was the worst seen in the last year (at least by the Science Operations staff): foggy (!), cold and very windy. April 1 and 2 were spent with the Paranal Engineering department, the Garching Optical Detector Group and other Instrumentation Division staff working overtime on one side to bring ISAAC up in imaging mode so that the first Service Mode episode of the Period could start, on the other to decontaminate the CCD in time for the first dark moon and the first FORS1 run.

It is a testimony of the excellent work of all the people involved that on April 3, the wind and humidity having abated to the more normal Paranal values, the first OBs could be executed on the sky. Paranal was finally a full-fledged astronomical Observatory!

From then on, the month spent in 'dry runs' to acquaint ourselves with the telescope and the instruments showed its results: it was immediately clear that the efficiency of the operations was quite high, even if some programmes were not as efficient as they could have been (the fact that ESO had decided to absorb the overheads being possibly a reason for this), the seeing was co-operating very nicely (though not all through the Period, alas), the instruments were behaving very well. Total downtime, both the weather and

the technical flavours, was less than 20%.

Ten days later the next challenge: the first Visiting Astronomers started coming to the mountain. I should probably explain that Service Mode and Visitor Mode, as seen from the Operations point of view, differ only in who makes the scientific decisions about 'what to do next'. A Paranal astronomer is always present to run the instrument, to advise the Visitor and to help preparing the OBs beforehand. Therefore the Visiting Astronomers can devote their time to analysing the data and decide on the observing strategy.

The experience with Visitor Mode has been very positive, the interaction with the Operations Astronomers on the whole resulting in satisfactory observations (or at least this is what we gather from the end of run reports!).

We have learned a lot during the first six months, and we have also made a few mistakes.

One thing that we have to clarify better to our "proposers" in the future is that a successful Service Observing Mode (SM) needs to include programmes designed for various types of conditions: if everybody wants 0.4 arcsecond seeing, photometric sky and be one day from new moon, it's very difficult that we can satisfy all requests...

In Period 63 there were two main issues that caused some confusion with our users: the oversubscription (especially of category A) SM programmes, and the constraints set.

The first is not a problem per se: oversubscribing the available time adds to the scheduling flexibility and makes for an efficient operation. Of course, it also creates unhappy users, who have to submit their OBs without guarantee of execution. The OPC ranking, which is our primary decision input, helped in selecting among programmes competing for the same conditions.

In P63 we were not helped by the time being assigned in terms of shutter open time: of the 600 available hours in Service Mode, 720 were allocated in P63. With the measured values of overhead (~30%) and downtime (~20%), we were oversubscribed by (1.3×720)/(0.8×600) ~ 2. Add to this that weather variability sometime caused the conditions to change during an exposure, so that it had to be repeated, adding to the oversubscription. We are actively studying ways to decrease the impact of this problem; in P63 we were lucky enough that part of the technical time (and some of the discretionary time) were not used, so that we put it into the SM pool, and were able to carry out more observations (see the statistics below).

The other problem we had is the constraints set: the number of programmes that could be observed when the seeing was > 1″ or the moon was up (for FORS), or for nights with cirrus was very small. In part this was compensated by the oversubscription, but in some cases it has been very difficult to decide what to observe. This problem is more acute at the end of a period (again, we are thinking of ways to improve this). Particularly demanding was the August full moon episode when ISAAC was not available for 7 nights, and we had to use FORS1 with very few programmes that made sense to execute.

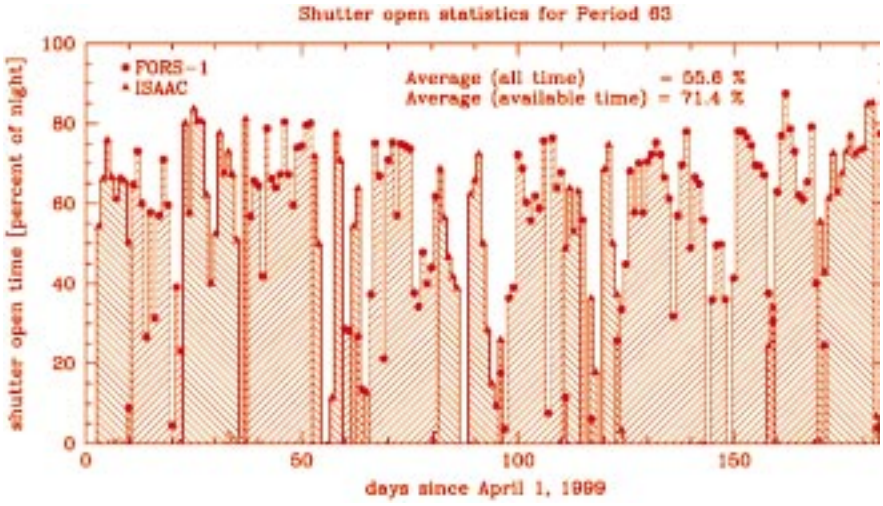

Figure 1.

Sometimes there is no alternative but to violate some constraint: when we had to do that, we always tried to compensate in some way (for example: higher than requested moon background usually meant that we would observe in better than requested seeing, to improve the contrast, or in the longest possible wavelength, where the effect is smallest, or both). Not always this has been possible; ranking has played a role (if a choice had to be made, we tried to avoid affecting very highly ranked programmes). But we have found ourselves in situations (fortunately few) where it was either observe something outside the constraints or keep the telescope idle.

Discussions are ongoing within ESO, and with the community, to minimise these problems in the future. Users can help too, by not requesting indiscriminately conditions that happen only a small fraction of the time.

In the following I would like to offer some statistics for Period 63. Some of this statistics comes from the engineering data stream that is recorded every night, much in the same way that satellite engineering data are recorded (indeed, this has proven to be among the best tools produced by the Commissioning team to understand the performance of the telescope and instruments).

Performance of Antu

During period 63 there have been 3907 presets (21 per night), 22,491 offsets (6 per preset) and 121,537 image analyses (98% of which resulted in an active optics correction). For those of you who have not yet had a chance to see the active optics in action, it is something really impressive: once you acquire a new field, the guide probe goes automatically to a guide star, acquires it, starts the image analysis and, usually about 30 seconds later, sends the first correction to the mirror actuators: at this point you see the guide star shrink to the outside seeing value, and you can start your science exposure (see http://www.eso.org/outreach/press-rel/pr-1999/phot-34-99.html).

This is the most visible difference with the way we used to do astronomy: from this moment on, the telescope is kept at the best focus, with the best optical figure for the pointing, all in parallel with the science observations and without requiring any additional time. The typical overhead to move to a new field, acquire a guide star, and start the active optics is about 5 minutes.

Downtime Statistics

One way to "measure" how well we did in Period 63 is to compute the total downtime. The technical downtime was 13,561 minutes (11.4% of the total available time). This statistics includes any observing time affected by the technical problem (e.g. a problem which can be fixed in 5 minutes but which has caused the loss of a, say, 30 min exposure would count as 35 min downtime).

The weather downtime was 12,700 minutes (10.7% of time). This includes clouds (5.6% of time), high winds (>18m/s) and high humidity (or combinations). Considering that P63 was during the southern winter, this percent loss does not seem surprising.

In total, therefore, we lost 22.1% of the time.

Weather

Of the 163 nights that were not lost to bad weather, 118 (72%) were ap-

parently photometric, 18 (11%) possibly photometric, 17 (11%) had thin cirrus and 10 (6%) had thick cirrus. We are currently finalising the analysis of the standard stars observations to confirm the number of "true" photometric nights.

The statistics on the seeing is based on 116,761 ASM data points, each averaging one minute of measurements. The median seeing in P63 was 0.76". The seeing was better than 1" 72% of the time, and better than 0.5" 13% of the time.

You may have heard that sometimes the seeing measured by the instruments on Antu is better than the outside seeing. Discounting wavelengths effect (i.e. yes, it is true that ISAAC with its 0.15″ pixels sometimes undersamples the atmospheric PSF), we have indeed seen this effect. It is however fairly rare, and needs special circumstances (in particular, the appropriate wind speed, a pointing such that the wind can flush the primary at the right angle, and an excellent seeing to start with). On some occasions, in service mode, we have had enough programmes in the queue that we could choose to observe in the right direction, and so took advantage of this. In general, however, and especially in visitor mode, it is an unlikely occurrence.

Operations Statistics

ISAAC was used 73 nights, or 40% of the time. FORS1 was used 110 nights. This reflects in part the instrumental problems described above, in part the actual time allocation (or the user preferences).

Once one discounts the downtime, there were 1484 available "observable" hours. Of these, 651 were used for FORS1 and 403 for ISAAC. This results in a total "shutter open" efficiency of 71% (see Figure 1). In period 63, the archive "ingested" 19,794 ISAAC frames and 24,039 FORS1 frames.

In Service Mode, we had 75 accepted programmes (40 in category A, 19 in B and 16 in C, or 40/19/16 for simplicity). The completion statistics is 34/16/11 (of which 13/10/8 are partial completions, usually meaning that most of the programme was carried out, the remainder being impossible to observe because of target RA or non realised constraints etc). The programmes not initiated were 0/3/5. The remainder (6/0/0) are category A open programmes that the Director General has allowed to carry over into Period 64 so that they can be finished.

The success of the first six months of operations is the result of the commitment and professionality of a very large number of people, both in Europe and in Chile. Naming all of them would look very much like the ESO internal organigram! However, I would like to mention at least the Science Operations Team at Paranal (now under the leadership of Gautier Mathys), the Paranal Engineering Department (Peter Gray), the User Support Group (Dave Silva) and the Data Flow Operations Group (Bruno Leibundgut) for their dedication and enthusiasm, and for their crucial contributions. Jason Spyromilio and his team delivered fully commissioned telescope and instruments. Massimo Tarenghi as director of Paranal provided oversight and direction to the whole process.

Special thanks to Jason, Gautier, Dave, Chris Lidman and Jose Parra for providing the statistics in this article.

E-mail: rgilmozz@eso.org

Configuration Management of the Very Large Telescope Control Software

F. CARBOGNANI, G. FILIPPI, P. SIVERA, ESO, Garching

1. Introduction

One of the elements of the success of the development, integration and commissioning of NTT, VLT and the attached Instruments has been the Configuration Management of the related Control Software. It has been based on the Code Archive and the VLT Software Problem Report (VLTSPR) procedure.

2. Code Archive

The code archive supports code configuration during development *and* integration on geographically distributed sites. The design keys are the following:

• The configuration item is the software module. This allows a reasonable but still simple flexibility in system configuration (a system is made up of 15 to 100 items, identified by their name and version, corresponding to 2000 to 20,000 files). Each module is a set of files organised in a fixed directory structure and has a unique name. Figure 1 gives the modules divided by VLT common software and applications.

• There is only one central archive. Users get local copies using a simple client server mechanism. In our projects, there is typically only one person at a time dealing with a specific part. A modification must be started, implemented and tested, then archived. During this period the module is locked.

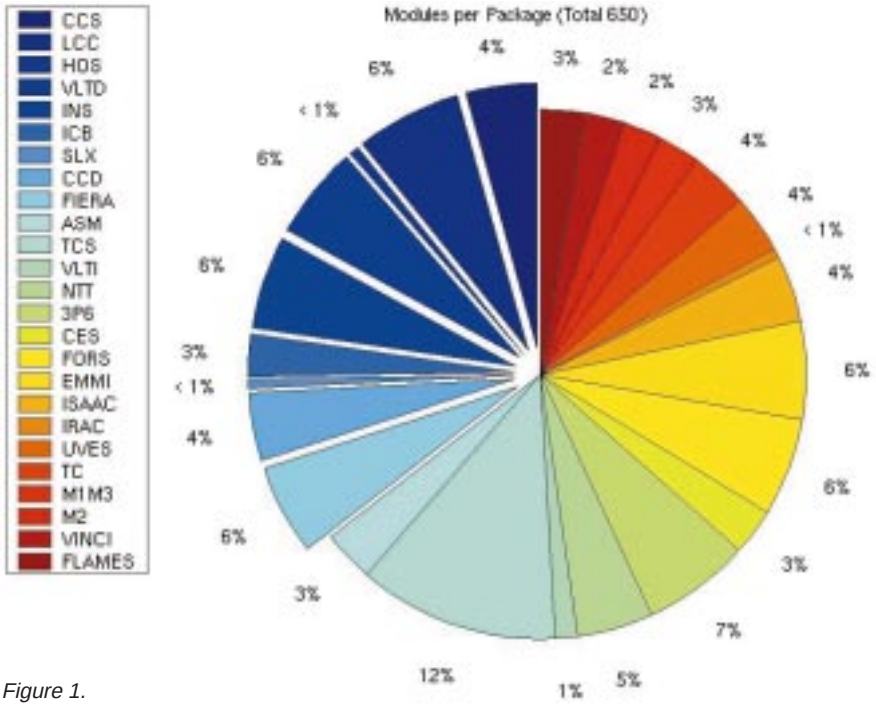

Figure 1.

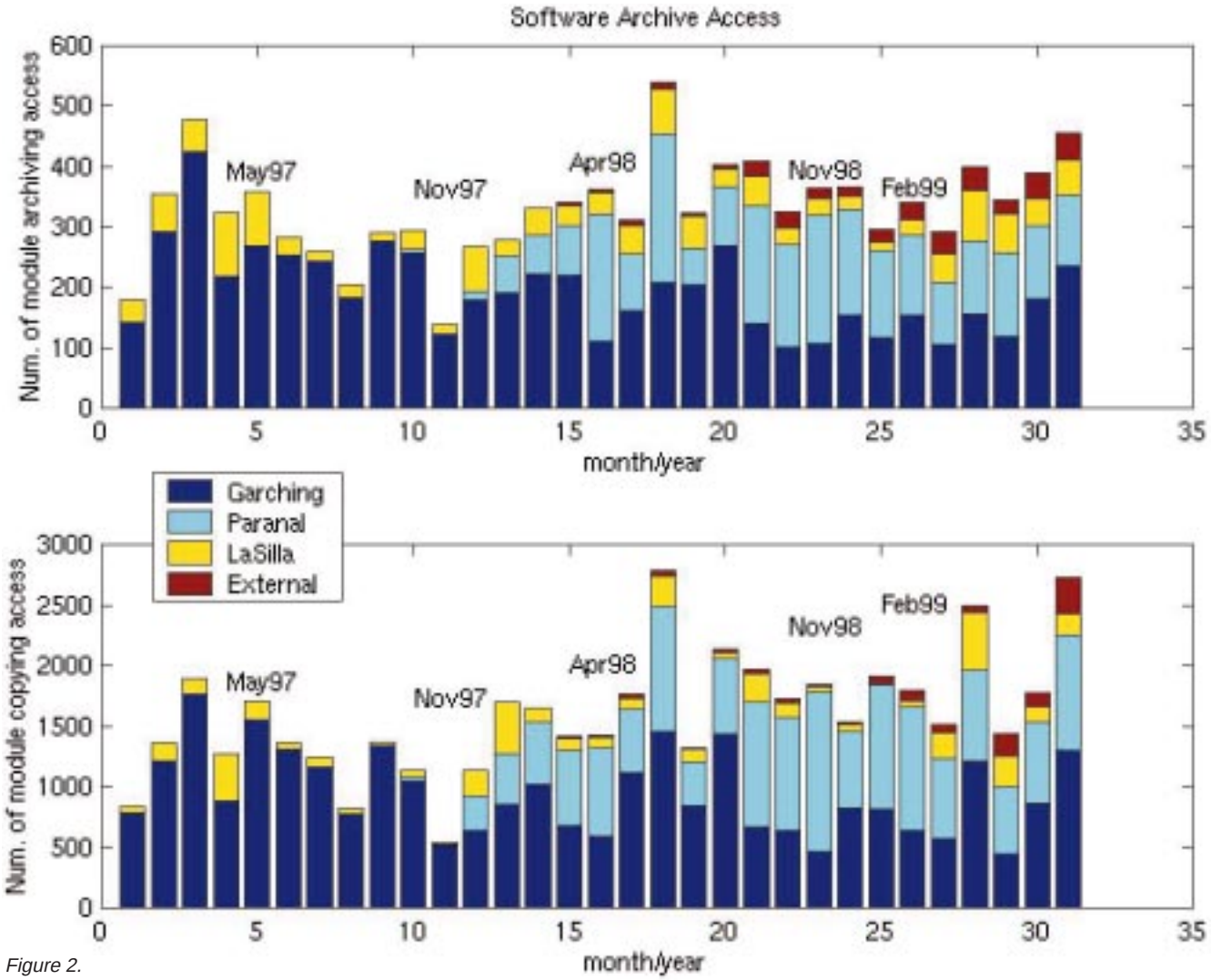

Figure 2.

• To allow experiments or patches on older versions, branches are also supported.

The code archive is implemented using RCS and a set of *ad hoc* programmes and scripts (cmm) implementing the client-server interaction and the user interface. The archive is physically located at the headquarters and used also by teams in Chile and several institutes.

Figure 2 gives the accesses per month for modification and for read-only mode. Currently approximately 60% of the accesses are from outside the headquarters and 25% from non-ESO sites. It can be remarked that the system was able to deal with more than 500 archive and 2500 read-only monthly accesses.

Figure 3 shows in detail the access made by non-ESO sites.

The central archive is not only the software repository, but it is also a management tool. In archiving a module, the developer tells all the other people "Hey, there is a new *consistent* and *tested* set of files that you can use!". This is very useful when several teams operating on different time zones do development and integration. Comparing the current configuration against the status of the archive, the integration responsible can see that new items have been produced. A glance to the comments stored by the developer to qualify the newly archived version is normally enough to decide whether to take the new version or not. In this way NTT, VLT and instruments have been developed, integrated and

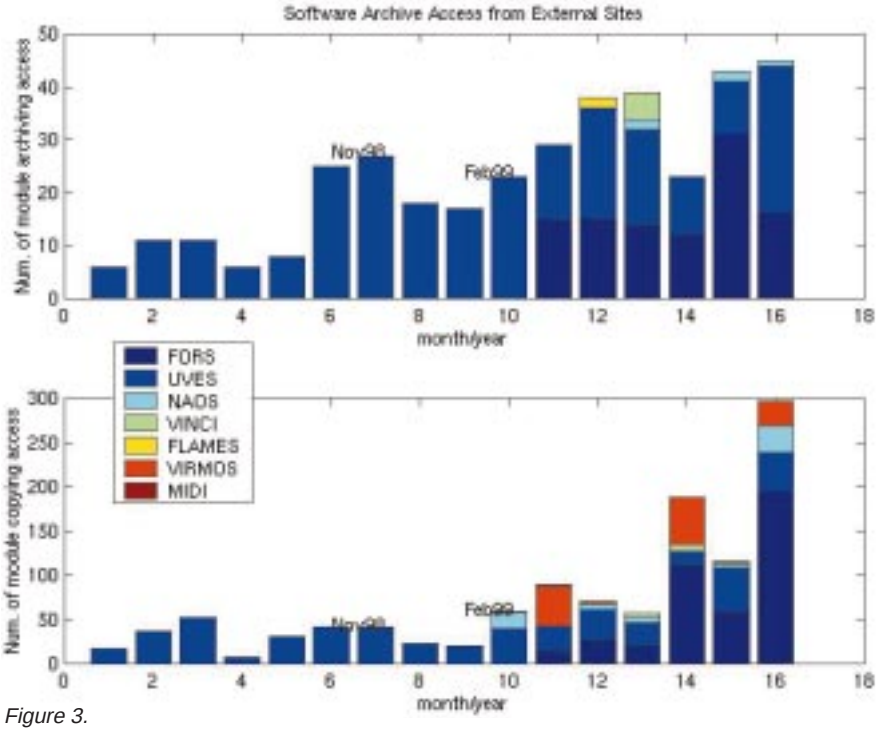

Figure 3.

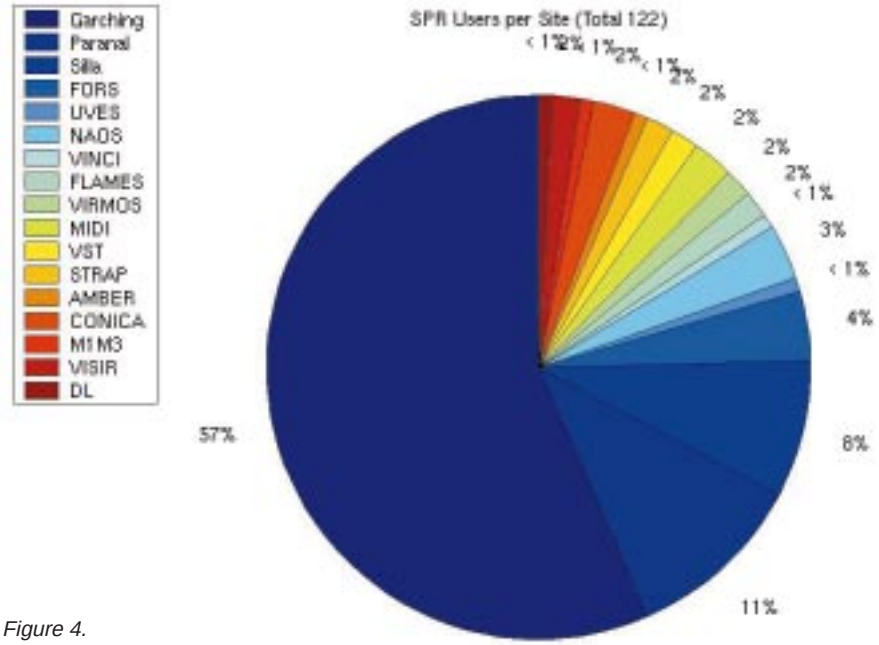

Figure 4.

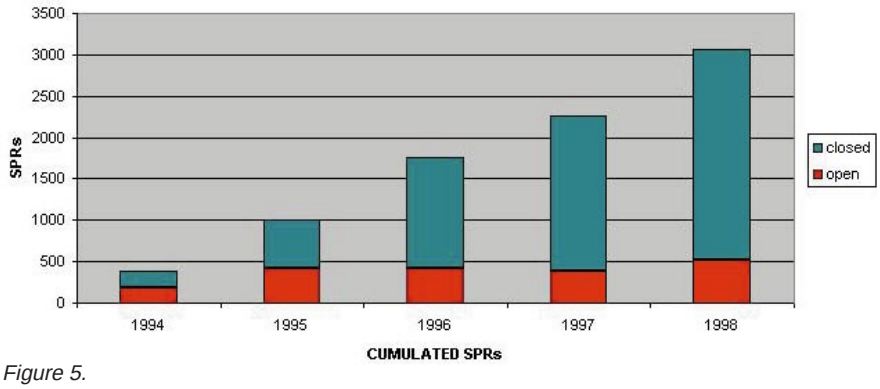

Figure 5.

commissioned on top of mountains at 2500 m in the middle of a desert, but involving people in several countries on both sides of the ocean. The Central Archive is hosted on a RAID system level 5, with hot-standby disk, and backed up in two different ways every day. This year the downtime of the server has been less than 8 days, corresponding to 2%, mainly during weekends. We are developing a better client-server mechanism and we plan to make the cmm software available on the public domain.

3. VLT Software Problem Report (VLTSPR)

The VLTSPR System is meant to be used by both internal and external users of VLT software to report errors in code or documentation or to propose a change. VLTSPR is built using the commercial tool Action Remedy (c) and has a Web Browser interface. This is the basic workflow of the system:

• Problem submitted, depending on the subject, some people are notified immediately

• The SPR is discussed in the Software Configuration Control Board meeting and a Responsible Person is appointed for the problem

• Responsible works on problem

• Responsible can close the SPR (must add a final remark on it)

• People can add comments any time.

At present there are about 120 names in the user database, 75% ESO users (both Europe and Chile), the remaining 25% from 13 external projects, some project have more sites. Figure 4 shows the present distribution of the VLTSPR users.

In Figure 5 the trend of the SPR archive over the years is shown. The number of open SPRs has always been kept under a physiological limit (about 500) that corresponds to what we are able to treat between two releases.

Figure 6 reports the distribution of the SPRs per area in 1997 and in 1998. As the project evolved, SPRs concerning the common software are decreasing, while the ones for the application part are going up, which is a sign of the integration activity that is now taking place.

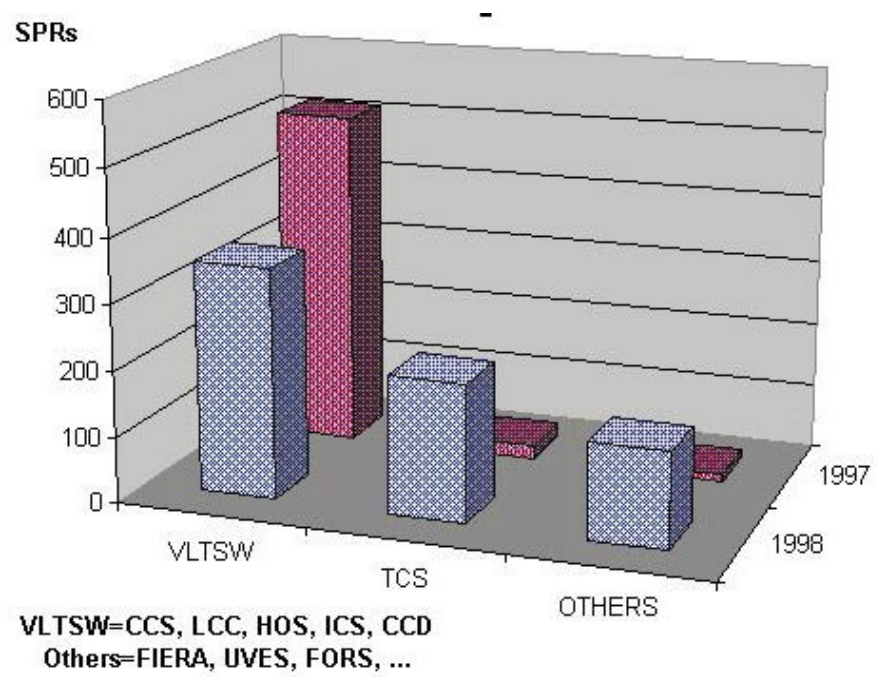

Figure 6.

4. Conclusion

Tools and Methodologies developed within the VLT Software Engineering Group have proved to be effective in supporting the VLT Software development. They can be seen as a concrete guideline and reference for all ESO internal projects and are proposed as baseline for all external collaborations.

This article is based on reports presented at ICALEPCS 99:

[1] G. Filippi, "Software Engineering for ESO's VLT project", *ICALEPCS* **93**.

[2] G. Filippi, F. Carbognani, "Software practices used in the ESO Very Large Telescope Control Software", *ICALEPCS* **99**.

E-mail: fcarbogn@eso.org

Java for Astronomy: Software Development at ESO/ST-ECF

M. DOLENSKY[1], M. ALBRECHT[2], R. ALBRECHT[1], P. BALLESTER[2], C. BOAROTTO[2], A. BRIGHTON[2], T. CANAVAN[2], M. CHAVAN[2], G. CHIOZZI[3], A. DISARÒ[2], B. KEMP[2]

[1]ESA/ST-ECF; [2]ESO/DMD; [3]ESO/VLT

Overview

The first part of this article discusses the Java computing language and a number of concepts based on it. After learning why Java is best suited for many applications in astronomy including ESO's JSky initiative and certain Web services there is a second part containing a collection of application briefs from software projects at ESO and ST-ECF. Appended is a list of contact points in house (Table 1) and an applet gallery (Table 2).

1. Why Java?

Here are the key features [1] that the authors felt were the most important arguments why Java was the first choice for their projects:

• Portability: There is only one version of source code and one version of binaries for all operating system-architectures and hardware platforms. As a result of the architecture-neutral capabilities, Java programmes execute on any platform for which a Java Virtual Machine (JVM) exists (e.g. Windows, Solaris, Mac OS, and Linux). Some web browsers come with a built-in JVM.

• JavaBeans Component Model = built-in support for code re-use: Java incorporates JavaBeans which is a software component model. The component model describes how to build an application from software components. In contrast to software libraries Beans provide an additional interface in order to support their re-use and customisation. The JavaBeans concept is widely supported by development tools.

• Common look and feel: There is built-in support of powerful GUI widgets (Swing classes) and common look and feel on different platforms.

• Applets: Applets are programmes running via web browsers. Therefore, no installation is necessary on the side of the web client and also no maintenance. Computations are performed on the client computer thereby off-loading our servers.

The next two bullet lists summarise more concepts and advantages as well as the weak points of Java technology.

More advantages and supported concepts

• Remote Method Invocation (RMI): RMI allows the execution of tasks on other machines.

• Jini: Jini defines a protocol for communication with devices. A device is, for instance, a disk drive, a TV, VCR or cellphone. With Jini there is no need for separate driver software. It's a very general implementation of plug and play capabilities.

• Enterprise JavaBeans (EJB): EJB is a specification for server side components based on JavaBeans. EJB components neither deal with server-side system-level programming nor with client-side interfaces and therefore form a middle tier containing business logic only. This gives much more flexibility when coping with changes of business rules.

• Lots of free software and a lively community with newsgroups

• Object-oriented: This implies encapsulation of data in objects and support of code-reuse.

• Security: Various security mechanisms prevent malicious code from being executed.

• Multi-threaded: Java supports thread synchronisation and enables an application to perform several tasks in parallel even if the underlying operating system is not capable of multitasking.

• Late binding: Java is capable of dynamically linking in new class libraries or instance variables at runtime.

• Robustness: Strict type checking, no pointers, no explicit memory (de)allocation, enforcing boundary checking when accessing arrays

Applet specific advantages

• No installation: Just requires a Java enabled web browser.

• Automatic software update: The latest software version is loaded whenever an applet is invoked. There exists only one copy of the software on the web server.

Weaknesses

• Rapid development led to a steady stream of new Java versions and framework specifications rendering it a moving target. It is only slowly settling down.

• Write once but install (in case of applications) and test everywhere: Platform specific bugs such as incompatibilities between JVMs are hard to detect and circumvent.

Table 1: Contact Points and Java Links in House.

Service	Contact Point
Java Interest Group (JIG) Mailing List	jig-list@web3.hq.eso.org Send mail to Tim Canavan tcanavan@eso.org for registration.
Java tools in archive and dmd UNIX domains	Bob Kemp bkemp@eso.org
Java tools for archive operations and ecf domain	Markus Dolensky mdolensk@eso.org
JSky Home Page	http://archive.eso.org/JSky/
JSky Mailing List	jsky@egroups.com Send mail to jsky-subscribe@egroups.com for registration.
JSky Repository	ftp://ftp.archive.eso.org/pub/jsky
P2PP Project Page	http://www.eso.org/~amchavan/projects/jp2pp/development-docs.html

Table 2: Applet Gallery.

Applet Name	Description	URL
ESO ETC	ESO Exposure Time Calculator	http://www.eso.org/observing/etc/
Isql	JDBC interface to databases	http://archive.eso.org:8009/sample/gateway.html
JIPA	Download Page of Java Image Preview Application	http://archive.eso.org/java/jipa1.35/
JPlot	Applet for Jitter Analysis	http://archive.eso.org/archive/jplot.html
Spectral	HST Preview Applet for Spectra	http://archive.eso.org/preview/preview/preview_hst/Y29E0305T/fits/spectral/4
TimeGraph [10]	Applet for System Load Monitoring	http://www.hq.eso.org/bin/tg?schema=sysload

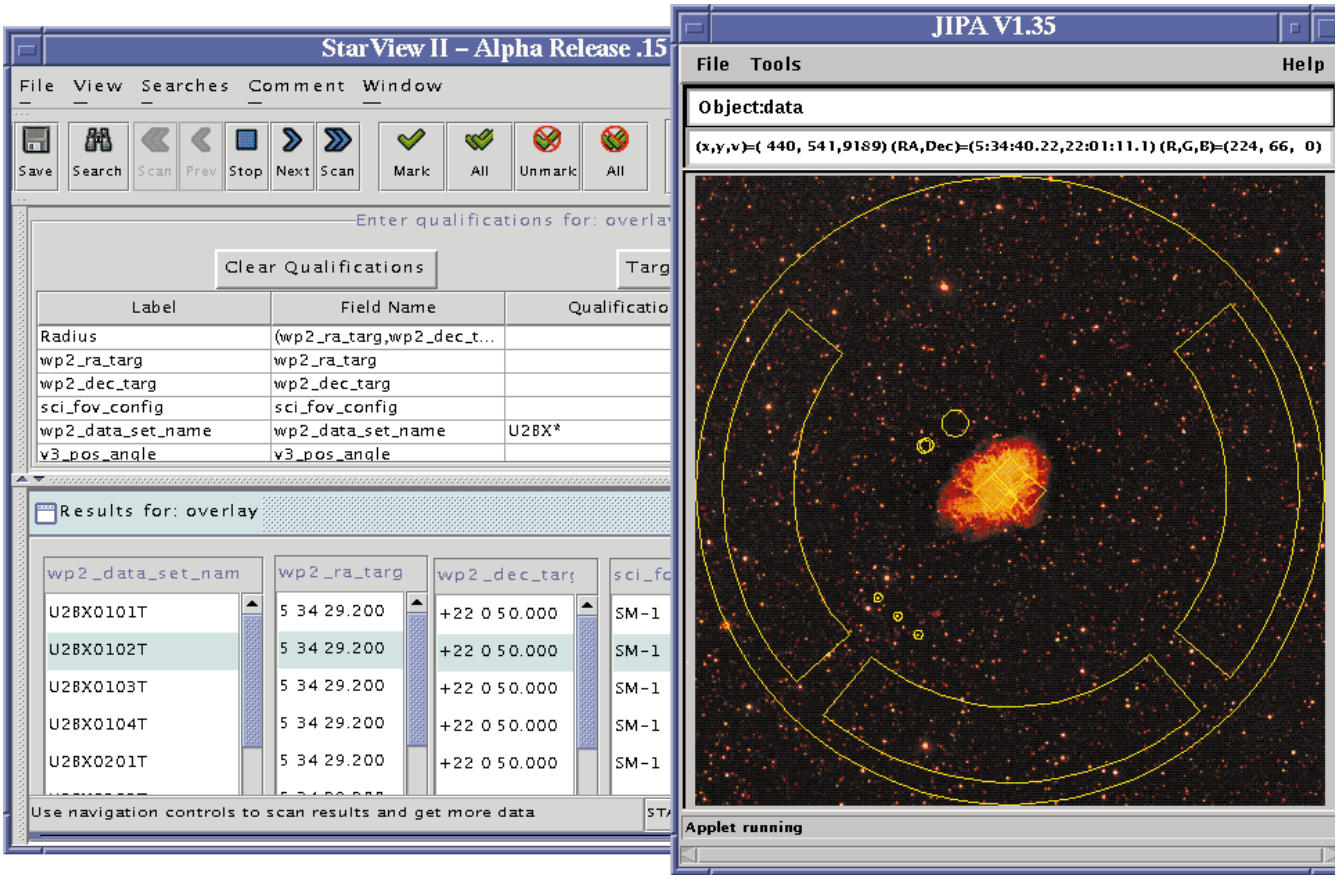

Figure 1: Alpha Release of STScI's archive browser StarView II. It uses ECF's utility JIPA to display a sky region from ESO's copy of the DSS catalogue together with an HST aperture overlay.

• Imposes strict adherence to object oriented design in contrast to C++. In fact, this could be seen as an advantage as well.

• Programmer has no direct control over system resources. Therefore flaws of built-in services like the garbage collection algorithm are hard to circumvent.

Applet specific weaknesses

• Security restrictions make it difficult to implement basic features like saving the programme status and printing.

• Lacking browser support, latency problem due to limited bandwidth and the lack of adequate caching mechanisms can lead to frustration of users.

2. Application Briefs

DBB – The Database Browser Project

The Database Browser Project is aimed at developing a library of Java classes which can be used to create interactive database browsing and editing tools. Many data-centred applications share a common structure: A user wants to select a set of items (rows) from a database according to some searching and sorting criteria, reviews a summary of the returned items, edits one or more items and saves the edited items back to the database. The DBB classes provide the application programmer with a set of tools to quickly develop interactive tools of that kind. By specialising the library, a programmer can fine tune the look and feel of the application to the desired level. DBB is used for the new Phase II Proposal Preparation System (P2PP) V.2.

DocumentView: A way of linking GUIs and Objects

DocumentView is a set of classes that link object properties with GUI components. For instance, one can link a text field widget with the title of an Observation Block (OB). Changes in each affect the other, and thus multiple GUI components displaying the property are kept synchronised. DocumentView is a component used for the P2PP tool described below.

A New Generation Phase II Proposal Preparation Tool

The successor to the current version of P2PP (Phase II Proposal Preparation System) is an application being developed using the Java programming language. The new version is largely backwards compatible with the current system, and its basic purpose is to provide help for the preparation of Observation Blocks (OBs) both at the observer's home institution and at the telescope.

The decision to rewrite version 2 of the system in Java was based on two fundamental requirements:

• To provide easier support for multiple platforms, since Java libraries are available for most operating systems and are extremely consistent in their behaviour across platforms.

• To provide a cleaner, more intuitive user interface. One of the main aims of the Swing graphics library for Java is to provide platform-independent high-level graphical components.

Design Patterns with names like Factory and Visitor [2] were used wherever reasonable in order to reduce the learning curve for future maintainers. P2PP V.2 can function as a 2- or 3-Tier client/server system with a relational database back end and an optional business object middle tier. However, users can work completely off-line, saving unfinished work on their local machine. Connection to the ESO OB repository is only needed in order to submit their OBs for execution.

Java Interface to VLT Control Software

This class library allows Java applications to interact with the non-Java VLT Control System. It provides interfaces to the the VLT Central Common Software. These interfaces are implemented as Java Native Methods, relying on the legacy VLT Common Software libraries implemented in C/C++.

The new library allows the development of high-level interfaces and VLT control applications in Java. It was made available for the first time as part of the OCT99 VLT Software Release.

P2PP V.2 uses this interface to transmit OBs to the VLT Unit Telescopes in Paranal and to get status information about their execution.

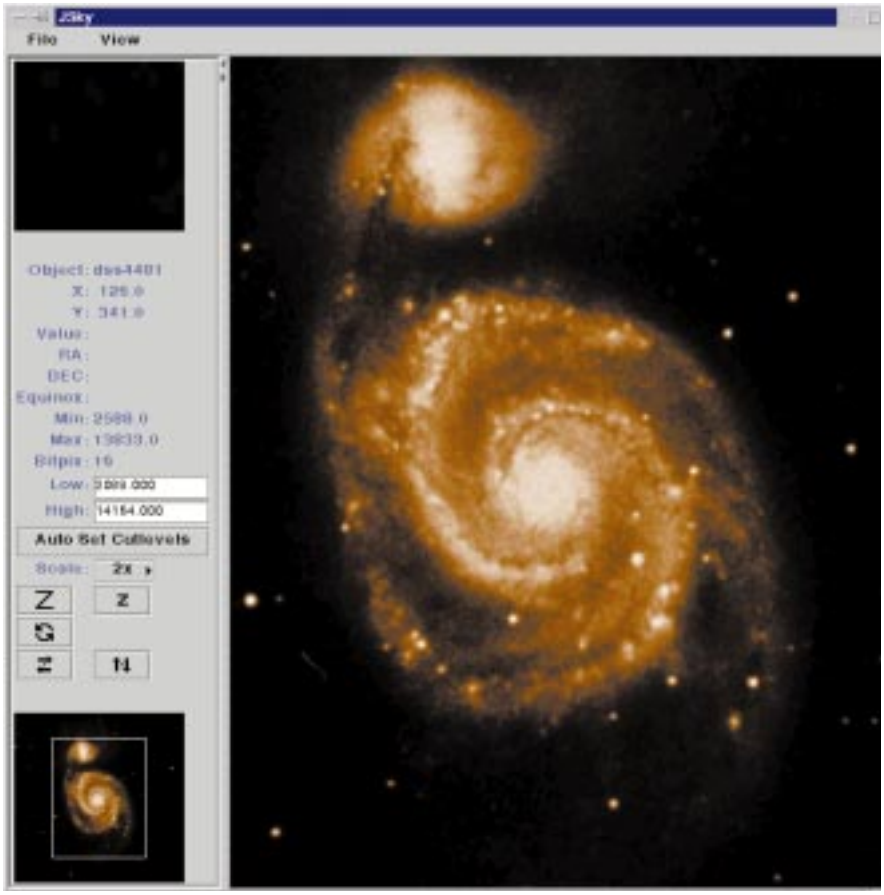

Figure 2: A first prototype of an image viewer has been developed, based on the JAI (Java Advanced Imaging) package from Sun.

Java Calibration Database Manager

The Calibration Database includes a collection of observation data and reduction procedures representing as completely as possible the observing modes and configurations of the different VLT instruments. The Calibration Database Manager is the standard application for browsing, editing, populating and aligning the local calibration database contents. This Java application is the interface between the pipeline local calibration database and the ESO archive system. It allows the ESO Quality Control Scientists of the Data Flow Operations group to request and submit files to the archive, and to structure calibration information to the formats supported by the pipeline and needed for long-term archival and trend analysis. The Calibration Database Manager and other quality control applications are described in more detail in a previous issue of *The Messenger* [3].

ESO Exposure Time Calculator

The user interface of the on-line Exposure Time Calculators provided for various VLT and NTT instrument as well as the Wide-Field Imager was implemented as a combination of HTML and Java. An observer specifies the relevant parameters in a web form, the necessary computation takes place on an ESO server and the results are returned in a page containing HTML text and a plot applet. The applet is based on Leigh Brookshaw's GNU plot library [4].

ST-ECF Applets for the Archive Interface

ECF started its efforts in this field about four years ago. Early on applets were released on the web. They are used for previewing HST spectra and images [5]. There is JPlot – a plot utility for jitter analysis of HST observations [6]. JPlot was used for quality control purposes in first place and later on put on-line as a public archive service. There is also Skymap, a simple applet that draws locations of HST parallel observations on a map.

As a logical next step, more ambitious projects followed which are currently accomplished in collaboration with other institutions like STScI and ISO IDC [7], [8]. The aim is a pure Java interface to both HST and ESO archives (Fig. 1) that will serve as a more powerful alternative to the current web interface.

JSky – Reusable Java Components for Astronomy

The JSky development effort aims to provide a library of reusable Java components for astronomy. Based on experiences with the Skycat application, the first components being developed are for image and catalogue display and manipulation. The goal is to eventually have a collection of general-purpose and astronomy-related JavaBeans that may be easily assembled into applications using a Bean Builder, ideally with little or no hand-written code necessary.

The prototype can display FITS images and supports zooming, panning, colour maps, and automatic cut level setting. Initial tests indicate that the performance is satisfactory for small images, as long as the JAI native library (mlib) is available. At the time of writing, this is only the case under Windows and Solaris, although a Linux version is due out soon. The current version does not yet handle large images well, but can be optimised to do so. The FITS reader is based on Thomas McGlynn's Java implementation, which currently always reads in the entire image. A future version will provide support for splitting the image into tiles, which is the only way to efficiently handle large images in JAI.

The image display application (Fig. 2) currently has a hard-coded layout. In the end, the goal is to build the application from JavaBeans and allow the users to change the layout, add new panel items, remove unwanted ones, etc.

The Java implementation of the catalogue browser looks pretty much like the Skycat version, so far, although this will likely change. The panel layout can be generated automatically, based on an eXtensible Markup Language (XML) catalogue description and the catalogue data itself may also be in XML [9]. The new catalogue interface should be more flexible than the Skycat version and allow various catalogue types to be supported by means of a catalogue registry.

JSky is an open development platform and contributions of general-purpose or astronomy-related software and components are welcome. There is a JSky home page [Table 1] as well as a JSky ftp repository [Table 1].

References

[1] A. Walsh, J. Fronchkowiak, 1998, "Java Bible", IDG Books Worldwide Inc, p. 7–18.
[2] Gamma et al., 1995, "Design Patterns: Elements of Reusable Object-Oriented Software", Addison-Wesley.
[3] P. Ballester, A. Disaro, D. Dorigo, A. Modigliani, J.A.Pizarro de la Iglesia, "The VLT Data Quality Control System", *The Messenger* **96**, p. 19.
[4] GNU Graph Class Library http://www.sci.usq.edu.au/staff/leighb/graph/
[5] Dolensky et al., 1998, "HST Archive Services Implemented in Java", *The Messenger* **93**, 26.
[6] Dolensky et al., 1998, "How the Analysis of HST Engineering Telemetry Supports the WFPC2 Association Project and Enhances FOS Calibration Accuracy", *The Messenger* **93**, 23.
[7] Binegar et al., 1999, "Browsing astronomical archives with StarView II and interacting with analysis tools such as JIPA", in ASP Conf. Ser., *ADASS* **99**, in press.
[8] http://archive.eso.org/~mdolensk/publ/jskybof/
[9] http://vizier.u-strasbg.fr/doc/astroxml.htx
[10] TimeGraph Download Page http://www.ece.utexas.edu/~tbieleck/

E-mail: mdolensk@eso.org

The ESO Public Imaging Survey

A. RENZINI and L. DA COSTA, ESO

1. Background

In the era of 4-m-class telescopes it was common to select targets and/or prepare observations using deep Schmidt plates for which full sky coverage was available down to $m \sim 23$. Now, in the blossoming era of 8-m-class telescopes one needs much deeper survey data to feed high-throughput, high-multiplex spectrographs able to reach at least two magnitudes deeper, or to find relatively rare objects such as clusters of galaxies, brown dwarfs, or trans-neptunian objects (for an extensive list of such potential targets see Renzini 1998, *The Messenger*, 91, 4). To a large extent, the scientific outcome of an 8-m-class telescope critically depends on the availability of preparatory imaging surveys, and the demand for deep and wide surveys will intensify as other large-aperture telescopes become operational world-wide and the competition becomes more and more fierce.

CCD and computer technology have evolved at a rapid pace over the last two decades, and multi-colour, digital imaging surveys of appropriate area and depth are within reach. Even though there are a number of ongoing optical/infrared digital all-sky surveys (DENIS, SDSS, 2MASS), none of them are particularly suitable for feeding targets for large telescopes (for most possible targets they are not deep enough) nor will they be publicly available in the near future. Surveys more suitable to large telescopes are being conducted at several observatories (e.g., CFHT, CTIO, La Palma, Kitt Peak) with the products becoming public within their respective communities. Groups with specific science goals are also conducting ambitious surveys, but again these data are unlikely to become accessible to general ESO users in a short-time scale.

To meet this challenge, in 1996, ESO took the initiative of proposing to carry out a public survey to fulfill at least some of the short-term needs of the ESO community in view of the first scientific runs of the VLT. Without hampering the possibility of groups to conduct their own surveys, a public survey offers a number of advantages. In particular, data can be used for a broad range of scientific applications, thus resulting in a substantial saving of telescope time (that can be as high as a factor of 10!), compared to the case in which each individual science group has to secure its own survey data. Moreover, public survey data can be easily complemented by "privately" acquired data for specific applications, such as in the case of second-epoch or narrow-band filter observations.

A Working Group (WG) was therefore appointed in 1996 to design the survey and to supervise the work of the Survey Team charged to carry out the observations, data reduction and distribution of survey products. Both the WG and the Survey Team were assembled from the community itself, with ESO providing the coordination and the required facilities and resources.

The main objectives of the resulting ESO Imaging Survey (EIS) were to conduct a public optical-IR imaging survey at the NTT, to reduce the data, construct object catalogues, and select from them special classes of objects of potential interest for VLT programmes. All this within a short time scale, before the start of operation of the first Unit Telescope of the VLT. In addition, EIS was seen as a first step towards developing an appropriate environment for carrying out future surveys, public as well as private. Indeed, the software tools developed by the programme were regarded as an integral part of the survey products, to be disseminated throughout the ESO community to facilitate the reduction and analysis of wide-area imaging data. The dissemination of such tools was seen as essential for the community to take full advantage of dedicated imaging telescopes such as the MPG/ESO 2.2-m telescope, now already in operation, and the VLT Survey Telescope (VST, Arnaboldi et al. 1998, *The Messenger*, 93, 30) to be installed on Paranal.

2. The EIS Project and the WFI Pilot Survey

In practice, to combine as far as possible wide-area coverage and depth, EIS consisted of two complementary projects: EIS-WIDE and EIS-DEEP. The goal of EIS-WIDE was to cover with EMMI@NTT four patches in the sky, 6 square degrees each, providing *V* and *I* data to a limiting magnitude of $V_{AB} \sim 24.5$ and $I_{AB} \sim 24$. This part of the survey was optimised to detect candidate clusters of galaxies at moderate to high redshift ($z \lesssim 1$). A ~ 2-square-degree fraction of one of the patches was also to be observed in U and B to allow for the identification of QSOs, metal-poor stars, etc.

The goals of EIS-DEEP were to cover with SUSI2 and SOFI three adjacent pointings in the Hubble Deep Field South including the fields covered by the various HST cameras, and four adjacent pointings in the AXAF deep field. In both cases the multicolour *UBVRI-JHK* data should have been deep enough to provide accurate photometric redshifts and to select Lyman-break galaxies. In practice, this required limiting magnitudes in the range 26–27 in the optical passbands and 23–24 in the infrared.

The one-year period (July 1997–July 1998) available to achieve the primary goals of EIS-WIDE represented a formidable task, as no consolidated experience existed at ESO or in the community. Apart from the limitations due to the weather, the goals were only met thanks to the enthusiastic response of many scientists from the community who brought their specific experience to ESO and to the resources made available at ESO to support the temporary relocation of these scientists. The contribution of ESO and ECF staff was also critical for several aspects of data processing, archiving, and distribution.

With the advent of the Wide Field Imager (WFI) at the 2.2-m telescope (Baade et al 1999, The Messenger, 95, 15) a "WFI Pilot Survey" was designed by the WG and recommended by the OPC to be conducted by the EIS Team. The scientific goal of the Pilot Survey was essentially to complete that part of the EIS-WIDE project that could not be done due to bad weather during the allocated nights (it is worth recalling the impact of El Niño in 1997–98). The "pilot" designation was meant to reflect the development period required for the major upgrade of the survey software to enable it to pass from one-CCD (EMMI) or two-CCD camera data to the eight 2k × 4k CCDs of WFI.

The companion article by da Costa et al. in this issue of The Messenger describes in some detail what was achieved by these surveys, with emphasis on the survey products. All the data from EIS-WIDE, EIS-DEEP and the WFI Pilot Survey were delivered to the community in due time. Over the last three Calls for Proposals (P63–P65), over 100 proposals for four different Panels, were based on the EIS data, or referred to EIS. Follow-up observations were conducted using ESO telescopes as well as other facilities to prune samples in preparation of VLT proposals. Targets selected from the EIS data were also used during Science Verification of UT1/Antu as well as of FORS1 Commissioning and Science Verification.

3. The Public Survey, Period 64 to 67

The usefulness of Public Surveys in support of VLT programmes being generally recognised, the WG at its meeting in September 1998 recommended ESO to issue a "Call for Ideas" for future public surveys to be conducted with the 2.2-m and NTT telescopes (The Messenger 94, 31). The resulting "ideas" were discussed in depth by the WG in March 1999, and two optimised proposals emerged. A small short-term proposal to complete the EIS-WIDE survey reaching the goals as originally stated, and a two-year Public Survey programme. The latter consists of three parts: (1) a deep multi-band (UBVRI) optical survey with the WFI over three fields of one square degree each; (2) a deep near IR survey with SOFI, covering two 450 square arcmin fields selected within the area observed in the optical; and (3) a shallower set of WFI observations in *V* and *I* of selected stellar fields in preparation for FLAMES at UT2/Kueyen (hereafter the "Pre-FLAMES Survey").

The selected fields for the deep optical/IR survey (hereafter Deep Public Survey, DPS) are given in Table 1. The main scientific drivers for this part of the Public Survey are the search for high-redshift objects: galaxies (e.g. Lyman-break galaxies), clusters and QSOs, as well as the possibility to derive photometric redshifts from such a large, homogeneous, multicolour database. The goals and requirements in terms of limiting magnitudes are similar to those of EIS-DEEP described above except that DPS is meant to cover a much larger area. The same database will also provide a unique and urgently needed tool for studies of Galactic structure and stellar populations. The DPS is therefore designed to provide targets for several of the first-generation VLT instruments, with emphasis on FORS1 and FORS2, ISAAC, UVES, VIMOS, and NIRMOS.

On the other hand, the Pre-FLAMES Survey is of crucial importance for stellar astronomy studies with the FLAMES System on UT2/Kueyen, where the OzPoz fibre positioner can pick up ~ 130 targets over a field of 25 diameter (well matched by the field of view of WFI) and feed the MEDUSA mode of GIRAFFE. Alternatively, 8 fibres from OzPoz could send the light of as many targets to UVES, over to the other Nasmyth platform of the same telescope (see Renzini 1999, *The Messenger*, 96, 13). The accuracy of fibre positioning, which requires accurate target coordinates to start with, is critical. Existing stellar catalogues fail to give the information that is necessary to operate FLAMES, i.e., coordinates with the required astrometric accuracy $\lesssim 0\farcs1$ rms) combined with multicolour information. The tentatively selected fields for the Pre-FLAMES Survey are listed on the EIS web pages. Interested scientists are welcome to give suggestions to complement and/or improve the list.

Table 1: Deep Public Survey Selected Fields.

Field	α(J2000.0)	δ(J2000.0)
Deep 1	22 43 00	–39 58 00
Deep 2	03 32 28	–27 48 00
Deep 3	11 22 00	–21 35 00

The Public Survey proposal was submitted as a Large Programme in response to the Call for Proposals for Period 64, applying for a total of 81 nights: for the DPS 54 nights at the 2.2-m telescope and 15 nights at NTT for its IR part, plus 12 nights at the 2.2-m telescope for the Pre-FLAMES Survey. This Large Programme was proposed for a two-year period, hence being distributed over ESO Periods 64 through 67. Details of the Public Survey, including the original proposal, can be found at http://http.hq.eso.org/science/eis/public-surveys/

This Public Survey "large proposal" was approved and recommended by the OPC, and 18 nights with WFI@2.2 and 8 nights with SOFI@NTT have been scheduled in Period 64. To increase the participation of the community in the Public Survey, an Announcement of Opportunity was also issued for groups in the community to carry out the observations and data reduction of the infrared part of the DPS, following the same guidelines of the EIS Team. Following an examination of the proposals, the WG has already selected the Team that will be in charge of this part of the survey (PI H. Jørgensen, Copenhagen).

The Public Survey in periods 64–67 will provide the ESO community with a competitive edge in the realm of the high-redshift universe as well as in stellar studies. Furthermore, it will allow the continuation of the development effort of EIS that will guarantee a smooth transition between the WFI@2.2 and the VST that will be equipped with ΩCam, four times larger than WFI in both field of view and number of pixels.

4. The Public Survey Products and Distribution

Among the many requirements of a Public Survey, the most important is perhaps that the data products be easily retrievable by external users. While this may seem trivial, practice has shown that it is not always simple to reconcile the needs of different users – with the implied large variety and size of the products – with other practical constraints such as efficiency and resources. In addition, data from ground-based optical observations are subject to atmospheric conditions and thus require more information to be properly characterised, relative to radio or space-based data.

The EIS/Pilot Survey project made available four kinds of data products: astrometrically and photometrically calibrated images, filtered and verified object catalogues drawn from single-colour coadded frames, derived catalogues such as colour catalogues, and target lists. Each release was also accompanied by papers describing the observations, data reduction, the different types of catalogues available and the target lists produced. The object catalogues were also essential to validate the data by computing simple statistics such as the number counts of stars and galaxies, colour-colour diagrams for point-sources and the two-point angular correlation function for galaxies. This allowed the photometric zero-points, star/galaxy classification, and uniformity of the data to be tested.

The primary reason for adopting this data release model was the strong desire to have verified data publicly available in the shortest possible time to meet the stringent deadlines imposed by the imminent start of the VLT regular operations, which began with the submission of the proposals for Period 63 (deadline October 1, 1998). However, this model is not the most suitable for long-term projects such as the Public Survey described in the previous section. The time baseline for the completion of the project is much longer, and intermediate products may be valuable for different applications. While it is obviously highly desirable to cut to the minimum the time lag between the collection of the survey data and the VLT follow-up, the sheer volume of the data expected from WFI@2.2m requires more time for detailed verification of the data products. In addition, users may have their own ideas on how to best extract catalogues for their specific scientific purposes, while final results for a given sky area can only be produced after all the observations are completed.

One solution to accommodate these various constraints is to provide both a prompt release, soon after an observation run is completed, and a more complete release on a time table synchronised with the ESO observing periods. In this framework one provides rapid access to reduced – but still unverified – data, thus allowing users to extract objects directly from the images. Meanwhile, the Survey Team will work to prepare complete and fully verified data releases. The aim is to strike a balance both between the needs of the community and the operational requirements, and between speed and quality. Following this approach, the distribution of data accumulated from the Public Survey will consist of prompt and final releases, which will occur on different time scales, as described below.

4.1. Prompt releases

The prompt releases will consist of products that are generated directly by the EIS-WFI pipeline. These will provide the opportunity for users to have a "quick-look" at the data soon after they have been acquired. These releases will consist of:

• Astrometrically and photometrically calibrated coadded images of dithered, single-pointing exposures and associated weight maps. The astrometric and photometric accuracy shall be better than 0.″05 and 0.1 mag,

• Catalogues of objects extracted from these images using SExtractor, in the form of FITS binary tables.

Such releases are expected to start as soon as the ongoing work of upgrading the EIS-WFI pipeline is completed and the new version properly tested, which should occur by the end of 1999.

These data together with SExtractor, LDAC and Drizzle softwares, which are publicly available and can be retrieved from the EIS home page, or directly from their respective authors, will enable users to work in parallel to the Survey Team, starting from the same basic data and at the same time. Users will, therefore, be able to evaluate the data and prepare, if they so desire, their own customised catalogues without having to rely solely on those derived by the Survey Team. Moreover, new tools are in the process of being installed which will further enhance the scope of work that can be done outside ESO without the need for distributing large amounts of raw or processed data.

4.2. Complete releases

Complementing these prompt releases, complete releases of verified data including all the data accumulated during all previous observing periods will occur every 6 months, namely on February 15 for odd periods and August 15 for even periods. These will include not only images but also a host of derived products which require more time for their proper preparation and verification. These releases will include:

• Tools to allow the extraction of image sections (cut-outs) from image mosaics and associated weight maps

• Co-added, mosaiced images of individual patches and associated weight maps

• Colour catalogues for multi-passband observations

with all image products being photometrically and astrometrically calibrated as specified above.

Each release will be followed by an update of the web and will be accompanied by papers prepared by the Survey Team. These papers are an integral part of the data distribution as they describe in detail the observations, the quality of the data, the data reduction and verification procedures, and the description of the content of the derived catalogues and of the methodology used in their preparation. These papers are also important as a reference, thereby recognising the commitment of ESO in producing the data and in making them available to the ESO community. While no direct scientific exploitation of the data will be done in these papers, they would still represent a reasonable reward for the members of the Survey Team for their effort in conducting such a survey of public utility.

5. Data Distribution Logistics

A daunting task for public wide-field imaging surveys is finding the ways and means of exporting the data to outside users. To give an indication of the scale of the problem it suffices to mention that the Pilot Survey alone has produced over 0.5 Terrabytes of data in roughly 11 nights of WFI observing, while 66 nights have been assigned for the Public Survey at the WFI@2.2. Even after co-addition of all dithered images, a single-passband 6-square-degree mosaic consists of 6.5 Gigabytes, and a complete data set for the recently observed EIS patches (combining data from EMMI and WFI) comprises 64 Gb of images and weight maps, and 32 Gb of context maps. The stellar fields comprise another 63 Gb of images. Therefore, with the presently available technology it is unrealistic to consider the distribution of pixel maps for an undetermined number of requests. To make the distribution possible, with the resources currently available at ESO for this task, a certain number of constraints are unavoidable. The distribution of bulk data must be limited to well-defined packages of reduced data, produced semi-automatically; distribution of large volumes of data must be limited to certain media, e.g. DLT model 7000 which store 35 Gb and are produced in about 2 hours (5 Mb/s). Large volumes of data cannot be requested by a simple click on the web page, but will have to be requested by submitting a statement of purpose which should include a scientific justification and demonstrate that resources are available at the home institute to handle the requested amount of data.

Note that even a single WFI frame (267 Mb) cannot be transferred by FTP in a reasonable time, under normal conditions. Major improvements will have to await the development of new storage media and of broadband technology. This also raises the issue of how rapidly and widely new storage media become available throughout European institutes. By now it should be clear that the rate at which images can currently be disseminated lags far behind the rate at which they are acquired.

In order to overcome this problem, the community is urged to consider using compressed images, which can lead to a significant reduction (as much as a factor of 500) in the size of the images. However, such compression schemes inevitably involve some loss of information and the scientific value of the resulting products depends on the specific application. Experiments conducted by the Survey Team indicate that for astrometric applications very little is lost, even for very large compression factors. In fact, the loss in accuracy is $\lesssim 0.5$ of pixel size, comparable to the estimated internal error of the astrometric solution. Examples of compressed images have been made available in the most recent data release. With the advent of the WFI it seems that the combination of compressed images for large fields and full resolution cut-outs for small regions should be seriously considered.

In summary, to a large extent the scope of the Survey Team work and the range of data products have been dictated by the recognition of the difficulties in exporting full-resolution images, as resulting from the direct experience with the EIS project, and the expected trend with the WFI@2.2 and the ΩCam at the VLT Survey Telescope. One needs to efficiently translate terabytes of imaging data into megabytes of useful information in the form of the various data products made available by the Survey Team (single and multi-band object catalogues, target lists, cut-outs, postage stamps). In this context it is important to emphasise once more that the primary goal of the ESO public surveys has been to support VLT observations and not to be an end in itself.

6. Future Plans

The Survey Team and the ESO Archive Group continue to explore other ways to provide external users with more flexibility in their use of the survey data. In the short term it will be possible to use the SKYCAT interface to run SExtractor on image cut-outs extracted from WFI mosaics, of sufficient size ($12' \times 12'$) to include the field-of-view of the FORSes and of individual VIMOS and NIRMOS cameras, regardless of their respective orientations on the sky. In the long term, efforts will be made to implement an object-oriented database which will allow users to fully explore the multi-dimensional position, magnitude and colour space defined by the objects extracted from the imaging surveys. The development of such a database, where astronomical objects extracted from survey data can be stored, updated and associated with all the information available from internal and external sources, and of tools for searching special categories of objects is an essential element for the efficient use of public survey data, as well as of all other imaging data that will also become publicly available after the proprietary period.

7. Conclusion

Besides the data, arguably one of the most important contributions of the EIS project has been to foster a collaboration between different European groups to develop a comprehensive imaging data analysis pipeline for the timely and full exploitation of the data that will become available from wide-field imagers. EIS has both benefited from and contributed to this ongoing effort, by capitalising on the available expertise and by providing data and a realistic framework and time-table to test concepts, designs and implementations of pipelines, database architecture and data archiving and distribution schemes. Since the first feasibility study carried out in 1995, over 30 people have contributed to the EIS effort among EIS visitors, WG members and ESO staff and fellows.

EIS has also provided a stimulating environment for the introduction of students to modern techniques of data reduction and analysis and the means to disseminate their experience throughout the community. This has been achieved by the EIS Visitor Programme which has sponsored long-term visits, ranging from 6 months to over 2 years, of 15 people over the past two years as well as short-term visits of leading experts acting as consultants. While about half of the long-term visitors have already returned to their home institutes, a large fraction continues to contribute to EIS in different ways.

As stated over two years ago, EIS was conceived as an experimental project not only to provide targets for the first year of VLT (see da Costa et al. in this issue of *The Messenger*) but also to explore the feasibility of conducting public surveys using dedicated wide-field imaging telescopes. Indeed, with its 9×9 arcmin field of view, EMMI@NTT was far from being the ideal instrument for wide area surveys. Yet, without the experience gained with EIS it would now be much more difficult to efficiently deal with the WFI@2.2 data, and in the medium term perspective with the almost 10 times larger data flow from the ΩCam@VST. EIS has served to prototype and build a framework for this type of long-range programme, essential for the whole ESO community to benefit from such telescopes, and to do so to the largest possible extent independently of the effective resources available at the individual institutes.

The new policy outlined here is meant to bring the data promptly to the users, while allowing the Survey Team more time to deliver the final products. Budget constraints obviously limit the size of the Survey Team, which cannot grow at the same pace as the data flow. Hopefully, this new model will stimulate new uses and checks of the data. Experience has shown that, regardless of the care taken, handling large volumes of data is a difficult task and only by the exhaustive use of the data in different applications can problems be detected. Therefore, the participation and the feedback from the users is essential to ensure the quality of the data. Users are also encouraged to periodically visit the EIS home page to monitor any new version of the various releases, and report any possible error.

8. Acknowledgements

We would like to thank the EIS Team and the ESO Archive Group for their continuing efforts to explore ways of improving the accessibility of the data by external users, as well as the NTT and 2.2-m Telescope Teams for their cooperation.

E-mail: arenzini@eso.org

ESO IMAGING SURVEY: Past Activities and Future Prospects

L. DA COSTA[1], S. ARNOUTS[1], C. BENOIST[1], E. DEUL[1,2], R. HOOK[3], Y. -S. KIM[1], M. NONINO[1,4], E. PANCINO[1,5], R. RENGELINK[1,2], R. SLIJKHUIS[1], A. WICENEC[1], S. ZAGGIA[1]

[1]*European Southern Observatory, Garching b. München, Germany*
[2]*Leiden Observatory, Leiden, The Netherlands*
[3]*Space Telescope – European Coordinating Facility, Garching b. München, Germany*
[4]*Osservatorio Astronomico di Trieste, Italy*
[5]*Dipartimento di Astronomia, Universtà di Padova, Italy*

1. Introduction

The ESO Imaging Survey (EIS) project is an ongoing effort to carry out public imaging surveys in support of VLT programmes. Background information on the original and future goals of the programme can be found in Renzini & da Costa (1997) and in a companion article by Renzini & da Costa in this issue of *The Messenger*.

The first phase of the project, which started in July 1997, consisted of a moderately deep, large-area survey (EIS-WIDE) and a deep optical/infrared survey (EIS-DEEP), with the observations being conducted at the NTT. EIS has recently reached another milestone with the completion of a Pilot Survey using the Wide-Field Imager (WFI) mounted on the MPG/ESO 2.2-m telescope at La Silla.

The purpose of this contribution is to briefly review the results of the original EIS and to give an update of the results obtained from the observations carried out as part of the Pilot Survey. The ongoing work to develop an advanced pipeline for handling data from large CCD mosaics and of facilities to make access to the data products easier to external users are also discussed.

2. EIS-WIDE

This part of the survey consisted of a mosaic of overlapping EMMI-NTT frames (9×9 arcmin) with each position on the sky being sampled twice for a total integration time of 300 sec. The observations were carried out i n the period July 97–March 98 and covered four patches of the sky south of $\delta = -20°$ and in the right ascension range $22^h < \alpha < 10^h$, thus producing targets suitable for the VLT almost year-round. The locations of these fields are shown in Figure 1 and their approximate centres are given in Table 1, which also lists the area covered in each passband. The typical depth of the survey, as measured from the co-added mosaics and with the magnitudes expressed in the AB system, is given in Table 2 which lists: in column (1) the passband; in column (2) the median seeing; in column (3) the 1σ limiting isophote; in column (4) the 80% completeness magnitude (e.g., Nonino et al. 1999); in

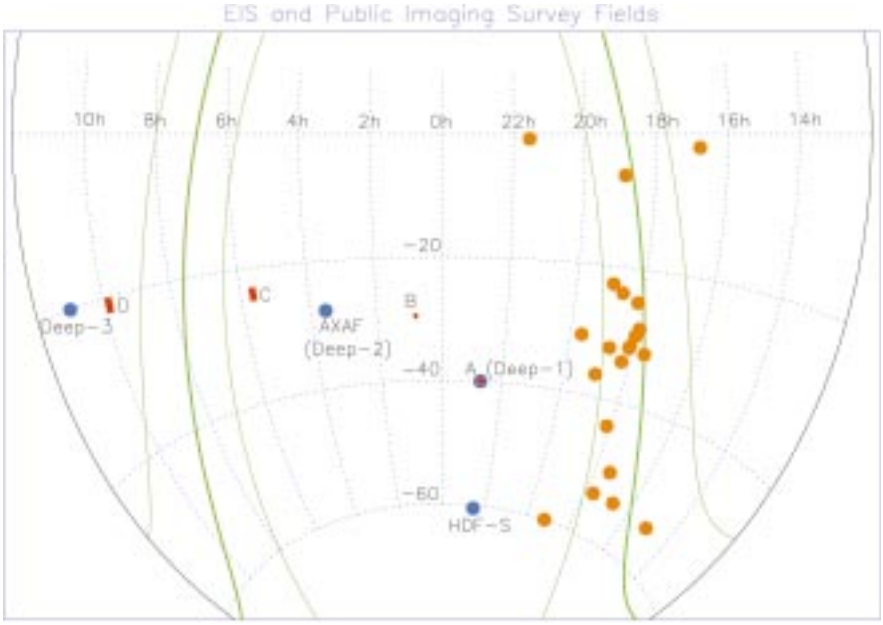

Figure 1: Sky projection showing the location of the original EIS-WIDE patches (red), the EIS-DEEP AXAF and HDF-S fields (blue), and the stellar fields of the Pilot Survey (orange). Also in blue are the new fields selected for the Deep Public Survey to be carried out in periods 64–67. Note that one of the regions selected coincides with patch A and the other with the EIS-DEEP AXAF field (see Fig. 2). The third field (Deep-3) has been selected in a region with lower absorption and less crowding than patch D. The right ascension range was chosen to distribute as much as possible the observations throughout the year.

Table 1: EIS-WIDE: Sky Coverage (square degrees).

Patch	α_{2000}	δ_{2000}	*B*	*V*	*I*
A	22 43 03	–39 58 30	–	1.2	3.2
B	00 48 22	–29 31 48	1.5	1.5	1.6
C	05 38 24	–23 51 54	–	–	6.0
D	09 51 40	–21 00 00	–	–	6.0
Total			1.5	2.7	16.8

column (5) the 3σ limiting magnitude within an aperture twice the median FWHM; and in column (6) the originally proposed magnitude limits (Renzini & da Costa 1997) expressed as in column (5). Note that these numbers are representative values since, as pointed out in the original papers (Nonino et al. 1999, Prandoni et al. 1999, Benoist et al. 1999), the observing conditions varied significantly during the course of the observations. Comparison of Tables 1 and 2 to the original goals of the survey (Renzini & da Costa 1997, and revised in da Costa 1997) shows that, while the desired limiting magnitudes were reached, not all the objectives were met. Among the most important omissions were the observations of a comparable area in V and of patch B in the U-band. The incompleteness was due to a combination of poor weather conditions and unexpected overheads in the observations. A total of about 42 nights were assigned to this part of the project out of which about 30% were lost due to the weather alone, compromising especially the coverage of EIS patches A and B. At the time, the Working Group (WG) in charge of overseeing the survey decided to postpone the U-band observations of patch B and the V-band observations of the other patches, giving priority to the I-band survey.

Table 2: EIS-WIDE: Limiting Magnitudes (AB system).

Filter	FWHM (arcsec)	μ_{lim} (mag arcsec^{-2})	80%	3σ (2 × FWHM)	3σ (proposed) (2 × FWHM)
B	1.0	26.5	24.6	24.2	24.2
V	0.8	26.2	24.4	24.0	24.5
I	0.8	25.5	23.7	23.7	24.0

Despite the smaller total area and the varying quality of the data, it was possible to meet most of the primary science goals of the survey. Particularly successful has been the *I*-band survey covering ~ 17 square degrees to a limiting magnitude I_{AB} ~ 23.5, currently the largest survey of its kind in the southern hemisphere. In addition the survey provided ~ 3 square degrees in *V I* and ~ 1.5 square degrees in *B V I*. From these data, samples of distant clusters of galaxies and quasar candidates were compiled (Olsen et al. l999a,b, Scodeggio et al. 1999, Zaggia et al. 1999) and used in several follow-up observations by different teams. The data, comprising astrometrically and photometrically calibrated pixel maps, derived catalogues and target lists, were made publicly available in March and July 1998 (Nonino et al. 1999, Prandoni et al. 1999, Benoist et al. 1999), meeting the planned deadlines. To ease the access to the data, a web interface was created to enable external users to request survey products, to extract image cutouts and to examine the selected targets on-line.

The accuracy of the relative astrometry is ~ 0.03 arcsec, making the coordinates sufficiently accurate for the preparation of multi-object spectroscopic observations. The internal accuracy of the photometric zero-point has been estimated to be better than 0.1 mag, consistent with the results obtained from comparisons with other data (e.g., DENIS). However, as more data in different passbands became available, gradients of the photometric zero-point, on a degree scale, have been noticed and are currently being investigated. The results of these investigations will be reported in due time.

3. EIS-DEEP

This part of the survey consisted of deep optical/infrared observations using SUSI2 and SOFI at the NTT of the HDF-S and AXAF fields shown in Figure 1. The original observations were carried out in the period August–November 1998, with all the data being publicly released December 10–12, 1998 (da Costa et al. 1999b, Rengelink et al. 1999). The release included fully processed and calibrated images, single-passband and colour catalogues, and a tentative list of *U*-and *B* dropouts. The centres of the different fields observed with SUSI2 and SOFI, chosen to provide some overlap, are given in Table 3. The data available for these fields are summarised in Tables 4 and 5 which provide, for each field, the following information: in column (1) the passbands available; in column (2) the total integration time; in column (3) the number of frames; in column (4) the final FWHM as measured on the co-added image; in column (5) the 1σ limiting isophote; in col-

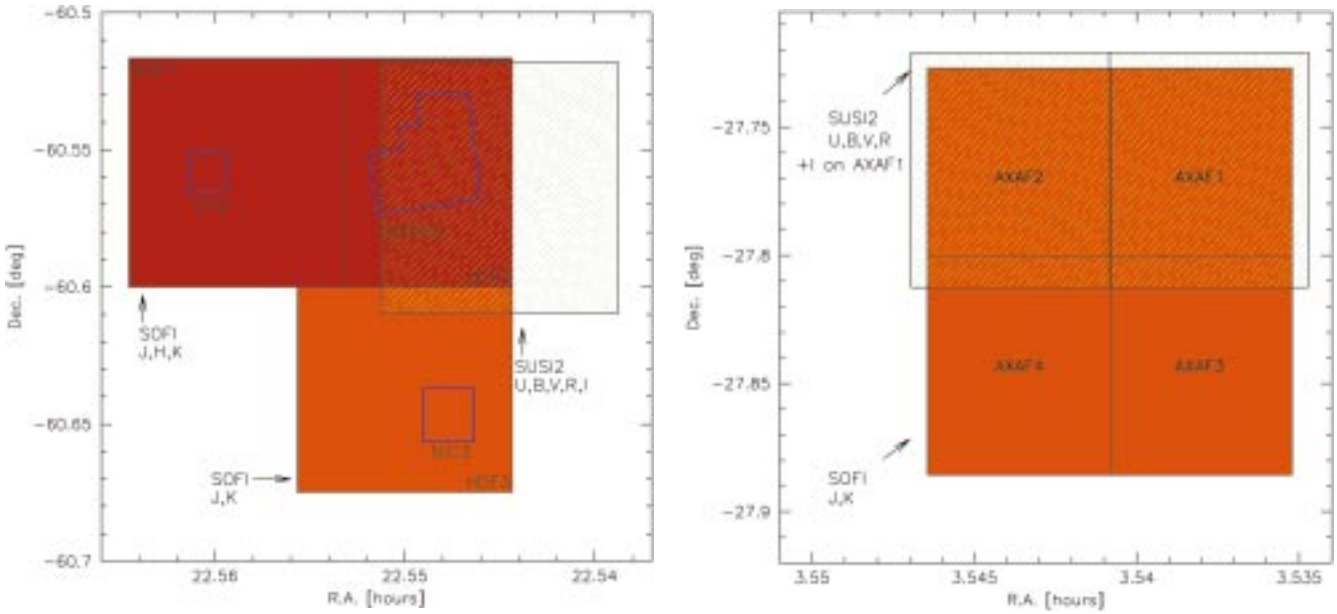

Figure 2: Schematic view of the various data sets available for the HDF-S and AXAF fields from optical/infrared observations conducted with SUSI2 and SOFI at NTT. The different colours denote the completeness of the multi-colour data.

Table 3: EIS-DEEP: SUSI2 and SOFI Pointings (J2000.0).

Field	α_{SUSI2}	δ_{SUSI2}	α_{SOFI}	δ_{SOFI}
HDF1	22 33 29	–60 33 50	22 33 32	–60 33 30
HDF2	22 32 42	–60 33 50	22 33 00	–60 33 30
HDF3	–	–	22 33 00	–60 37 59
AXAF1	03 32 16	–27 46 00	03 32 17	–27 46 10
AXAF2	03 32 38	–27 46 00	03 32 37	–27 46 10
AXAF3	–	–	03 32 17	–27 50 35
AXAF4	–	–	03 32 37	–27 50 35

Table 4: EIS-DEEP: HDF-S Observations (magnitudes in the AB system).

Filter	t_{total} (sec)	N_f	FWHM (arcsec)	μ_{lim} (mag arcsec^{-2})	3σ (2 × FWHM)	3σ (proposed) (2 × FWHM)
HDF1						
J	10800	180	1.37	25.7	23.6	24.2
H	3600	60	0.91	25.1	23.4	23.7
Ks	10800	180	0.90	24.9	23.1	23.1
HDF2						
U	17800	22	1.00	28.2	26.3	26.6
B	6600	22	0.84	28.2	26.5	25.7
V	12250	49	1.27	28.3	26.5	25.8
R	5500	22	1.05	27.3	25.4	26.0
I	8800	44	1.11	27.0	25.0	26.2
J	10800	180	0.90	26.2	24.4	24.7
H	7200	120	0.85	24.9	23.2	24.2
Ks	18000	300	0.96	25.5	23.7	23.6
HDF3						
J	5820	97	1.18	25.5	23.5	24.2
Ks	7440	124	0.86	24.9	23.2	23.1

umn (6) the limiting magnitude of a 3σ detection within an aperture twice the FWHM. In Table 4 the last column lists the originally proposed limiting magnitudes for EIS-DEEP, expressed as those in column (7), assuming a 1 arcsec seeing (da Costa & Renzini 1998). To help visualise the fields and the different sets of data available, Figure 2 shows a schematic view of the EIS-DEEP observations of the HDF-S and AXAF fields, with the colours indicating the completeness of the multi-colour data. In the case of HDF-S the location of the WFPC2, STIS and NIC3 HST fields and their relation to the location of the EIS-DEEP fields are also shown.

The highest priority was given to the observations of the HDF2 (WFPC2) field for which data in eight passbands are available, by and large reaching the required magnitude limits, with the notable exception of the *I*-band. Note that in this field the *J* and *Ks* observations reach half-magnitude fainter limits than those in the other fields, as suggested by the WG (da Costa & Renzini 1998). Even though it was not possible to complete the observations in all the passbands for all the fields, the data gathered provide ~150 square arcmin in *J Ks* and ~80 square arcmin in *UBVRI*. When combined, the optical/infrared deep observations provide a coverage of 15 and 25 square arcmin in eight and seven passbands, respectively. These numbers include the recently released data for the HDF-S STIS and NICMOS fields from observations conducted in July 1999 (see EIS home page). Unfortunately, due to bad weather, no new optical data were obtained during the four half nights scheduled in July 1999 at the NTT, and the *R I* images of HDF1, taken in 1998, proved to be unsuitable due to poor seeing and stray

light. The incompleteness of the EIS-DEEP data relative to the original goals is primarily due to the optical observations which were affected by both poor weather and a variety of technical problems in 1998. An attempt to complete the optical coverage of the HDF1 (STIS) field will be made in June–July 2000, while the AXAF field has been chosen to be one of the three fields selected for the new Deep Public Survey as shown in Figure 1 (see Renzini & da Costa 1999).

4. WFI@2.2 Pilot Survey

With the announcement of the commissioning of the WFI@2.2m, the WG recommended the undertaking of a pilot multi-colour survey over the area already covered in *I* – band, including the missing U-band observations of patch B. The motivation was to complete the original goals of EIS-WIDE and to steer the upgrade of the pipeline to cope with CCD-mosaics and the corresponding order of magnitude increase in the volume of data.

Even though originally proposed to be carried out in dark time over the observing Periods 62 and 63, some adjustments had to be made to accommodate the WFI commissioning period. In the end, a total of 30 hours was used for the Pilot Survey observations during the commissioning period in January 1999, and a total of 8.5 nights in the months of April, May and September. The observations consisted of five 4-minute dithered exposures, which allowed the coverage of 0.5 square degrees/hour in a single pass-band including overheads. A total of 18 square degrees were observed, covering patches C and D in *B* and *BV*, respectively. The *B*-filter was used first because it was the only broad-band filter available during commissioning. In mid-September new observations of Patches A and B were conducted in *V* and *U* but the data have not yet been reduced at the time of writing. Table 6 shows the current status of the EIS-WIDE patches after combining the data available from EMMI at the NTT with those from the Pilot Survey, including the September 1999 run. These data together with the 17 hours scheduled in service mode for Period 64 should allow the completion of about 1.5 square degrees in *UBVI* and 15 square degrees in *BVI*. These data should greatly broaden the range of applications that can benefit from the EIS public survey to produce samples for follow-up observations with the VLT. Preliminary estimates of the median seeing and limiting magnitudes reached in *B* and *V* from the data gathered so far using the WFI are given in Table 7.

Some of the scheduled time was unsuitable for the observation of the patches, either because the EIS-WIDE fields

Table 6: WFI Pilot Survey: Sky Coverage (square degrees).

Patch	U	B	V	I
A	–	1.0	1.2	3.2
B	1.25	1.5	1.5	1.6
C	–	6.0	6.0	6.0
D	–	6.0	6.0	6.0
Total	1.25	14.5	14.7	16.8

Table 7: WFI Pilot Survey: Limiting Magnitudes (AB system).

Band	FWHM (arcsec)	μ_{lim} (mag arcsec^{-2})	80%	3σ (2 × FWHM)
B	0.9	26.8	24.5	25.0
V	1.0	26.4	24.1	24.6

Table 5: EIS:DEEP: AXAF Observations (magnitudes in the AB system).

Filter	t_{total} (sec)	N_f	FWHM (arcsec)	μ_{lim} (mag arcsec^{-2})	3σ (2 × FWHM)
AXAF1					
U	17000	21	0.90	28.0	26.1
B	6600	22	1.10	28.0	26.4
V	5500	22	0.88	27.7	25.7
R	5500	22	0.89	27.5	25.9
I	12600	21	1.31	27.0	24.9
J	10800	180	0.99	25.7	23.8
Ks	10800	180	0.95	24.9	23.2
AXAF2					
U	13000	16	0.90	27.8	26.0
B	5400	18	1.10	27.9	25.8
V	5500	22	0.88	27.7	26.1
R	5500	22	0.89	27.5	25.7
J	10800	180	0.90	25.8	24.1
Ks	10800	180	0.90	24.8	23.1
AXAF3					
J	10800	180	0.90	25.4	23.7
Ks	10800	180	1.00	24.7	22.9
AXAF4					
J	10800	180	0.70	25.6	24.1
Ks	7200	120	1.00	24.4	22.6

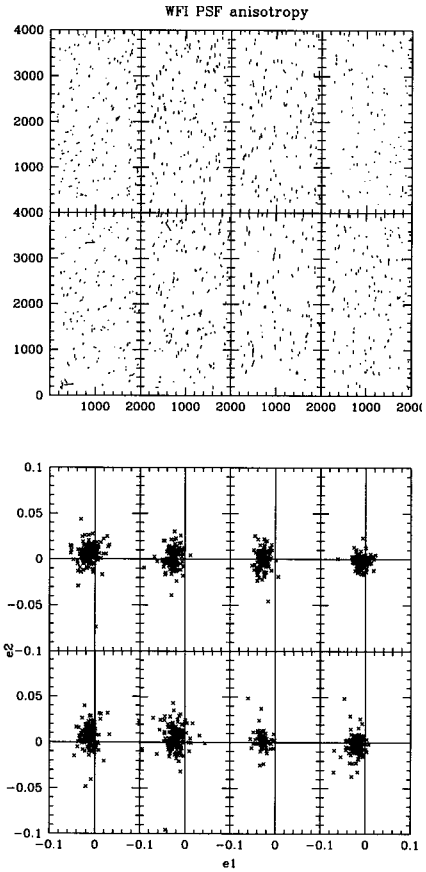

Figure 3: Vector representation of the pattern of the PSF anisotropy and the amplitude of its components for each chip of the CCD mosaic, as measured on a V-band image obtained from a 20-min exposure.

Figure 4: Colour image of a section of EIS patch D combining BV images of WFI with I-images of EMMI. ▶

Figure 5: A 16.1 × 9.4 arcmin section of the co-added I-band image, rebinned to a scale of 0.5 arcsec/pixel, of the cluster NGC 6558 located in Baade's window. The regions devoid of objects are associated with the interchip gaps.

were not visible or because the nights were too bright. In these periods, a set of selected stellar fields were observed as a test case for future preparatory programmes for GIRAFFE and UVES using the fibre-positioner FLAMES, thus anticipating part of the Public Survey observations now planned for P64–67, the so-called Pre-Flames Survey recommended by the WG in their meeting in March 1999 (see Renzini & da Costa 1999). The selected fields (Figure 1) included Baade's window, globular (GC) and open clusters (OC). A total of 22 fields (5.5 square degrees) given in Table 8 were observed in different passbands. A full description of the available data can be found on the web.

Altogether the observations from January to April 1999 yielded 400 Gby of raw data at a rate of about 40 Gby/night (0.5 Mb/sec), including calibration frames (standard stars, dome and sky flats). All the data have been processed, using the upgraded EIS-WFI pipeline, and publicly released on September 9, 1999.

Preliminary results show that the performance of the WFI@2.2 exceeds expectations and demonstrate its competitiveness in the area of wide-field imaging surveys. Analysis of the images shows that the point-spread function is very uniform across the entire field of view and that PSF distortions are small ~ 2%. This is illustrated in Figure 3 where the spatial distribution of the po-

larisation vector, representing the amplitude and direction of the PSF distortions, and the distribution of the amplitude of its two components are shown for each CCD chip of the WFI camera.

To illustrate the results obtained by the pipeline, Figure 4 shows a colour composite of a section of patch D (23 × 19 arcmin) constructed from the combination of WFI *B* and *V* mosaics with the EMMI *I*-band mosaic. Since one of the primary goals of Pilot Survey is to complement the *I*-band observations, the co-addition of the WFI images was carried out on the EMMI pixel scale, about 10% larger than that of the WFI. By dithering the WFI exposures and by co-adding the available frames using the weight maps, the final coadded mosaic shows no noticeable evidence of the inter-chip gaps, with the least sampled regions having an exposure time about 60% of that obtained in the best sampled regions. Another example can be found in Figure 5, where the co-added *B*-band image of the globular cluster NGC 6558, observed with 0.6 arcsec seeing, is shown. Note that in this case only two images have been co-added and the regions devoid of stars are the remains of the interchip gaps.

The co-addition is carried out after the astrometric calibration of each input frame. Figure 6 shows the distribution of the differences in the coordinates of 700,000 pairs of stars in patch D from independent astrometric solutions obtained for different WFI *V*-band frames. The rms of the distribution is ~ 0.04 arcsec, an estimate of the internal accuracy of the astrometric solution. This result shows that the position of the targets extracted from the survey data can be directly used to position the slits and fibers of VLT spectrographs such as FORS1, FORS2, VIMOS, NIRMOS and FLAMES. However, even though a satisfactory astrometric solution was determined for the stellar field shown in Figure 5, problems are still found in calibrating crowded fields. Procedures to astrometrically calibrate these fields, including proper modelling of the optical distortions, are still being investigated. These issues as well as a full description of the observations, data reduction and derived products will be presented in forthcoming papers.

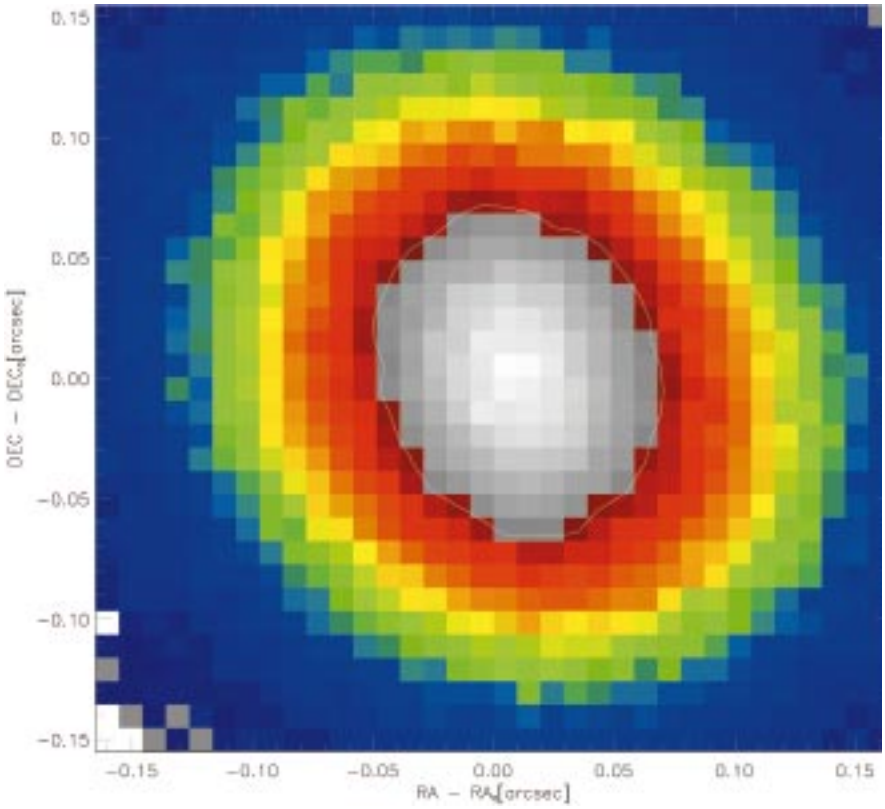

Figure 6: Distribution of the differences in the coordinates of 700,000 pairs of stars in patch D obtained from the independent astrometric calibration of different WFI frames. The solid contour corresponds to the half-maximum of the distribution, encompassing 62% of the points.

Table 8: WFI Pilot Survey: Stellar Fields.

Object Name	Object Type	α_{1950}	δ_{1950}	Filters
Baade Window (1)	Bulge	17 55 28	–28 45 20	B, V, I, z
Baade Window (2)	Bulge	17 56 04	–29 13 14	B, V, I, z
Baade Window (3)	Bulge	18 00 00	–29 52 13	B, V, I
Baade Window (4)	Bulge	18 05 33	–31 27 04	B, V, I
Baade Window (5)	Bulge	18 07 02	–31 46 27	V, I
Baade Window (6)	Bulge	18 15 10	–33 58 38	V, I
NGC 6218	GC	16 47 14	–01 56 52	B, V, I
NGC 6397	GC	17 40 41	–53 40 25	B, V, I
NGC 6544	GC	18 07 20	–24 59 51	B. V, I
NGC 6809	GC	19 39 59	–30 57 44	B, V, I
NGC 7089	GC	21 33 29	–00 49 23	B, V, I
NGC 6752	GC	19 10 51	–59 58 55	B, V, I
NGC 6541	GC	18 08 02	–43 42 20	B, V, I
NGC 6681	GC	18 43 12	–32 17 31	B, V, I
NGC 6656	GC	18 36 24	–23 54 12	B, V, I
NGC 6717	GC	18 55 06	–22 42 03	B, V, I
NGC 6723	GC	18 59 33	–36 37 54	B, V, I
IC 4651	OC	17 24 42	–49 57 00	B, V, I
NGC 6405	OC	17 36 48	–32 11 00	B, V, I
NGC 6208	OC	16 45 30	–53 4400	B, V, I
NGC 5822	OC	15 01 30	–54 09 00	B, V, I
NGC 6705	OC	18 51 06	–06 16 00	B, V, I

5. Data Handling

One of the most demanding tasks of the EIS project has been the development of a data reduction pipeline in parallel to the observations which have used four different instruments (EMMI, SUSI2, SOFI and WFI@2.2m) in a period of two years. Adaptation of the software to this rapidly changing environment has been by far the most challenging aspect of the project, which will hopefully subside in the next couple of years. This not only impacts the development effort but also the data reduction and verification which depend on the stability of the pipeline.

The original EIS pipeline was developed over a period of one year, starting in April 1997, by assembling existing software (IRAF, SExtractor, LDAC and Drizzle) adapted to the specific needs (detector and observing strategy) of the EIS-WIDE survey. The task was facilitated because most tools were devel-

oped by astronomers in the Member States who participated in this development. At the time, the data volume was relatively small, which greatly facilitated the handling and processing of the data. Most of the work focused on the interfacing of the different processing blocks and in producing scripts to control the processing essentially in batch mode. A lot of effort was also spent in the design and implementation of a database which was primarily used for bookkeeping.

After the first EIS data release in March 1998, an upgrade was carried out to incorporate ECLIPSE (Devillard, Jung & Cuby 1999) for the reduction of SOFI data and to handle the two-CCD mosaic of SUSI2. Even though time-consuming, implementing these add-ons did not require major changes in the design of the pipeline.

The advent of the WFI, on the other hand, required a major overhaul driven by the sheer volume of the data. New hardware was required as well as a major re-design of the pipeline architecture. Over the past year new machines have been added, the number of processors available in each server increased, disk and memory capacities expanded and DLT tape units installed. In parallel, during the past six months significant modifications have been made to the pipeline software, even though the basic algorithms remain essentially the same. A more sophisticated control system has been developed to administer the resources of the system, to retrieve/store images in the tape library, to supervise the reduction process and to communicate with an expanded implementation of the database in a variety of ways. The new pipeline allows the reduction of both single CCD (SOFI and other single-chip instruments) and mosaics (e.g., SUSI2, WFI) and parts of the code have been optimised and parallelised to increase the overall throughput to match the expected input data rate. Finally, the pipeline has been made more user-friendly and uniform in order to facilitate its maintenance and integrity, to prevent discontinuities caused by the constant changes of Survey Team members and to allow it to be run by other interested users.

Broadly speaking the pipeline consists of four logical blocks:

1. Image Processing – this module performs the usual image processing steps removing instrument signatures and astrometrically and photometrically calibrating each individual WFI frame. It then performs the co-addition of dithered WFI frames, producing a single FITS image from which object catalogues are extracted. These are the basic products produced automatically by the pipeline which are then transferred to the archive for quick-look releases.

2. Image Mosaicing – this module deals with the production of image mosaics, which implies adjustments of the photometric zero-point, of final object catalogues, extracted from the co-added images using the most recent and extensively tested version of SExtractor, and of colour catalogues constructed either by the association of objects detected in each passband or by the use of a reference image (e.g., χ^2-image).

3. Quality control – this module carries out the quality control of the data. It monitors image distortions, computes the rms distribution of the residuals of the astrometric solution, compares the astrometry of the objects extracted in different passbands and checks the spatial uniformity of the photometric zero-point. It also performs a preliminary scientific evaluation of the data. It culls object catalogues, computes simple statistics such as number counts, colour-colour diagrams, colour distributions and the two-point angular correlation function for objects classified as galaxies. The results are compared with other available data to check the photometric zero-points, the star-galaxy classification and uniformity of the object catalogues.

4. Target Selection – this module is used to produce a variety of target lists. It also produces image postage stamps (typically 2×2 arcmin) in different passbands of the selected objects for visual inspection. In time, other facilities are expected to be added, in particular for searches for variable and proper-motion objects. Among many possible applications, a major goal is to define secondary-standards in the surroundings of the traditional Landolt fields, essential to monitor the zero-point of the different chips in the CCD-mosaic.

Even though the backbone of the pipeline is in place, a lot of work remains to be done, especially on the control system, in order to allow the process to be fully automated. Time benchmarks of different parts of the pipeline demonstrate that most of the modules are operating at a rate ~ 0.2 Mpixels/sec. For instance, it currently takes about 7 hours to process 20 WFI frames and produce the results required for a quick-look release of a square degree worth of data. This corresponds to 2 hours of observations in the wide-angle-survey mode adopted by the Pilot Survey. Even though preliminary, these numbers show that the current pipeline is capable of coping with the volume of data being produced by the survey. Furthermore, the pipeline is not yet fully implemented and tested and there still is considerable room for improving the system throughput. The final consolidation of the software should last until the end of 1999, with a final target date of April 1, 2000. A detailed description of the available software will be presented in the "EIS-WFI Pipeline Primer" currently in preparation by the Survey Team.

6. Data Access

Unlike radio surveys and other public surveys carried out in space, ground-based optical imaging surveys require considerably more information to characterise the data available. An arduous and time-consuming task, given the time pressure and limited personnel, has been to establish adequate channels of communication between the Survey Team and the community at large to describe the progress of the project and to provide the necessary information about the observations and the various data products available. In this first phase this was accomplished by posting as much information as possible on the web, by periodically reviewing the status of the project in *The Messenger* (da Costa 1997, da Costa et al. 1998, da Costa & Renzini 1998) and by submitting and circulating papers with each data release.

During the first phase, requests for large volumes of data from different groups have been processed by the ESO Archive Group and about 100 Gby of data have been delivered in various forms. The requests originated from 11 countries, including all of the ESO member states. According to current guidelines, catalogues are available world-wide, but images are restricted to ESO member states, with the exception of those of the HDF-S fields. Table 9 shows a summary of data requests listing the product and the number of requests up to September 1999. The access to the EIS home page has increased by a factor of 5 over the period of the survey. It currently averages about 30,000 hits/month, reaching peaks twice as high after a data release. About one-third of these hits are from research institutes in Europe and abroad, constantly monitoring the progress of the survey, while the rest are from the general public. In this respect, it is worth noting the popularity of the EIS image gallery, with about 35,000 images being retrieved from the web. A total of about 4500 data requests have been processed so far, about half of which asked for derived products such as target lists and catalogues. By expanding the scope of the observations to other areas of application and by im-

Table 9: Summary of Data Requests (September 1999).

Product	Number of Requests
Bulk Data	50
Cutouts	1128
Mini-images	319
Target Lists	737
EIS-Deep catalogues	1440
HDF-S images	821
TOTAL	4495
Gallery Images	34538

proving the interface with the public, these numbers are likely to increase significantly.

7. Future Developments

With the recent approval of a two-year Large Programme to conduct a Public Survey (see Renzini & da Costa 1999) with the WFI and SOFI, it is now possible to envision a more stable operation leading to the production of more standard data sets. In this framework, new ways of making the data accessible to the community will be explored. Quick-look releases of the data, distribution of compressed data and the implementation of new on-line features are being considered as described by Renzini & da Costa (1999). These, together with the other products already available should provide users with a large range of options and greater flexibility to explore the available data.

A considerable effort is also underway to implement a flexible design to store the objects extracted from the public survey images in a database which will allow users to directly select and display objects according to their positions in the sky, their magnitudes and their colours without any reference to a specific catalogue. The database will be a dynamic entity that will grow in time as information from new observations of different sky regions or repeated observations of the same objects are continuously added to it. The implementation of such a database and database tools where astronomical objects extracted from survey data can be stored, updated and associated with all the information available from internal and external sources is an essential element for the successful use of the Public Survey data. The need for such databases transcends EIS and several groups in Europe involved in wide-field imaging surveys are tackling the same problem (e.g. Terapix, ΩCam). These various groups are exchanging ideas, and a preliminary implementation has recently been tested by the EIS Survey Team, in collaboration with the ESO Archive Group, using the Objectivity database. As the work on the pipeline is consolidated, the attention of the software developers in the Survey Team will focus on this critical area which is a key element for the efficient scientific exploitation of the survey data.

8. Conclusions

After two years of observations, software development, data reduction and distribution, nearly all the data from the ongoing Public Surveys (EIS-WIDE, EIS-DEEP and Pilot Survey) are publicly available. The only exceptions are the data gathered from observations conducted with the WFI in September 1999 and some data taken with the narrow-band *z* filter for which no proper calibration is currently available. The EIS experience has been extremely valuable for the new Public Survey to be conducted in Periods 64–67, as important lessons have been learned in handling large volumes of data, in setting up rules for automatically processing images and recipes for data quality control, and in ways and means of exporting the data to the users in an adequate form and in a timely fashion. With the accumulated experience from four previous releases and with the major development phase drawing to a close, new ways of making the data available are being considered which will hopefully provide interested users with a broader range of products as well as more flexibility and thus contribute to the scientific exploitation of the VLT.

9. Acknowledgements

We would like to thank A. Renzini for his effort in steering the imaging survey, the WG members for their scientific input and former EIS team members for their contribution over the years. Special thanks to E. Bertin for addressing the innumerable questions and requests posed by the EIS team and for introducing new features to SExtractor as needed and to T. Erben for his help in the analysis of the PSF.

References

Benoist et al. 1999, *A&A*, **346**, 58.
da Costa, L., 1997, *The Messenger*, **88**, 34.
da Costa. L. et al., 1998, *The Messenger*, **91**, 49.
da Costa, L. & Renzini, A., 1998, *The Messenger*, **92**, 40.
da Costa, L. et al., l999b, A&A, in press (astro-ph/9812105).
Devillard, N., Jung, Y. & Cuby, J.G., 1999, *The Messenger*, **95**, 5.
Nonino, M. et al. 1999, *A&A Supp.*, **137**, 51.
Olsen et al. 1999a, *A&A*, **345**, 681.
Olsen et al. 1999b, *A&A*, **345**, 363.
Prandoni et al. 1999, *A&A*, **345**, 448.
Renzini, A. & da Costa, L., 1997, *The Messenger*, **87**, 23.
Renzini, A. & da Costa, L., 1999, in this issue of *The Messenger*.
Rengelink et al., 1999, *A&A*, submitted (astro-ph/9812190).
Scodeggio et al. 1999, *A&A Supp.*, **137**, 83.
Zaggia, S. et al. 1999, *A&A Supp.*, **137**, 75.

E-mail: ldacosta

VLT/ISAAC and HST/WFPC2 Observations of NGC 3603

*B. BRANDL[1], W. BRANDNER[2], E.K. GREBEL[3] AND H. ZINNECKER[4]**

[1]Cornell University, Ithaca; [2]University of Hawaii, Honolulu;
[3]University of Washington at Seattle; [4]Astrophysikalisches Institut Potsdam

1. Abstract

We have studied NGC 3603, the most massive visible HII region in the Galaxy, with VLT/ISAAC in the near-infrared (NIR) J_s, H, and K_s-bands and HST/WFPC2 at Hα and [N II] wavelengths. In this *Messenger* article we describe the data analysis and some first results from both our complementary observations.

Our HST/WFPC2 gave us an unprecedented high-resolution view of the interstellar medium in the giant HII region and its ionisation structure. Among the findings are two gigantic gas columns (similar to the famous "elephant trunks" in M16) and three proplyd-like structures. The emission nebulae are clearly resolved; all three nebulae are tadpole shaped, with the bright ionisation front at the head facing the central cluster and a fainter ionisation front around the tail pointing away from the cluster. Typical sizes are 6000 A.U. × 20,000 A.U. The nebulae share the overall morphology of the proplyds ("PROto PLanetarY DiskS") in Orion, but are 20 to 30 times larger in size.

The VLT observations are the most sensitive near-infrared observations made to date of a dense starburst region, allowing us to investigate with unprecedented quality its low-mass stellar population. Our sensitivity limit to stars detected in all three bands corresponds to 0.1 $M_\odot$ for a pre-main sequence star of age 0.7 Myr. Our observations clearly show that sub-solar-mass stars down to at least 0.1 $M_\odot$ do form in massive starbursts.

2. Introduction

NGC 3603 is located in the Carina spiral arm (RA = 11h, DEC = –61°) at a distance of 6–7 kpc. It is the only massive, Galactic HII region whose ionising central cluster can be studied at optical wavelengths, due to only moderate (mainly foreground) extinction of A_V = 4–5 mag (Moffat 1983; Melnick et al. 1989). The OB stars (> 10 $M_\odot$) and stars with the spectral signatures of Wolf-Rayet (W-R) stars contribute more than 2000 $M_\odot$ to the cluster mass. Normally, W-R stars are evolved supergiants that have long left the main sequence and have ages of 3–5 Myr. In NGC 3603, however, the W-R stars also show hydrogen absorption lines in addition to the typical W-R features. It is believed that these stars are still main-sequence, core hydrogen-burning stars that are so massive and so close to the Eddington limit that they are loosing their outer envelopes through fast winds, and thus resemble evolved W-R stars. In comparison to the Orion Trapezium system, NGC 3603 with its more than 50 O and W-R stars producing a Lyman continuum flux of 10^{51} s^{-1} (Kennicutt 1984; Drissen et al. 1995) has about 100 times the ionising power of the Trapezium cluster.

With a bolometric luminosity $L_{bol} > 10^7$ $L_\odot$, NGC 3603 has about 10% of the luminosity of 30 Doradus and looks in many respects very similar to its stellar core R136 (Brandl et al. 1996). In fact, it has been called a Galactic clone of R 136 but without the massive surrounding cluster halo (Moffat, Drissen & Shara 1994). In many ways NGC 3603 and R136 can be regarded as representative building blocks of more distant and luminous starburst galaxies (Brandl, Brandner & Zinnecker 1999, and references therein). So the best way to study collective star formation in a violent environment is by examining these regions on a star-by-star basis. Until recently, observations of the entire stellar populations were limited to the massive stars by sensitivity or wavelength restrictions. The formation of low-mass stars in starburst regions is of particular interest. Fundamental questions that arise in this context are: Does the slope of the IMF vary on small scales? Do low-mass stars in a starburst event form together with the most massive stars or do they form at different times or on different timescales? And finally, one might even ask if low-mass stars form at all in such environments?

In addition, NGC 3603 is an ideal laboratory to study individual (!) star formation. Some young stars in the vicinity of massive stars are surrounded by partially ionised circumstellar clouds with cometary shape, so-called protoplanetary disks ("Proplyds"), ionised from the outside (Churchwell et al. 1987; O'Dell et al. 1993). FUV photons (13.6 eV > hν > 6 eV) heat up the inside of the proplyd envelope and lead to the dissociation of molecules in the outer layers of the circumstellar disk (Johnstone et al. 1998). The resulting evaporation flow provides a steady supply of neutral atoms to the ionisation front and leads to the development of a cometary tail (McCullough et al. 1995; Störzer & Hollenbach 1999). Until recently, only one other proplyd had been found outside the Orion nebula. It is located in the vicinity of the O7V star Herschel 36 in the Lagoon Nebula (M8, Stecklum et al. 1998).

3. VLT/ISAAC Observations

We observed NGC 3603 through the J_s = 1.16–1.32 μm, H = 1.50–1.80 μm, and K_s = 2.03–2.30 μm broadband filters using the NIR camera ISAAC on ANTU, the first VLT unit telescope. The observations were made during the 4 nights of April 4–6 and 9, 1999, in service mode when the optical seeing was equal to, or better than, 0.4″ in 1-minute exposures. Such seeing was essential for accurate photometry in the crowded cluster and increased our sensitivity to the faintest stars. The majority of our data were taken under photometric conditions.

Our observing strategy was to use the shortest possible frame times of 1.77 seconds to keep the number of saturated stars to a minimum. However, due to the system's excellent sensitivity, about two dozen of the brightest stars ended up being saturated. Nevertheless, this does not impose a problem to our study of the low-mass stars. Thirty-four short exposures were co-added to an effective one-minute exposure, the minimum time per pointing required to stabilise the telescope's active optics control system. Between the 1-minute pointings we moved the telescope by up to 20″ offsets in a random pattern. This approach has several advantages:

- Enlargement of the observed field of view (FOV) with maximum signal-to-noise (S/N) in the cluster centre.
- Reduction of residual images and other array artefacts, using the median filtering technique.

*Our collaborators on the project described in this article are Y.-H. Chu, H. Dottori, F. Eisenhauer, A.F.J. Moffat, F. Palla, S. Richling, H.W. Yorke and S. D. Points.

• Derivation of the "sky" from the target exposures using the median filtering technique. No additional time for "blank" sky frames outside the cluster was required.

The sky frames have been computed using between 15 and 37 subsequent exposures per waveband and night, and careful eye-inspection showed that all sources have been efficiently removed using our modified median filtering technique which returns the lower 1/3 instead of the mean (1/2) value.

We subtracted the sky background and flat-fielded each exposure using the twilight flat-fields provided by ESO. The relative position offsets were derived from cross-correlating the images; the exposures were co-aligned on a 0.5×0.5-pixel sub-grid for better spatial resolution, and then added together using the median filtering technique. The resulting images are $3\farcm4 \times 3\farcm4$ in size with pixels of $0\farcs074$. The effective exposure times of the final broadband images in the central $2\farcm5 \times 2\farcm5$ are 37, 45, and 48 minutes in J_s, H, and K_s, respectively.

Figure 1: Three-colour image of NGC 3603 composed from J_s (blue), H (green), and K_s-band (red) images. Intensities are scaled in logarithmic units. The field of view is $3\farcm4 \times 3\farcm4$. North is up, East to the left. The insert to the lower right is a blow-up of the central parsec^2.

Figure 1 shows the impressive 3-colour composite image that has recently been the subject of an ESO press release. (http://www.eso.org/outreach/press-rel/pr-1999/pr-16-99.html). The brightest star in the FOV (80″ northeast of the core) is the red supergiant IRS 4 (Frogel, Persson, & Aaronson 1977). To the south of the cluster is a giant molecular cloud (GMC). Ionising radiation and fast stellar winds from the starburst cluster are excavating large gaseous pillars. Located about 20″ to the north of the cluster centre is the blue supergiant Sher 25. This supergiant is unique because its circumstellar ring and bipolar outflows form an hourglass structure similar to that of SN 1987A (Brandner et al. 1997a, 1997b). The image also shows the three proplyd-like objects that have recently been discovered by Brandner et al. (2000) (see Fig. 2 for details). About 1′ south of the central cluster, we detect the brightest members of the deeply embedded protocluster IRS 9.

In order to derive the photometric fluxes of the stars we used the IRAF implementation of DAOPHOT (Stetson 1987). We first ran DAOFIND to detect the individual sources, leading to $\approx$ 20,000 peaks in each waveband. Many of these may be noise or peaks in the nebular background and appear only in one waveband. In order to reject spurious sources, we required that sources be detected independently in all three wavebands, and that the maximal deviation of the source position centroid between different wavebands be less than 0.075″. The resulting source list contains 6967 objects in the entire FOV. We then flux-calibrated the images using the faint NIR standard stars from the lists by Hunt et al. (1998) and Persson et al. (1998). Because of the stringent requirements on the seeing, the PSF did not noticeably change during our observations and the systematic photometric errors are dominated by uncertainties in the aperture offsets. (A detailed error analysis will be part of a subsequent paper). Comparing our photometric fluxes of numerous sources with the fluxes derived by Eisenhauer et al. (1998) yields a systematic offset of 0.1^m in J_s and 0.05^m in K_s.

4. HST/WFPC2 Observations

On March 5, 1999 we obtained deep narrow-band Hα (F656N, $2 \times$ 500s) and [NII] (F658N, 2×600s) observations. The Planetary Camera (PC2) chip was centred on the bipolar outflow structure around the blue supergiant Sher 25. The three Wide Field Camera (WF) chips covered the central cluster and the HII region to the South of Sher 25. In addition, we retrieved and analysed archival HST data, which had originally been obtained in July 1997 (PI Drissen). The

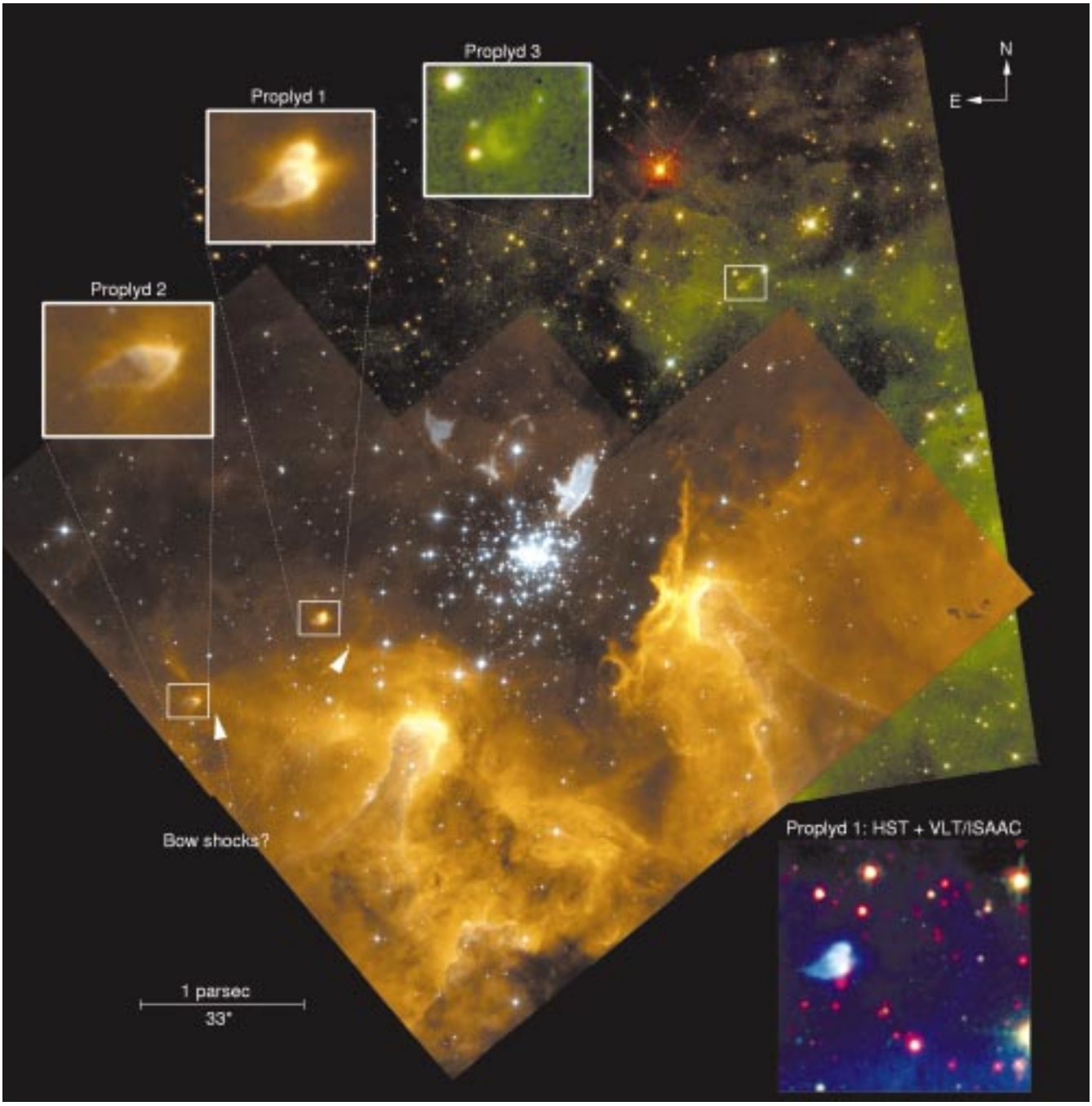

Figure 2: WFPC2 observations of NGC 3603. North is up and East is to the left. The upper part of the image consists of the archive data with the following colour coding: F547M (blue), F675W (green), F814W (red). Overlaid are our new WFPC2 data with the F656N data in the red channel, the average of F656N and F658N in the green channel, and F658N in the blue channel. The location of the three proplyd-like emission nebulae is indicated. The insert at the lower right is a combination of WFPC2 F656N (blue) and F658N (green) and VLT/ISAAC Ks (red) observations.

PC2 was centred on the cluster, and the three WF chips covered the area north-west of the cluster. We combined individual short exposures in F547M (8×30s), F675W (8×20s), and F814W (8×20s) to produce images with effective exposure times of 240s, 160s, and 160s, respectively.

The HST/WFPC2 observations are presented in Figure 2. The figure shows an overlay of two composite colour images. The upper part of the image consists of the archive data with the following colour coding: F547M (blue), F675W (green), F814W (red). Overlaid are our new WFPC2 data with the F656N data in the red channel, the average of F656N and F658N in the green channel, and F658N in the blue channel. The locations of the proplyds are marked by small boxes, and enlargements of the boxes are shown in the upper part of Figure 2. Proplyd 3 has only been observed in intermediate and broad-band filters and thus stands out less clearly against the underlying background when compared to Proplyds 1 and 2. The insert at the lower right shows a colour composite of HST/WFPC2 F656N (blue) and F658N (green) data and VLT/ISAAC K_s data (red).

5. Results and Interpretation

All three proplyds are tadpole shaped and rim brightened, with the extended tails facing away from the starburst cluster. The portion of the ionised rims pointing towards the cluster are brighter than the rims on the opposite side. The central parts of the proplyds are fainter than the rims, with a noticeable drop in surface brightness between the head and the tail. Proplyds 2 and 3 exhibit a largely axisymmetric morphology, whereas Proplyd 1, which is also the one closest to the cluster, has a more complex structure. Un-

like the convex shape of the heads of the other proplyds, Proplyd 1 has a heart-shaped head with a collimated, outflow-like structure in between. One possible explanation for the more complex morphology of Proplyd 1 might be that it is actually a superposition of two (or maybe even three) individual proplyds or that the photoevaporative flows of several disks in a multiple system interact to produce this complex single structure.

At distances of 7.4″ and 2.9″ from Proplyd 1 and 2, respectively, faint arc-like Hα emission features are seen on the WFPC2 frames. The arcs are located in the direction of the cluster, and may be the signatures of bow shocks created by the interaction of proplyd winds with the winds from the massive stars in the central cluster. Additional faint filaments located between the nebulae and the central ionising cluster can be interpreted as bow shocks resulting from the interaction of the fast winds from the high-mass stars in the cluster with the evaporation flow from the proplyds.

Low-resolution spectra obtained with EFOSC2 at the ESO/MPI 2.2-m telescope of the brightest nebula, which is at a projected separation of 1.3 pc from the cluster, reveal that it has the spectral excitation characteristics of an ultra compact H II region with electron densities well in excess of 10^4 cm^{-3}. The near-infrared data reveal a point source superimposed on the ionisation front.

The striking similarity of the tadpole-shaped emission nebulae in NGC 3603 to the proplyds in Orion suggests that the physical structure of both types of objects might be the same. Our hydrodynamical simulations (Brandner et al. 2000) reproduce the overall morphology of the proplyds in NGC 3603 very well, but also indicate that mass-loss rates of up to 10^{-5} Mo yr^{-1} are required in order to explain the size of the proplyds. Due to these high mass-loss rates, the proplyds in NGC 3603 should only survive 10^5 yrs. Despite this short survival time, we detect three proplyds. This indicates that circumstellar disks must be common around young stars in NGC 3603 and that these particular proplyds have only recently been exposed to their present harsh UV environment.

The point source close to the head of Proplyd 3 is already detected on the broadband HST/WFPC2 observations (see Figure 2). The WFPC2 images show that the point source is actually located in front of Proplyd 3 and thus very likely not physically associated with it. The infrared source in Proplyd 1 is also detected as an underlying, heavily reddened continuum source in the spectrum. A more detailed analysis of ground based optical images and spectra of the proplyds and other compact nebulae in NGC 3603 will be presented in Dottori et al. (2000).

The figure on page 1 of this issue of *The Messenger* shows the resulting colour-magnitude diagrams (CMD) derived from our VLT data. The left plot contains all stars detected in all 3 wavebands within the entire FOV of 3.′4 × 3.′4 (6 pc × 6 pc). Since NGC 3603 is located in the Galactic Plane we expect a significant contamination from field stars. To reduce this contribution we followed a statistical approach by subtracting the average number of field stars found in the regions around the cluster at r > 75″ (central plot) per magnitude and per colour bin (0.5 mag each).

The accuracy of our statistical subtraction is mainly limited by three factors: first, we cannot rule out that low-mass pre-main-sequence stars are also present in the outskirts of the cluster. Second, because of crowding on one hand and dithering which leads to shorter effective integration times outside the central 2.′5 × 2.′5 on the other hand, the completeness limit varies across the FOV. Third, local nebulosities may hide background field stars. However, none of these potential errors affects our conclusions drawn from the CMD. The resulting net CMD for cluster stars within r < 33″ of NGC 3603 is shown at the right in the figure on page 1. We overlaid the theoretical isochrones of pre-main sequence stars from Palla & Stahler (1999) down to 0.1 $M_\odot$. We assumed a distance modulus of $(m–M)_\odot$ = 13.9 based on the distance of 6 kpc (De Pree et al. 1999) and an average foreground extinction of $A_V = 4.5^m$ following the reddening law by Rieke & Lebofski (1985).

Applying the isochrones to measured magnitudes could be misleading since the theoretical calculations include only stellar photospheres while the stars still may be surrounded by dust envelopes and accretion disks. This would lead to excess emission in the NIR and make the stars appear younger than they actually are. Typical excess emission of classical T-Tauri stars in the Taurus-Auriga complex have been determined as DH = 0.2^m, and DK = 0.5^m (Meyer, Calvet & Hillenbrand 1997). The upper part of the cluster-minus-field CMD clearly shows a main sequence with a marked knee indicating the transition to pre-main-sequence stars. The turn-on occurs at $J_s \approx 15.5$ mag (m ≈ 2.9 $M_\odot$). Below the turn-on the main-sequence basically disappears. We note that the width of the pre-main sequence in the right part of the figure on page 1 does not significantly broaden toward fainter magnitudes, indicating that our photometry is not limited by photometric errors. The scatter may in fact be real and due to varying foreground extinction, infrared excess and evolutionary stage. In that case the left rim of the distribution would be representative of the "true" colour of the most evolved stars. Fitting isochrones to the left rim in the CMD yields an age of only 0.3–1.0 Myr. Our result is in good agreement with the study by Eisenhauer et al. (1998) but extends the investigated mass range by about one order of magnitude toward smaller masses and covers also a much larger area.

Because of ≈ 10 magnitudes range in luminosities in the crowded core region, our sensitivity limits of $J_s \approx 21^m$, $H \approx 20^m$ and $Ks \approx 19^m$ don't appear to be exceedingly faint (and are about 3 magnitudes above ISAAC's detection limit for isolated sources). However, only VLT/ISAAC's high angular resolution, PSF stability, and overall sensitivity enabled us to study the sub-solar stellar population in a starburst region on a star-by-star basis.

Acknowledgements: We would like to thank the ESO staff, in particular those involved in the service observations, for their excellent work.

References

Brandl, B., et al. 1996, *ApJ*, **466**, 254.
Brandl, B., Brandner, W. & Zinnecker, H. 1999, Star Formation 1999, eds. T. Nakamoto et al., in press.
Brandl, B., et al. 1999, *A&A Letters*, **352**, L69.
Brandner, W., et al. 1997a, *ApJ*, **475**, L45.
Brandner, W., et al. 1997b, *ApJ*, **489**, L153.
Brandner, W., et al. 2000, *AJ*, in press (January 2000 issue).
Churchwell, E., Felliw, M., Wood, D.O.S. & Massi, M. 1987, *ApJ*, **321**, 516.
De Pree, C.G., Nysewander, M.C. & Goss, W.M. 1999, *AJ*, **117**, 2902.
Dottori, H., et al. 2000, subm. to *A&A*.
Drissen, L., Moffat, A.F.J., Walborn, N. & Shara, M.M. 1995, *AJ*, **110**, 2235.
Eisenhauer, F., Quirrenbach, A., Zinnecker, H. & Genzel, R. 1998, *ApJ*, **498**, 278.
Frogel, J.A., Persson, S.E., Aaronson, M. 1977, *ApJ*, **213**, 723.
Hunt, L.K., et al. 1998, *AJ*, **115**, 2594.
Johnstone, D., Hollenbach, D. & Bally, J. 1998, *ApJ*, **499**, 758.
Kennicutt, R.C. Jr. 1984, *ApJ*, **287**, 116.
McCullough, P.R., Fugate, R.Q., Christou, J.C. Et al. 1995, *ApJ*, **438**, 394.
Melnick, J., Tapia, M. & Terlevich, . 1989, *A&A*, **213**, 89.
Meyer, M.R., Calvet, N., & Hillenbrand, L.A. 1997, *AJ*, **114**, 288.
Moffat, A.F.J. 1983, *A&A*, **124**, 273.
Moffat, A.F.J., Drissen, L., & Shara, M.M. 1994, *ApJ*, **436**, 183.
O'Dell, C.R.O., Wen, Z. & Hu, X. 1993, *ApJ*, **410**, 686.
Palla, F. & Stahler, S. W. 1993, *ApJ*, **418**, 414.
Palla, F. & Stahler, S.W. 1999, *ApJ*, in press (20 Nov).
Persson, S.E. et al. 1998, *AJ*, **116**, 247.
Stecklum, B., Henning, T., Feldt, M., et al. 1998, *ApJ*, **115**, 767.
Stetson, P.B. 1987, *PASP*, **99**, 191.
Störzer, H. & Hollenbach, D. 1999, *ApJ*, **515**, 669.
Zinnecker, McCaughrean & Wilking 1993, Protostars and Planets III, eds. E.H. Levy & J.I. Lunine (University of Arizona Press), 429.

E-mail: brandl@astrosun.tn.cornell.edu

From Intracluster Planetary Nebulae to High-Redshift Lyα Emitters

R.P. KUDRITZKI and R.H. MÉNDEZ, Munich University Observatory
J.J. FELDMEIER and R. CIARDULLO, Dept. of Astron. and Astrophys., Penn State University
G.H. JACOBY, Kitt Peak National Observatory, Tucson
K.C. FREEMAN, Mt. Stromlo and Siding Spring Observatories
M. ARNABOLDI and M. CAPACCIOLI, Osservatorio Astronomico di Capodimonte, Napoli
O. GERHARD, Astronomisches Institut, Universität Basel
H.C. FORD, Physics and Astronomy Dept., Johns Hopkins University, Baltimore

1. Introduction

The fact that the spectra of planetary nebulae (PNs) are dominated by strong emission lines, with a very weak continuum, has two interesting consequences for extragalactic work. First, PNs in other galaxies are easily detectable: we need two images of a galaxy, one taken through a narrow-band filter transmitting a strong nebular emission (e.g. [O III] λ5007) and another taken through an off-band filter which does not transmit any strong nebular line. In the on-band image the PN appears as a point source. Since the nebular continuum is so weak, the point source should be invisible in the off-band image. By blinking the two images, and provided that the off-band image is deep enough, it is easy to identify the PNs. Second, for each detected PN we can measure an accurate radial velocity, because all the flux we have detected is concentrated at the redshifted wavelength of the emission line. Thus we can take a good spectrogram in an exposure time not much longer than what we need for the imaging. Since PNs are preferentially discovered in the outskirts of galaxies, where the surface brightness is lower, this means that PNs are ideal test particles for studies of rotation and mass distribution in the halos of the corresponding galaxies. Typical examples of such studies are Hui et al. (1995) on NGC 5128, and Arnaboldi et al. (1996) on the Virgo cluster galaxy NGC 4406. Here begins an unusual chain of unexpected results.

2. Intracluster PNs

The giant galaxy NGC 4406 is characterised by a negative redshift (–230 km s^{-1}), and indeed many of its PNs, discovered by Jacoby et al. (1990) and measured by Arnaboldi et al. (1996), have the expected redshifts. However, 3 of these PNs turn out to have redshifts typical of the Virgo cluster (around 1300 km s^{-1}). The conclusion was that these 3 PNs do not belong to NGC 4406; they must be members of an intergalactic or intracluster diffuse stellar population in the Virgo cluster, and only by chance they appear projected upon NGC 4406. Direct evidence of the existence of red giants belonging to this Virgo intracluster stellar population was subsequently reported by Ferguson et al. (1998), who worked with the Hubble Space Telescope. These red giants are too faint for spectroscopic studies. In contrast, the intracluster PNs offer an ideal opportunity to learn about the kinematic behaviour and perhaps even the abundances of the diffuse stellar population. A search for intracluster PNs in different positions across the Virgo cluster started immediately and produced dozens of PN candidates (Méndez et al. 1997, Feldmeier et al. 1998).

The "on-band/off-band" narrow-band filter technique used to discover the PN candidates allows the detection of a single emission line. This is not necessarily the desired [O III] λ5007; it might be another emission line at higher z, redshifted into the on-band filter, like [O II] λ3727 at z = 0.35, or Lyα at z = 3.14. In previous work (e.g. Méndez et al. 1997) we argued that most of our detections had to be real PNs because (a) the surface density of emission-line galaxies derived from previous studies (for example Thompson et al. 1995) was not high enough to explain all the detections; (b) the luminosity function of the detected sources, if we assume them to be at the distance of the Virgo cluster, is in good agreement with the PN luminosity functions derived in several Virgo galaxies (Jacoby et al. 1990).

Then we decided to take deep VLT+FORS spectrograms of several intracluster PN candidates, located in Field 1 of Feldmeier et al. (1998) and in the smaller field observed by Méndez et al. (1997; in what follows the "La Palma Field" or LPF, because the discovery images were taken with the 4.2-m William Herschel Telescope at La Palma). Our purpose was first of all to measure radial velocities and provide spectroscopic confirmation of the PN nature of the candidates, since a few of them could be high-redshift sources. Second, we were hoping to detect the very faint diagnostic emission lines necessary for reliable abundance determinations, at least for a few of the brightest intracluster PN candidates. This was not to be; in what follows we report the unexpected outcome of our first VLT run. Here we will restrict our description to the LPF, where the most interesting objects are located. A paper with a complete report has been submitted to *ApJ*.

3. Observations and First Results

In April 1999 we used the VLT UT1 with FORS in multi-object spectroscopic mode (MOS) with grism 300V. We defined 1 arcsec wide slitlets for several PN candidates in the LPF, and added slitlets for 2 objects suspected to be QSOs or starbursts because they were visible (although much weaker) in the off-band discovery image (Méndez et al. 1997). Some other slitlets were placed on stars or galaxies in the field, in order to check the slitlet positioning (done by taking a short exposure without grism through the slitlets) and to help locate the dispersion lines as a function of position across the field, which is important for the correct extraction of spectra consisting of isolated emission lines.

After completing 5 exposures of the initial MOS configuration, each 40 minutes long, the surprising result was that our targets in the LPF were confirmed as emission-line objects, but none of them is a PN. If we expose long enough, a PN must show not only [O III] λ5007, but also [O III] λ4959, which is three times weaker. In none of our sources could we find the second [O III] line. The spectra show only a strong, isolated and narrow emission line at wavelengths from 5007 to 5042 Å (encompassing the full width of the on-band discovery filter), and nothing else.

Of the 2 QSO or starburst candidates, one was confirmed as a QSO at z = 3.13, showing a typical broad-lined Lyα and several other emissions, including C IV λ1550. The other one appears to be a starburst region (one strong, isolated and narrow emission line, with faint continuum).

In this way we found ourselves unable to work on the expected intracluster PNs, and facing a different problem, namely, we had to identify the isolated emission. Was it [O II] λ3727 at $z = 0.35$, or could it be Lyα at $z = 3.13$? We defined a new MOS configuration, placing the slitlets so as to cover as much wavelength range towards the infrared as possible. We were able to take three exposures with this new MOS configuration. Based on the absence of any other emission line in our spectra, we could rule out all the alternatives, e.g. if the detected emission were [O II] λ3727 redshifted into the on-band filter, then we should see other features, like Hβ, the [O III] lines and Hα, at the corresponding redshift. A similar argument can be used to reject Mg II λ2798 at $z = 0.79$. There is only one possible identification: Lyα at $z = 3.13$. We had unwillingly found a nice collection of high-redshift Lyα emitters, which was an adequate compensation for the loss of the expected intracluster PNs.

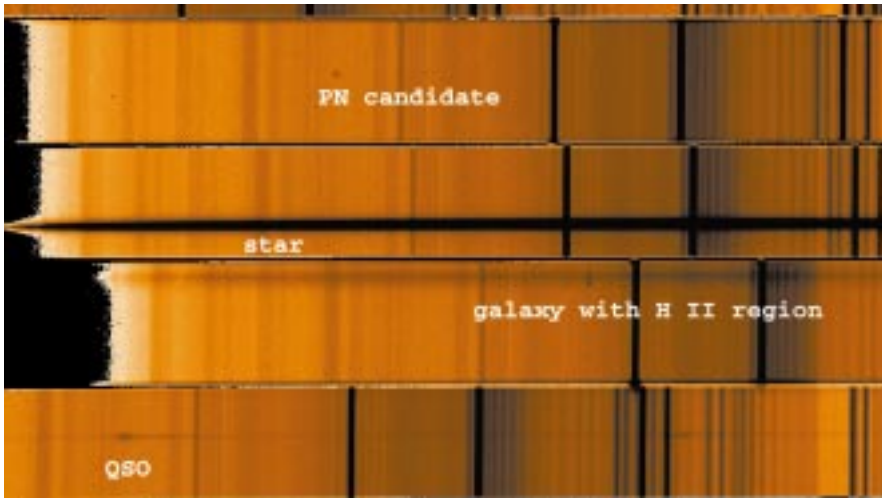

Figure 1. A section of an image produced by coadding 3 MOS exposures of the La Palma Field (LPF), taken with FORS. Here 4 of the 19 FORS slitlets are shown. These spectra, taken during new moon, are dominated by strong sky emissions. From top to bottom: (1) one of our intracluster PN candidates, now re-identified as a high-redshift Lyα emitter; (2) a foreground star; (3) a low-redshift galaxy showing a bright H II region at the edge, where Hβ and the [OIII] emissions λλ4959, 5007 are visible; (4) one of the QSO or starburst candidates, confirmed as a QSO. The strong and broad emission line is Lyα at z = 3.13. A weak continuum is visible. C IV λ1550 is visible to the right, flanked by strong sky emissions.

4. How Could This Happen?

Not just a few, but all the sources we tested with FORS are high-redshift galaxies. However it would be wrong to conclude that intracluster PNs do not exist. In fact, multi-object spectroscopy with the AAT and the 2-degree-field (2df) fibre spectrograph has confirmed the PN nature of many Virgo intracluster candidates, by detecting both [O III] emissions at 4959 and 5007 Å (Freeman et al. 1999). What happened to us is that the surface density of intracluster PNs in the LPF appears to be much lower than in other places across the Virgo cluster, probably indicating some degree of clumpiness in the distribution of the diffuse intracluster population. This will be verified by wide field surveys currently in progress.

There is another aspect to consider: the rather small area of the LPF (50 arcmin^2). Given a small area and a low surface density, the total number of intracluster PNs is small, and it becomes very improbable to find bright PNs. It seems that the fraction of high-redshift Lyα sources in the on-band/off-band samples is higher at faint magnitudes, thus explaining the detections in the LPF. We conclude that it is more efficient to search for intracluster PNs using wide-field survey cameras, like the WFI at the ESO 2.2-m telescope. With a larger area the total number of PNs increases and it is more probable to find bright ones; at brighter magnitudes the fraction of high-redshift Lyα emitters is smaller.

5. Properties of the Lyα Emitters

The weak (in most cases undetected) continuum implies a large Lyα equivalent width, between 20 and 200 Å in the rest frame. For these typical equivalent widths the most probable explanation is H II regions ionised by recently formed massive stars (e.g. Chariot and Fall 1993). The observed Lyα fluxes are between 2×10^{-17} and 2×10^{-16} erg cm^{-2} s^{-1}. Adopting $z = 3.13$, $H_0 = 70$ km s^{-1} Mpc^{-1} and $q_0 = 0.5$ we get a luminosity distance of 1.8×10^4 Mpc, which implies Lyα luminosities for our sources between 2×10^8 and 2×10^9 $L_\odot$. These numbers depend on our assumptions about the cosmological parameters: for a flat universe with $\Omega_0 = 0.2$, $\Omega_\Lambda = 0.8$, and the same z and H_0 as above, the luminosity distance becomes 3×10^4 Mpc, and the Lyα luminosities become larger by a factor 2.8. Our Lyα emitters are quite similar to those recently found by Hu (1998), Cowie & Hu (1998) and Hu et al. (1998) at redshifts from 3 to 5.

Using simple population synthesis models, on the assumption that these sources are produced by star formation with a Salpeter initial mass function and a lower mass cut-off of 0.5 $M_\odot$, we have concluded (Kudritzki et al. 1999 *ApJ* submitted) that the nebulae are nearly optically thick and must have a very low dust content, in order to explain the high observed Lyα equivalent widths. These galaxies must differ substantially from the typical Lyman break galaxies detected through their U-dropout; those are characterised by a strong continuum (needed for their very detection) and weak or absent Lyα emission. We attribute this difference to a lower dust content of our objects.

For the cosmological and star formation parameters we adopted, the total stellar mass produced would seem to correspond to the formation of rather small galaxies, some of which are perhaps destined to merge. However, one of our sources might become a serious candidate for a proto-giant spheroidal galaxy if we assumed continuous star formation, a low mass cut-off of 0.1 $M_\odot$ in the IMF, and a flat accelerating universe with $\Omega_0 = 0.2$ and $\Omega_\Lambda = 0.8$.

The implied star formation density in our sampled comoving volume is probably somewhat smaller than, but of the same order of magnitude as, the star formation density at $z \sim 3$ derived by other authors from Lyman-break galaxy surveys (see e.g. Steidel et al. 1999). This result agrees with the expectation that the Lyα emitters are a low-metallicity (or low-dust) tail in a distribution of star-forming regions at high redshifts. Finally, the Lyα emitters may contribute as many H-ionising photons as QSOs and Ly-break galaxies at $z \sim 3$ (see e.g. Madau et al. 1998). They are therefore potentially significant for the ionisation budget of the early universe.

6. Future Work

Now we would like to do some additional work on these Lyα emitters. In particular we would like to use ISAAC; we expect the strongest [O II] and [O III] forbidden lines as well as Hβ to be detectable with the Short Wavelength arm of ISAAC in Medium Resolution spectroscopic mode. This would allow us to either determine or (in the case of non-detection) put an upper limit to the metallicity. It might also be possible to clarify to what extent the production of Lyα photons can be attributed to AGN activity in-

stead of recent massive star formation. The firm detection of an infrared continuum would help to constrain the characteristics and total mass of the stellar populations through comparison with population synthesis models.

References

[1] Arnaboldi M., Freeman K.C., Méndez R.H. et al. 1996, *ApJ* **472**, 145.
[2] Charlot S., Fall S.M. 1993, *ApJ* **415**, 580.
[3] Cowie L.L., Hu E.M. 1998, *AJ* **115**,1319.
[4] Feldmeier J.J., Ciardullo R., Jacoby G.H. 1998, *ApJ* **503**, 109.
[5] Ferguson H.C., Tanvir N.R., von Hippel T. 1998, *Nature* **391**, 461.
[6] Freeman K.C. et al., 1999, in Galaxy Dynamics: from the Early Universe to the Present, ASP Conf. Ser., eds. F. Combes, G.A. Mamon, V. Charmandaris, in press, astro-ph/9910057.
[7] Hu E.M. 1998, ASP Conf Ser. 146, p. 148.
[8] Hu E.M., Cowie L.L., McMahon R.G. 1998, *ApJ* **502**, L99.
[9] Hui X., Ford H.C., Freeman K.C., Dopita M.A. 1995, *ApJ* **449**, 592.
[10] Jacoby G.H., Ciardullo R., Ford H.C. 1990, *ApJ* **356**, 332.
[11] Madau P., Haardt F., Rees M.J. 1998, preprint astro-ph/9809058 (4 Sep 1998).
[12] Méndez R.H., Guerrero M.A., Freeman K.C. et al. 1997, *ApJ* **491**, L23.
[13] Steidel C.C., Adelberger K.L., Giavalisco M. et al. 1999, preprint astroph/ 9811399v2 (23 Jan 1999).
[14] Thompson D., Djorgovski S., Trauger J. 1995, *AJ* **110**, 96.

E-mail: kudritzki@usm.uni-muenchen.de

VLT Spectroscopy of the $z = 4.11$ Radio Galaxy TN J1338–1942

C. DE BREUCK[1,2], W. VAN BREUGEL[2], D. MINNITI[2,3], G. MILEY[1], H. RÖTTGERING[1], S.A. STANFORD[2] and C. CARILLI[4]

[1]*Sterrewacht Leiden, The Netherlands (debreuck,miley,rottgeri@strw.leidenuniv.nl)*
[2]*Institute of Geophysics and Planetary Physics, Lawrence Livermore National Laboratory, Livermore, U.S.A. (wil,adam@igpp.llnl.gov)*
[3]*P. Universidad Católica, Santiago, Chile (dante@astro.puc.cl)*
[4]*National Radio Astronomy Observatory, Socorro, USA (ccarilli@nrao.edu)*

High-redshift radio galaxies (HzRGs) play an important role in cosmology. They are likely to be some of the oldest and most massive galaxies at high redshifts, and can therefore constrain the epoch at which the first generation of stars were formed. The near-IR Hubble $K-z$ diagram of powerful radio galaxies shows a remarkably tight correlation from the present time out to $z = 5.19$, despite significant K-corrections (van Breugel et al. 1998, 1999). This indicates that we can follow the evolution of the hosts of HzRGs from near their formation epoch out to low redshift ($z \lesssim 1$), where powerful radio sources inhabit massive elliptical galaxies (e.g. Lilly & Longair 1984; Best, Longair & Röttgering 1998). For example, at $z \sim 3$, we observe a change in the observed K-band morphologies of HzRGs from large-scale low-surface brightness emission with bright radio-aligned clumps at $z \lesssim 3$ to smooth, compact structures, sometimes showing elliptical shapes, like their ocal Universe counterparts (van Breugel et al. 1998). These surrounding clumps have properties similar to the UV dropout galaxies at similar redshifts (Pentericci et al. 1999), and indicate that HzRGs often reside in (proto-)cluster environments. This evolution picture seems consistent with the hierarchical clustering formation models (e.g. Kauffmann et al. 1999), where massive objects form by accretion of smaller systems located in over-dense regions.

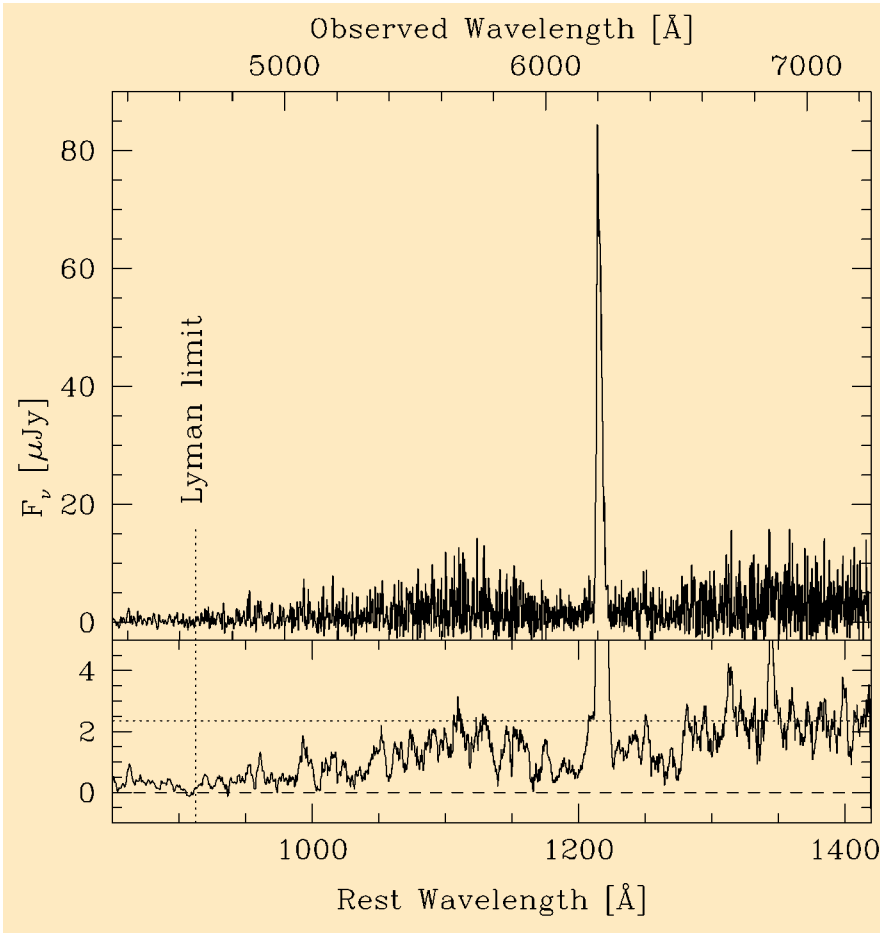

Figure 1: VLT spectrum of TN J1338–1942. The lower panel has been boxcar smoothed by a factor of 9 to better show the shape of the Lyα forest and the Lyman limit.

Detailed studies of HzRG can then be compared with the predictions of the hierarchical clustering scenarios.

Using newly available radio surveys, we have begun a systematic search for $z > 3$ radio galaxies (De Breuck et al. 2000), to be followed by more detailed studies of selected objects.

During the second week of VLT Antu operations in April 1999, we used FORS1 to obtain a spectrum of the second highest redshift radio galaxy from our sample, TN J1338–1942 at $z = 4.11$. We discovered this object in March 1997 using the ESO 3.6-m telescope (De Breuck et al. 1999a). The purpose of these VLT observations was to study the Lyα emission and the UV-continuum.

We used the 600R grism with a 1.3″ wide slit, and integrated for 47 min. The spectrum, shown in Figures 1 and 2, is dominated by the bright Lyα line ($F_{Ly\alpha} = 2 \times 10^{-15}$ erg s^{-1} cm^{-2}) with a rest-frame equivalent width of 210±50Å, a typical value for HzRGs.

Most notable from Figure 2 is the large asymmetry in the emission profile, consistent with a very wide (~ 1400 km/s) blueward depression over the entire spatial extent of the emission (~10 kpc). Similar asymmetries have been detected in other HzRGs, and have been interpreted as due to absorption by cold HI gas in a halo surrounding the radio galaxy (e.g. van Ojik et al. 1997; Dey 1999). The Lyα profile is well fit by a simple model consisting of a Gaussian emission profile and a single Voigt absorption function (see Figure 2). This model constrains the HI column density in the range $3.5 \times 10^{19} - 1.3 \times 10^{20}$ cm^{-2}. From this, we derive the total mass of the absorber at $2 - 10 \times 10^7$ $M_\odot$, which is comparable or slightly less than the total HII mass, as derived from the Lyα emission (De Breuck et al. 1999b). These results show that TN J1338–1942 is surrounded by a large reservoir of gas.

We also detect continuum emission in TN J1338–1942, only the second time this is reported in the spectrum of a $z > 4$ radio galaxy. The continuum, shown in the bottom panel of Figure 1, shows a discontinuity across the Lyα line, and a tentative detection of the Lyman limit. The flux deficit bluewards of Lyα is interpreted as HI absorption along the cosmological line of sight, and is described by the parameter

$$D_A = \langle 1 - \frac{f_\nu(\lambda 1050-1170)_{obs}}{f_\nu(\lambda 1050-1170)_{pred}} \rangle$$

(Oke & Korycanski 1982). For TN J1338–1942, we measure $D_A = 0.37 \pm 0.1$, similar to the $D_A = 0.45 \pm 0.1$ measured for the $z = 4.25$ radio galaxy 8C 1435+64 (Spinrad et al. 1995). Both these D_A values for $z > 4$ radio galaxies are significantly lower than the D_A values found for quasars at these redshifts (Schneider et al. 1991). Although based on only two measurements, our results suggest that the foreground HI absorption (≡ D_A) in quasars could have been overestimated because the highest redshift ($z > 4$) quasars have been found from samples with an optical colour selection, thereby excluding quasars with relatively small breaks across Lyα.

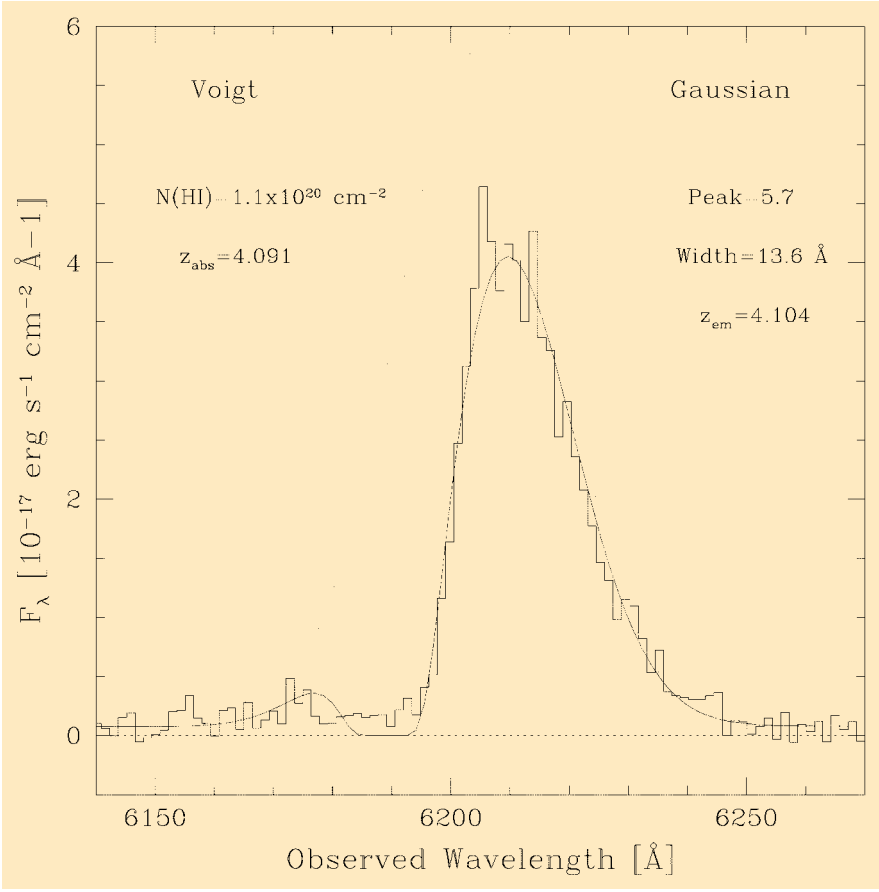

Figure 2: Part of the spectrum around the Lyα line. The solid line is the model consisting of a Gaussian emission profile (dashed line) and a Voigt absorption profile with the indicated parameters.

It is therefore particularly important to expand the number of objects at $z > 4$ selected by techniques other than optical colours. Radio galaxies are the brightest objects at these redshifts which are not out-shined by their central AGN like in quasars. Using the high sensitivity of the VLT instruments, we will be able to study at the same time the origin and evolution of their giant luminous halos or ionised gas, and the neutral HI gas surrounding them.

Acknowledgements. The work by C.D.B., W.v.B., D.M. and S.A.S. at IGPP/LLNL was performed under the auspices of the US Department of Energy under contract W-7405-ENG-48. D.M. is also supported by Fondecyt grant No. 01990440 and DIPUC. This work is supported in part by the Formation and Evolution of Galaxies network set up by the European Commission under contract ERB FMRX-CT96-086 of its TMR programme.

Bibliography

[1] Best, P. N., Longair, M. N., & Röttgering, H.J.A. 1998, *MNRAS*, **295**, 549.
[2] De Breuck, C., van Breugel, W., Röttgering, H., Miley, G., & Carilli, C. 1999a, in "Looking Deep in the Southern Sky", ed. R. Morganti & W. Couch (Berlin Heidelberg: Springer), p. 246.
[3] De Breuck, C. van Breugel, W., Minniti, D., Miley, G., Röttgering, H., Stanford, S. A., & Carilli, C. 1999 *A&A*, 1999b, **352**, L51.
[4] De Breuck, C., van Breugel, W., Röttgering, H., & Miley, G.2000, A&AS, submitted.
[5] Dey, A. 1999, in 'The Most Distant Radio Galaxies', ed. H. Röttgering, P. Best M. Lehnert (Amsterdam: KNAW), p. 19.
[6] Kauffmann, G., Colberg, J.M., Diaferio, A., & White, S. D. M. 1999, *MNRAS*, **303**, 188.
[7] Lilly, S. J. & Longair, M., 1984, *MNRAS*, **211**, 833.
[8] Oke, J.B., & Korycanski, D.G., 1982, *ApJ*, **255**, 11.
[9] Pentericci, L. et al. 1999, *A&A*, **341**, 329.
[10] Schneider, D. P., Schmidt, M, & Gunn, J.E. 1991, *AJ*, **101**, 2004.
[11] Spinrad, H., Dey, A., & Graham, J.R. 1995, *ApJ*, **438**, 51.
[12] van Breugel, W., Stanford, S. A., Spinrad, H., Stern, D., & Graham, J.R. 1998, *ApJ*, **502**, 614.
[13] van Breugel, W., De Breuck, C., Stanford, S. A., Stern, D., Röttgering, H., & Miley, G. 1999, *ApJ*, **518**, 61.
[14] van Ojik, R., Röttgering, H., Miley, G., & Hunstead, R. W. 1997, *A&A*, **317**, 358.

Weighing Young Galaxies – an Occasional Observer Goes to Paranal

S. WHITE, Max-Planck Institute for Astrophysics, Garching

"The VLT is Europe's great leap forward, heralded as a new window on the distant universe. Surely we can think of some joint projects that will turn the Americans green!" Trying to rally the troops at the annual meeting of our EC-funded "Galaxy Formation" network forced me to think about where the VLT pay-off might really come. A talk from Alan Moorwood provided some valuable ideas. The first efficient near-IR spectrograph on an 8-metre telescope could detect Hα past redshift 2 and [OII] 3727 to redshift 5. How about getting kinematics for distant galaxies like those in the Hubble Deep Fields or the infamous "Steidel" objects? This would have to clarify their relation to nearer, dearer, but (perhaps) more boring galaxies. Of course, I'd never taken an infrared spectrum of anything, but why not start now?

In a new field it's always important to get good help. My chance came with the news that Nicole Vogt was moving to IoA in Cambridge, one of the partners in our network. Californian graduate students now regularly present theses full of 10-metre data, and Nicole's contained Keck rotation curves for 15 galaxies out to redshift 0.8. Data for fifty more were rumoured to be in the pipeline. Some discussion showed that ISAAC could get Hα rotation curves for her most distant Keck galaxies (observed in [OII] 3727 on Hawaii) and, more interestingly, could extend the accessible redshift range by at least a factor of two. All we had to do was to find suitable candidates and to bang away for a few hours under the famous Paranal observing conditions. A proposal was duly dispatched suggesting a pilot study in the Hubble Deep Field South. We were elated when the Observing Programmes Committee gave us (most of) the time.

Travelling to Paranal from Garching makes one appreciate the virtues of remote observing. The shops at Paris CDG and in Buenos Aires were interesting but the attractions of neither place compensated for the long hours spent on planes and in airport lounges. The ESO guest house in Santiago, seemingly stuck in a genteel time warp between encroaching high-rise apartments, provided a welcome rest, but was spoiled somewhat by the need to get up long before breakfast in order to catch a taxi to catch a plane to catch a taxi to catch the once-a-day ESO bus to Paranal. The bus itself, complete with green baize curtains, reclining seats and movie videos, was a surreal but surprisingly comfortable way to end the odyssey. It dumped us under a clear blue sky in front of a small city of temporary buildings which appeared to have been built on the Moon. Not Ithaca, perhaps, but it turned out to be too deceptively luxurious to be considered Spartan.

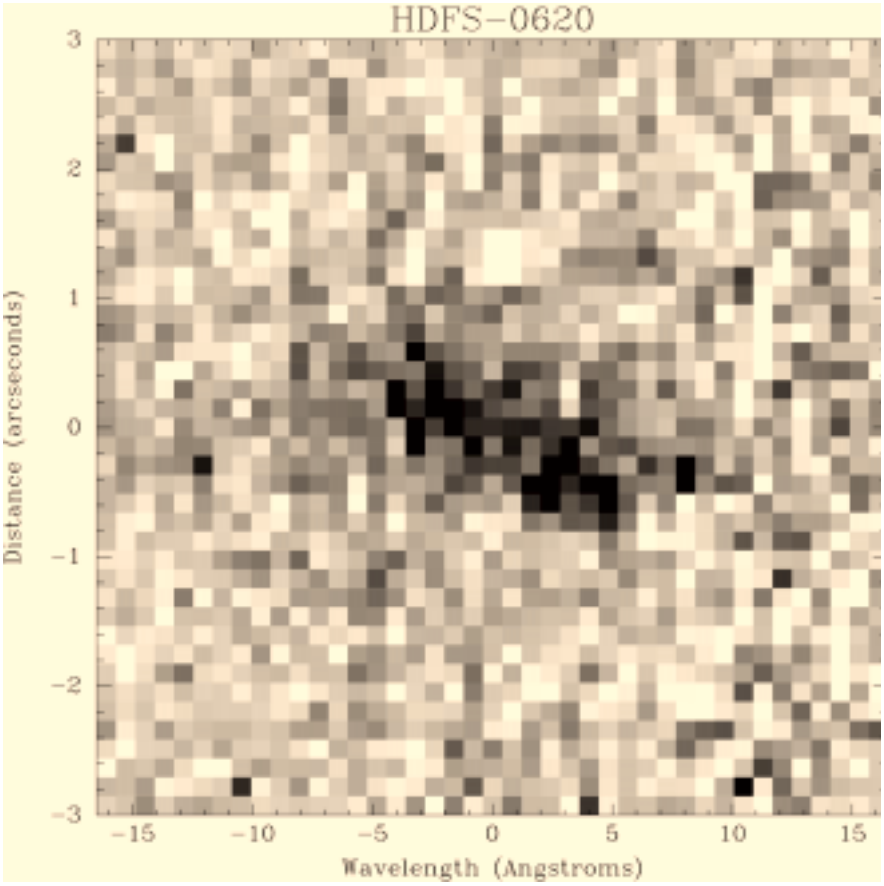

H-band spectrum of the Hα emission line for disk galaxy HDFS–0620, observed with VLT+ISAAC in high-resolution mode. The galaxy has a redshift of z = 1.29, placing the Hα emission at λ = 1.5 μm, in a clear region of the H-band IR window of the atmosphere between night-sky emission lines. The gas can be traced across almost 2 arcseconds (15 kiloparsecs) along the major axis of the galaxy, yielding a rotation curve with a total observed amplitude of order 180 km/s.

In the two days before our run started we learned the novel joys of P2PP, creating enough OBs (Observing Blocks) for the more seasoned observers to decide that we were quite definitely crazy. Our problem was that it isn't easy to decide how bright a distant object is likely to be in the Hα line when all you have is broadband photometry.

Furthermore, we had to make do with photometric redshifts for most of our candidates, so we weren't sure where Hα would fall relative to the night sky. Finally, there just aren't any "big" spirals beyond redshift 1 in the Hubble Deep Field South; our best candidates were all dwarf or irregular systems. As a result we needed plenty of flexibility to adjust our programme in light of experience at the telescope – and so plenty of OBs. The inevitable drawbacks of a pilot project...

Our first night at the telescope we learned a number of things.

(1) ESO looks after its VLT observers extremely well. The night assistant attended to all telescope-related issues, including guide-star acquisition. We never had to think about such things. The support scientist knew the instrument and its performance inside out and had written all the available quick-look software. As a result he could help us assess our data as soon as they were taken. Finally, the shift manager always showed up whenever things got complicated.

(2) The telescope points and tracks like a dream. Our reference stars always arrived within a few seconds of the centre of the field, our offsets all worked to a small fraction of an arcsecond, even over several arcminutes, and the telescope drifted by only a couple of tenths of an arcsecond even after tracking for two hours.

(3) The instrument and the conditions really can be "as advertised". The see-

ing on the detector rarely got worse than 0.5 arcsec and there were extended periods when it was 0.3 arcsec. Furthermore the long-slit spectra taken by ISAAC sky-subtracted well and had a cosmetic quality quite comparable to that of good optical spectra.

(4) Even with the best equipment under the best conditions, a hard project is still hard. Our first couple of candidates showed no clear detection after a couple of hours of integration, leaving us uncertain whether their photometric redshifts were in error, their emission lay under a sky line, or was just very weak. We were greatly relieved when our third target showed strong Hα at $z \sim 1.3$ with a clear detection of galactic rotation.

Our second night was equally good and brought several more detections as well as some further "blanks". We finished with a feeling of achievement; galaxy kinematics really can be studied beyond redshift one. This night also brought an unexpected (and probably illegal) glass of champagne as the UVES commissioning team, working 20 metres away on the UT2 console, obtained their first *bona fide* quasar spectrum. It was certainly impressive; the Lyα forest could be seen booming through right down to the atmospheric cut-off. As we boarded the bus the following afternoon at the start of the long trek home, we felt sure we would be returning soon despite the distance.

(swhite@mpa-garching.mpg.de)

Sunset on Paranal (Photographer: Herbert Zodet).

Science with the Atacama Large Millimetre Array

"Science with the Atacama Large Millimetre Array" was the title of an international conference held at the Carnegie Institution in Washington, DC, in early October. In order to increase public attention on the ALMA project, NRAO had organised a press briefing on October 7, enabling journalists to meet with scientists and key representatives of the ALMA partnership. The press briefing followed a reception in the US Congress. In addition, ESO, PPARC and NRAO mounted small exhibitions at the Carnegie Institution itself.

C. Madsen

ANNOUNCEMENTS

The La Silla 2000+ Report Now Available

The Working Group "La Silla 2000+" has completed its work, based on the replies to the questionnaire survey of the Users Committee (see *The Messenger* No. 95, p. 38). A total of 256 colleagues from the ESO countries participated in this survey, a very gratifying turnout.

The report of the Working Group, which contains a set of recommendations for the future of the La Silla facilities (1999–2006) has been submitted to the Director General of ESO (June 1999).

The final "La Silla 2000+ Report" (with colour figures) is now available on the Web at the following address:

http://www.eso.org/gen-fac/commit/ls2000pl1.html

The Working Group wishes to thank all of those who answered the questionnaire. Special thanks go to the ESO Remedy Team, and in particular to Rein Warmels who helped to design the questionnaire and prepare the figures in the Report.

The report will now be discussed in the relevant ESO committees.

Birgitta Nordström
Chair, ESO Users Committee and the WG "La Silla 2000+"

The NEON Observing School

The Network of European Observatories in the North (NEON) organises an observational Euro summer school sponsored by the European Community. This school is taking over from the former, discontinued, ESO/OHP summer school and intends to run on a yearly basis.

The participating observatories are: Asiago Observatory (Italy), Calar Alto Observatory (Germany-Spain) and Haute-Provence Observatory (France), with additional tutorial assistance from ESO.

The purpose of the school is to provide an opportunity to gain practical observational experience at the telescope, in observatories with state-of-the-art instrumentation. To this effect, the school proposes tutorial observations in small groups of 3 students, under the guidance of an experienced observer, centred around a small research project and going through all steps of a standard observing programme. Some complementary lectures will be given by experts in the field.

The school is open to students working on a PhD thesis in Astronomy and which are nationals of a Member State or an Associated State of the European Union. The working language is English. Up to eighteen participants will be selected by the organising committee and will have their travel and living expenses paid, if they satisfy the EC rules (age limit of 35 years at the time of the Euro Summer School).

The first NEON Euro summer school will take place at the Calar Alto Observatory in Spain, from

July 10 to 22, 2000

Instructions and full practical details can be found on the school Web site when this announcement appears in print.

Applicants are expected to fill in an application form that will be available on the Web site, with a curriculum vitae and a description of previous observational experience, and to provide a letter of recommendation from a senior scientist.

The provisional application deadline is March 31st, 2000.

The school Web site is hosted by the
EAS Web site at: http://www.iap.fr/eas/schools.html

Secretary of the school: Mrs Brigitte RABAN at IAP, 98bis, Bd Arago, F-75014 PARIS.

Michel Dennefeld, Co-ordinator of the NEON school.

PERSONNEL MOVEMENTS

(1st October 1999–30th November 1999)

International Staff

ARRIVALS

EUROPE

BRISTOW, Paul (GB), Science Data Analyst/Programmer
BROWN, Anthony (NL), Fellow
DIMMLER, Martin (D), Electronics/Control Engineer
ESKDALE, Jane (AUS), Secretary/Group Assistant
GAILLARD, Boris (F), Associate
GONÇALVES C., Anabela (P), Fellow
RITTER, Heiderose (D), Associate
RIVINIUS, Thomas (D), Fellow
SARTORETTI, Paola (I), Scientific Application Developer
TUELLMANN, Ralph (D), Student
VAN ECK, Sophie (B), Fellow
ZAGGIA, Simone (I), Fellow

CHILE

ATHREYA, Ramana (IND), Fellow
GALLIANO, Emmanuel (F), Student
MARCONI, Gianni (I), Operations Staff Astronomer
TAMAI, Roberto (I), Mechanical Engineer

DEPARTURES

EUROPE

BALON, Serge (F), Technical Assistant
BRESOLIN, Fabio (I), Fellow
FERRARI, Marc (F), Associate
FUCH, Rainer (D), Legal Advisor
HILL, Susan (GB), Archive Operator
KORNWEIBEL, Nicholas (AUS), Software Engineer
LATSCH, Hedwig (D), Administrative Clerk
SCODEGGIO, Marco (I), Fellow

CHILE

SCHUMANN, Erich (D), Catering La Silla

Local Staff

DEPARTURES

DIAZ,Jorge,
RAMIREZ, Luis,
LECAROS, Fernando,
FERNANDEZ DE C., Rodrigo,

ARRIVAL

TAPIA, Mario, Mechanical Engineer

MESSENGER INDEX 1999 (Nos. 95–98)

SUBJECT INDEX

ANNOUNCEMENTS

AUTHOR INDEX

ESO, the European Southern Observatory, was created in 1962 to "… establish and operate an astronomical observatory in the southern hemisphere, equipped with powerful instruments, with the aim of furthering and organising collaboration in astronomy …" It is supported by eight countries: Belgium, Denmark, France, Germany, Italy, the Netherlands, Sweden and Switzerland. ESO operates at two sites. It operates the La Silla observatory in the Atacama desert, 600 km north of Santiago de Chile, at 2,400 m altitude, where several optical telescopes with diameters up to 3.6 m and a 15-m submillimetre radio telescope (SEST) are now in operation. In addition, ESO is in the process of building the Very Large Telescope (VLT) on Paranal, a 2,600 m high mountain approximately 130 km south of Antofagasta, in the driest part of the Atacama desert. The VLT consists of four 8.2-metre and three 1.8-metre telescopes. These telescopes can also be used in combination as a giant interferometer (VLTI). The first 8.2-metre telescope (called ANTU) is since April 1999 in regular operation, and also the second one (KUEYEN) has already delivered pictures of excellent quality. Over 1200 proposals are made each year for the use of the ESO telescopes. The ESO Headquarters are located in Garching, near Munich, Germany. This is the scientific, technical and administrative centre of ESO where technical development programmes are carried out to provide the La Silla and Paranal observatories with the most advanced instruments. There are also extensive astronomical data facilities. In Europe ESO employs about 200 international staff members, Fellows and Associates; in Chile about 70 and, in addition, about 130 local staff members.

The ESO MESSENGER is published four times a year: normally in March, June, September and December. ESO also publishes Conference Proceedings, Preprints, Technical Notes and other material connected to its activities. Press Releases inform the media about particular events. For further information, contact the ESO Education and Public Relations Department at the following address:

EUROPEAN
SOUTHERN OBSERVATORY
Karl-Schwarzschild-Str. 2
D-85748 Garching bei München
Germany
Tel. (089) 320 06-0
Telefax (089) 3202362
ips@eso.org (internet)
URL: http://www.eso.org

The ESO Messenger:
Editor: Marie-Hélène Demoulin
Technical editor: Kurt Kjär

Printed by
J. Gotteswinter GmbH
Buch- und Offsetdruck
Joseph-Dollinger-Bogen 22
D-80807 München
Germany

ISSN 0722-6691

Contents